

# TECHNISCHE UNIVERSITÄT MÜNCHEN

Lehrstuhl für Ernährungsmedizin / Lehrstuhl für Biofunktionalität der Lebensmittel

## Influence of adipogenesis and high fat diet on the development of cell stress markers in adipose tissue

Stephanie May

Vollständiger Abdruck der von der Fakultät Wissenschaftszentrum Weihenstephan für Ernährung, Landnutzung und Umwelt der Technischen Universität München zur Erlangung des akademischen Grades eines

Doktors der Naturwissenschaften

genehmigten Dissertation.

Vorsitzender: Univ.-Prof. Dr. J. J. Hauner

Prüfer der Dissertation:

1. Univ.-Prof. Dr. D. Haller

2. Priv.-Doz. Dr. T. Skurk

Die Dissertation wurde am 08.05.2013 bei der Technischen Universität München eingereicht und durch die Fakultät Wissenschaftszentrum Weihenstephan für Ernährung, Landnutzung und Umwelt am 06.09.2013 angenommen



## Zusammenfassung

Adipositas hat gravierende Effekte auf die Entwicklung von Krankheiten, wie zum Beispiel Insulinresistenz/Typ 2 Diabetes mellitus sowie arterielle Hypertonie. Diese metabolischen Krankheiten sind mit einer niedrig-gradigen Entzündung assoziiert. Das Gleichgewicht von Proteinsynthese und Proteinfaltung spielt dabei in den Zellen eine wichtige Rolle. Dieses Gleichgewicht kann durch äußere Einflüsse - exzessive Nahrungsaufnahme, Sauerstoffmangel oder Hitzeeinwirkungen - gestört sein, so dass Signalwege (UPR) aktiviert werden. Diese laufen als Proteinantwort im Endoplasmatischen Retikulum (erUPR) sowie im Mitochondrium (mtUPR) ab. Ziel der Arbeit war es herauszufinden, welche Rolle erUPR und mtUPR bei der adipogenen Differenzierung spielen. Des Weiteren, wollten wir verstehen wie erUPR und mtUPR die Entwicklung von Adipositas beeinflussen können.

*In vitro* konnten wir zeigen, dass sich der Verlauf von Markerproteinen der erUPR (Grp78, p-eIF2 $\alpha$  und CHOP) während der adipogenen Differenzierung stark verändert. Zusätzlich konnten wir in allen untersuchten Zelllinien nachweisen, dass Cpn60 (als Marker für die mtUPR) während der Adipogenese ansteigt und aus diesem Grund ein wichtiges Kernstück in der Funktion von Fettzellen darzustellen scheint. Des Weiteren wird während der Adipogenese der ER-assoziierte Abbau (ERAD), aber keine durch JNK induzierte Entzündungsreaktion aktiviert. *In vivo* zeigten sich vergleichbare Ergebnisse mit C57BL/6N Mäusen. Mit Hilfe der Grp78<sup>+/-</sup> Maus können wir eine Kompensation des heterozygoten Knock-outs durch die Steigerung des ERAD erkennen. Cpn60<sup>+/-</sup> Mäuse zeigten einen Phänotyp mit der Tendenz eine Entwicklung von Adipositas vorzubeugen. Dieser Phänotyp stellte sich allerdings nur bei den Tieren unter Normal-Diät dar, da diese leichter sind, kleinere Fettzellen haben und weniger Triglyzeride in Leber und Plasma vorweisen. Zusätzlich konnten wir auch hier einen Anstieg des ERAD ausmachen.

Zusammenfassend zeigt sich, dass die Adipogenese kein Stressfaktor per se ist. Beide Signalwege – die erUPR sowie die mtUPR – werden durch die Adipogenese beeinflusst und das teilweise Fehlen von Grp78 oder Cpn60 führt zu einer Aktivierung des ERAD.



## Abstract

Obesity has detrimental effects on the development of pathological conditions like insulin resistance/ type 2 diabetes and cardiovascular disease (CVD). These metabolic disorders usually develop on a common low-grade inflammatory background. The balance of protein synthesis and protein folding plays an essential role in the physiology of all cells. Protein homeostasis could be disturbed by environmental stress situations, such as nutrient excess, hypoxia in white adipose tissue (WAT) and/or a situation triggered by physiological stress like heat. The response pathways could be identified in the endoplasmic reticulum (erUPR) and also in mitochondria (mtUPR). Thus, the aim of this work was to investigate the role of erUPR and mtUPR in adipogenic differentiation. Furthermore, we want to contribute to the understanding of how the erUPR and the mtUPR influence the development of obesity.

*In vitro*, we could show that markers for the erUPR (Grp78, p-eIF2 $\alpha$  and CHOP) alter during the course of differentiation. Additionally, we described that in all cell models investigated Cpn60 (as a marker of the mtUPR) increase during adipogenesis and therefore seems to be very important for the correct development of adipocytes. Furthermore, the cells activated an ER-associated degradation (ERAD) by induction of VCP, but the inflammation pathway activated by JNK was not induced. *In vivo*, we showed that C57BL/6N mice at different ages behave more like the *in vitro* human cell culture models for adipogenesis than like the murine 3T3-L1 cell line. For the Grp78<sup>+/-</sup> mice we observed a compensatory adaptive response to counteract the critical requirement of Grp78 in maintaining ER homeostasis via up-regulation of ERAD. For the Cpn60<sup>+/-</sup> mice we saw a mildly beneficial phenotype to prevent obesity but only in the group under normal diet. The Cpn60<sup>+/-</sup>-Ctrl mice showed lower body weight, smaller adipocytes and less triglyceride in the liver and the plasma. In the WAT of Cpn60<sup>+/-</sup> mice we observed an increase in VCP.

In conclusion, adipogenesis is not a condition to activate erUPR and mtUPR per se. Both response pathways are affected by the development of obesity and the partial deletion of Grp78 as well as Cpn60 leads to an activation of the ERAD.



## **Table of contents**

<b>ZUSAMMENFASSUNG .....</b>	<b>3</b>
<b>ABSTRACT .....</b>	<b>5</b>
<b>TABLE OF CONTENTS .....</b>	<b>7</b>
<b>INTRODUCTION .....</b>	<b>11</b>
<b>Obesity.....</b>	<b>11</b>
Obesity - Type 2 Diabetes mellitus and inflammation .....	11
<b>Adipose tissue .....</b>	<b>12</b>
Adipose tissue function and morphology .....	12
Adipogenesis and adipose tissue growth .....	14
Adipose tissue function and metabolic diseases .....	15
<b>Cellular stress signaling .....</b>	<b>16</b>
The endoplasmic reticulum and the erUPR .....	17
erUPR and inflammation in obesity .....	19
Mitochondria and the mtUPR.....	20
Mitochondrial dysfunction in obesity .....	21
<b>High fat diet and animal models.....</b>	<b>23</b>
Grp78 <sup>+/-</sup> mice and Cpn60 <sup>+/-</sup> mice .....	23
<b>AIM OF THE WORK.....</b>	<b>25</b>
<b>MATERIAL AND METHODS .....</b>	<b>27</b>
<b>Cell culture .....</b>	<b>27</b>
3T3-L1 cell culture .....	27
SGBS cell culture .....	27
Primary human preadipocytes cell culture.....	28
<b>Patients.....</b>	<b>29</b>
Isolation of primary human preadipocytes .....	29
Isolation of primary human adipocytes .....	29
Fractionation of human adipocytes.....	30
<b>Animals .....</b>	<b>31</b>
Experimental setup.....	31
Genotyping of the mouse .....	31

## Table of contents

Polymerase chain reaction (PCR) for genotyping .....	32
Housing .....	34
Diets .....	34
Minispec NMR analysis .....	36
Indirect calorimetric measurement .....	36
IP-GTT .....	37
Sacrificing and sample collection .....	37
Bomb-calorimetric measurement .....	37
Paraffin embedding .....	38
Hematoxylin-Eosin (HE)-staining .....	38
<b>Adipocyte differentiation, fat storage and adipocyte size .....</b>	<b>39</b>
GPDH (glycerol-3-phosphate dehydrogenase) measurements .....	39
DAPI Staining .....	39
Oil-Red-O staining in cell culture .....	39
Oil-Red-O staining of liver .....	40
Determination of adipocyte size in adipose tissue .....	40
Triglyceride measurement in plasma samples .....	41
Triglyceride measurement in liver tissue .....	41
<b>ELISA .....</b>	<b>41</b>
Adipokine-ELISA .....	41
Insulin-ELISA .....	41
<b>Protein expression .....</b>	<b>42</b>
Protein isolation (cell culture) .....	42
Protein isolation (tissue samples) .....	42
Bicinchoninic acid (BCA) method .....	42
Western blot .....	42
<b>Statistical analysis .....</b>	<b>44</b>
<b>RESULTS .....</b>	<b>45</b>
<b>In vitro assessment of UPR markers during adipogenic differentiation .....</b>	<b>45</b>
Qualitative assessment of housekeeping proteins in adipocytes of different sizes .....	45
UPR markers during differentiation of primary isolated human preadipocytes as well as SGBS cells .....	48
UPR markers during differentiation of murine 3T3-L1 cells .....	54
<b>Assessment of UPR markers in primary isolated mature adipocytes and in clinical samples from a tissue bio bank .....</b>	<b>58</b>
<b>Measurement of UPR markers in different mouse models .....</b>	<b>61</b>
Development of adipose tissue in C57BL/6N mice of different ages .....	61
Grp78 <sup>+/-</sup> mice – a basal characterization under a high fat diet .....	63
Cpn60 <sup>+/-</sup> mice – A basal characterization under a high fat diet .....	74



<b>DISCUSSION</b> .....	<b>85</b>
<b>UPR during adipogenic differentiation</b> .....	<b>85</b>
Markers of the UPR vary during the process of adipogenic differentiation .....	85
ERAD and inflammation are important during the process of adipogenic differentiation.....	87
<b>UPR in different mouse models</b> .....	<b>89</b>
Characteristics of adipose tissue in C57BL/6N mice of different ages .....	89
Age and duration of high fat feeding is an important factor for protection of obesity in Grp78 <sup>+/-</sup> mice .....	92
Cpn60 <sup>+/-</sup> mice establish a mild phenotype under normal conditions .....	94
<b>LIST OF FIGURES AND TABLES</b> .....	<b>99</b>
List of Figures .....	99
List of Tables .....	100
<b>ABBREVIATIONS</b> .....	<b>101</b>
<b>REFERENCES</b> .....	<b>105</b>
<b>PUBLICATIONS AND PRESENTATIONS</b> .....	<b>123</b>
<b>ACKNOWLEDGEMENTS</b> .....	<b>125</b>
<b>CURRICULUM VITAE</b> .....	<b>127</b>



## **Introduction**

### ***Obesity***

Nowadays, obesity is a common condition in the general population of developed and developing countries.<sup>1</sup> Obesity is defined as a medical situation with an excess gain in white adipose tissue (WAT). This in turn may have an adverse effect on health and could induce the risk of developing a number of medical problems. For example, the metabolic syndrome (MetS), a cluster of cardiovascular risk factors comprising abdominal obesity, glucose intolerance/type 2 diabetes mellitus, dyslipidemia and hypertension could develop.<sup>2</sup> The susceptibility to obesity can be explained by a chronic imbalance between high caloric intake and energy consumption due to reduced physical activity. Additionally, it is thought to be dependent of the genetic background.<sup>3,4</sup>

The BMI (body mass index), is a heuristic proxy for human body fat based on an individual's weight and height<sup>5</sup> and is defined as the individual's body weight divided by the square of his or her height. According to the World Health Organization (WHO) people are overweight (pre-obese) if the calculated BMI is between 25 and 30 kg/m<sup>2</sup> and obese if it is greater than 30 kg/m<sup>2</sup>. Alone, it is not a good indicator for the health risk assessment in overweight and obese individuals. Moreover, the adipose tissue distribution is very important to estimate the risk to develop related diseases.<sup>6</sup> Individual's with an abdominal type of obesity (so-called apple-shaped) have a higher risk for cardiovascular and/or metabolic diseases. In contrast, a gluteo-femoral adipose tissue distribution seems to be protective as less health complications arise.<sup>7</sup>

### ***Obesity - Type 2 Diabetes mellitus and inflammation***

Obesity has detrimental effects on the development of pathological conditions like insulin resistance/ type 2 diabetes and cardiovascular disease (CVD)/ atherosclerosis.<sup>8-10</sup> In 1988, it was proposed that individuals with insulin resistance have a higher risk for CVD.<sup>11</sup> The definition of the insulin resistance syndrome seems to be a logical choice to provide a pathophysiological construct with which to view the different abnormalities and clinical syndromes that occur more commonly in

insulin-resistant individuals. Diabetes mellitus type 2 (T2D) is a metabolic disorder of insulin secretion by the pancreas and the inability of the tissues in the body to respond to this hormone. It is characterized by high blood glucose in the context of insulin resistance and a relative insulin deficiency.<sup>12</sup> It is well accepted, that obesity and increased abdominal fat distribution are the most important factors which induce the risk of developing T2D, although other factors, such as genetic predisposition, age, hypertension, dyslipidemia, glucose intolerance and physical inactivity exist. T2D is a chronic disease which is often associated with a shorter life expectancy<sup>13</sup>, a higher risk of CVD and stroke, as well as kidney failure.<sup>14</sup>

All these conditions, are considered to grow on a common low-grade inflammatory background.<sup>15,16</sup> Although the origin of the subclinical inflammatory state is not fully understood at least two factors may contribute to this situation. Firstly, it was shown that immune cells colonize the stromal vascular fraction (SVF) of adipose tissue.<sup>17,18</sup> Secondly, adipocytes have been shown to demonstrate secretorily active cells including pro-inflammatory chemokines and cytokines.<sup>19-21</sup> In turn, these mediators exert the potential to induce activation not only of macrophages but also of lymphocytes.<sup>22,23</sup>

Although adipocytes exhibit a high capacity to produce pro-inflammatory factors, it is currently unclear to which extent these cells contribute to the observed inflammatory status in plasma. This status is affected by an elevated circulation of inflammatory cytokines and adipokines, such as interleukin (IL) 6, C-reactive protein (CRP) and plasminogen activator inhibitor-1 (PAI-1).<sup>1</sup> Since adipose tissue expansion is linked to increased levels of IL-6 and PAI-1 within the tissue, it is also assumed that some of these factors contribute to the low-grade inflammatory status.<sup>15</sup>

## ***Adipose tissue***

### *Adipose tissue function and morphology*

Adipose tissue is an organ with various functions. It is composed of around 80% fat, which is stored in adipocytes. Adipose tissue could be explained like a loose connective tissue predominantly consisting of adipocytes. The (mature) function of adipose tissue is to store energy in form of neutral lipids. In recent years, adipose tissue has been recognized as an endocrine organ, which produces hormones and a

large number of various adipokines.<sup>24,25</sup> Moreover, expanded adipose tissue secretes various pro-inflammatory cytokines, chemokines and certain complement factors. Therefore, adipose tissue is involved in several functions such as the immune response.<sup>26,27</sup>

The weight of the adipose tissue in healthy humans ranges between 12 to 30% (depending on gender) of total body weight. According to the localization and function one can distinguish between WAT, brown adipose tissue (BAT) and bone marrow fat.

Further on, it should be focused only on WAT. WAT contains several cell types, with the highest percentage of cells being adipocytes, which contain univacuolar fat droplets. Other cell types include fibroblasts, macrophages and endothelial cells. The adipose tissue also contains adipocyte precursors (**Fig. I1**).<sup>28</sup>

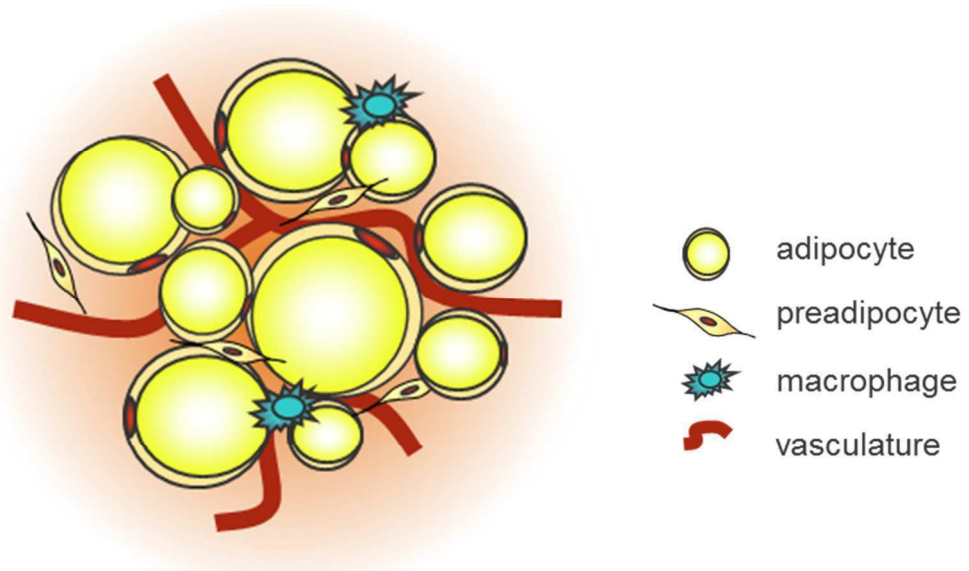


**Fig. I 1: Basic structure of white adipose tissue (modified from Klaus S.<sup>28</sup>)**

The white adipose tissue (WAT) contains mature adipocytes to store lipids. A small percentage of cells are preadipocytes, with the ability to differentiate into mature adipocytes. Also other cell types like macrophages and endothelial cells colonize the WAT. Endothelial cells also exist in the WAT.

The WAT is responsible for storing energy and it is essential for energy homeostasis.<sup>29</sup> However, fatty acids (FA) are not only stored in case of surplus calorie availability. Also under normal conditions FA are constantly stored in and released from the adipose tissue. FA as well as glucose are taken up by adipocytes and stored as triglycerides. The storage is catalyzed by insulin, which is normally stimulated by high blood sugar level after a meal. The process, which converts triglycerides into FA and glycerol, is called lipolysis and appears during periods of fasting.<sup>29</sup>

Adipogenesis and adipose tissue growth

Adipose tissue is a highly dynamic organ with a substantial turnover.<sup>30</sup> During tissue expansion two major mechanisms can take place to facilitate the storage of excess energy. First, adipose tissue growth may be caused by an increased lipid load per adipocyte (hypertrophy) and/or second an increased number of adipocytes (hyperplasia).<sup>31</sup> Although it is suggested that adipocyte hypertrophy might be responsible for the majority of metabolic abnormalities, it is currently unclear how differentiating adipocytes behave under these growth conditions. The formation of new adipocytes from preadipocytes is a central process (adipogenesis) during adipose tissue growth and it is therefore essential to understand the underlying mechanisms.

It could be shown that numbers of white adipocytes increase during the development of animals but are relatively constant in the mature fat pad.<sup>32</sup> Similar findings have been obtained in humans, but within adult human WAT, adipocytes seem to undergo an annual turnover of approximately 10%.<sup>33</sup> Thus, adipogenesis obviously takes place in adults to maintain the adipose compartment. Whether this annual turnover has a crucial role in the development of obesity remains unclear.

The process of adipogenesis follows a strict course. First, mesenchymal stem cells (MCSs) switch over to committed white preadipocytes, a course mediated by factors, such as extracellular matrix (ECM) stiffness, confluence or cell shape.<sup>34</sup> White preadipocytes can become mature white adipocytes upon the addition of adipogenic stimuli. Such factors are for example glucocorticoids, insulin, cyclic adenosinmonophosphate (AMP) and triiodothyronine (T<sub>3</sub>).<sup>35</sup> The process of adipogenesis is very complex and still under investigation (**Fig. I2**).<sup>34</sup> Undifferentiated preadipocytes can expand their volume several fold during differentiation due to increasing lipid inclusion. Furthermore, cell size in mature adipocytes can vary from under 70 µm to more than 120 µm in diameter.<sup>36</sup>

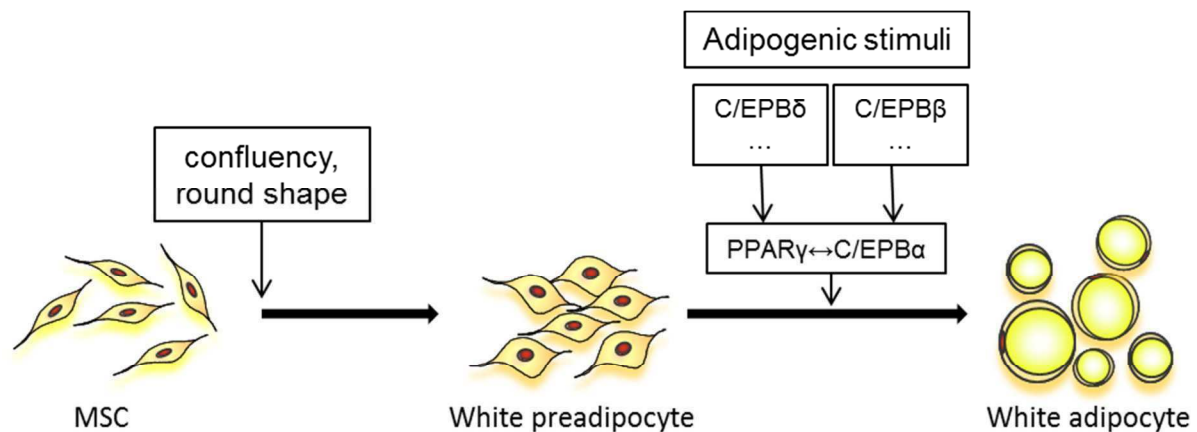


**Fig. I 2: Schematic course of adipogenic progression (modified from Cristancho, AG et al.<sup>34</sup>)**

The formation of mesenchymal stem cells (MSCs) into white preadipocytes could be mediated, e.g. by extracellular matrix (ECM) stiffness, confluence and/or cell shape. White preadipocytes differentiate into mature white adipocytes. This process needs adipogenic stimuli, like glucocorticoids, insulin and cyclic AMP. The total progress is called adipogenesis.

### Adipose tissue function and metabolic diseases

Adipose tissue in humans comes more and more into focus in view of metabolic diseases. Under a high nutrient excess WAT expands and obesity occurs. In this context a lot of metabolic diseases arise, which usually grow on a common low-grade inflammatory background. Although the origin of elevated inflammation markers is unknown there is a clear association of obesity and fat mass.<sup>33</sup> Especially fat cell size was shown to be a significant determinant for the production of pro-inflammatory mediators (**Fig. I3**).<sup>36,37</sup>

Although adipocytes exhibit a high capacity to produce pro-inflammatory factors<sup>20,21</sup> it is currently unclear to which extent these cells contribute to the observed inflammatory status in plasma. The obese adipose tissue is also colonized by various subsets of immune cells, which (when activated) also exhibit a high potency to release a similar pattern of immune effectors.<sup>38-40</sup> For example, macrophages may either show an anti-inflammatory M2 phenotype or may produce high amounts of pro-inflammatory mediators upon activation.<sup>41</sup> The hypothesis, that predominantly non-fat cells may produce these factors is supported by various reports.<sup>42</sup>

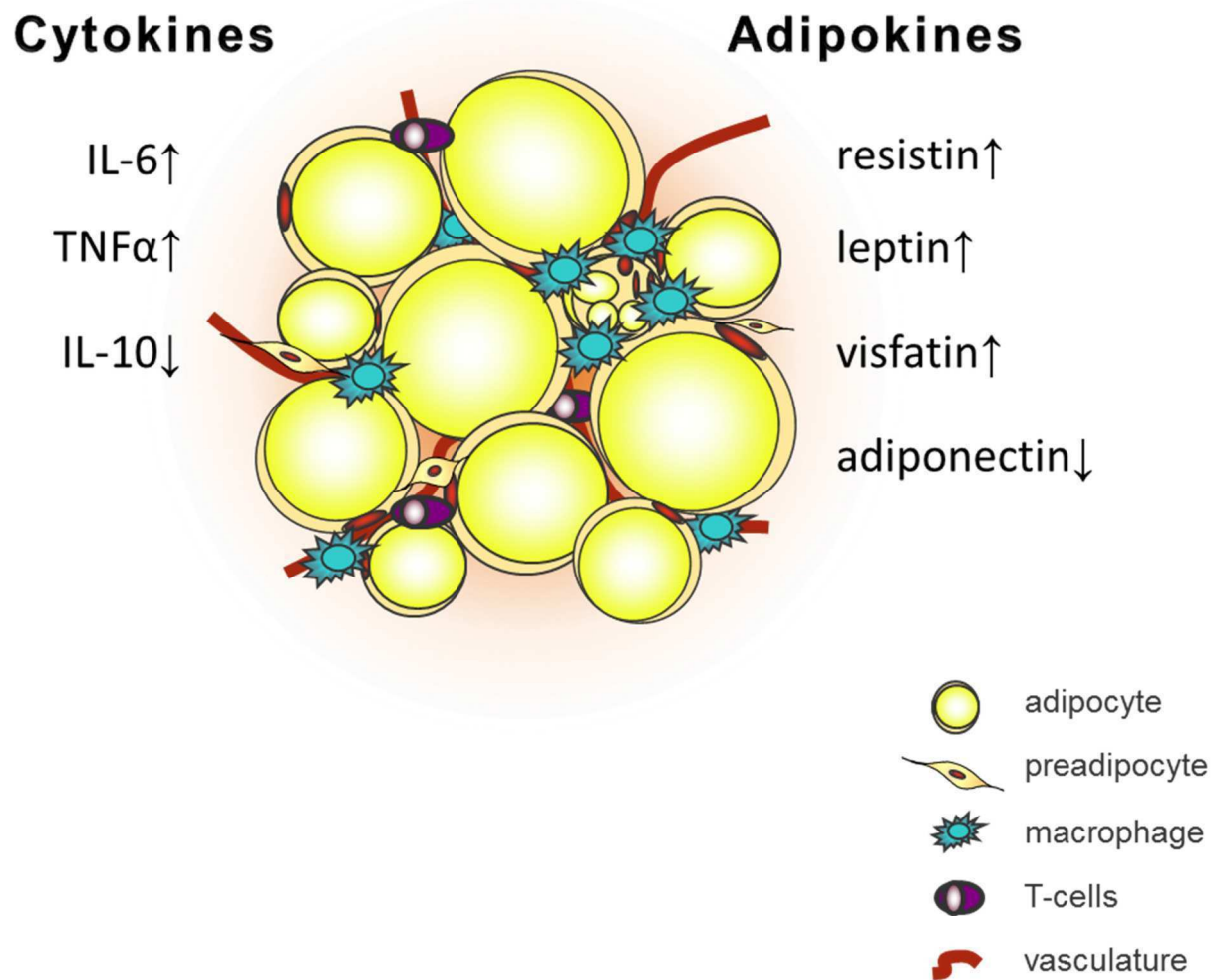


**Fig. I 3: Secretory pattern of WAT in obese subjects (modified from Hauner H.<sup>43</sup>)**

WAT secretes a variety of factors under pathophysiological conditions. Some of these factors are anti-inflammatory and some are pro-inflammatory. IL (interleukin)-6, TNF- $\alpha$  (tumor necrosis factor- $\alpha$ ) and IL-10 are cytokines, which could also be secreted by other cells. Resistin, visfatin, leptin and adiponectin are adipokines in the narrow sense, exclusively secreted by the adipose tissue.

### **Cellular stress signaling**

The balance of protein synthesis and protein folding, which is maintained by a network of molecular pathways including chaperones and proteases plays an essential role in the physiology of all cells. Protein homeostasis is sustained by preventing the aggregation of newly synthesized proteins and promoting the efficiency of folding and assembly.<sup>44</sup> However, protein homeostasis could also be affected by environmental stress situations, such as nutrient excess, hypoxia in the WAT and/or a condition triggered by physiological stress or inflammation. The responses to increased unfolded and misfolded proteins include several signal



transduction pathways. Usually, these pathways are summarized as unfolded protein response(s) (UPRs). Such response pathways could be identified in the cytosol,<sup>45</sup> in the endoplasmic reticulum<sup>46</sup> and also in mitochondria.<sup>47</sup> The major actors in UPRs are chaperones, which assist in folding and prevent aggregation of proteins. Under normal conditions which are characterized by a condition of physiological homeostasis, chaperones of the heat shock protein (HSP) family bind to stress sensor proteins. For this reason the signaling of the UPRs is repressed under normal situations. Upon negative stress situations explained before, chaperones disassociate from the stress sensor proteins and UPRs are activated.<sup>44,46</sup>

### The endoplasmic reticulum and the erUPR

The endoplasmic reticulum (ER) in eukaryotic cells is a specialized cytosolic organelle for protein folding and maturation.<sup>46,48</sup> Surface as well as secreted proteins of various compartments are translocated in an extended, unfolded state through the so called translocon, a protein channel in the ER membrane. Consequently, processes adversely affecting ER-function either by the accumulation of unfolded or misfolded proteins within the ER, increased protein synthesis rates or energy and nutrient fluctuations cause ER-stress.<sup>49,50</sup> These conditions activate conserved signaling pathways known as the UPR in the ER. The erUPR is designed to restore cell homeostasis by increasing the capacity to clear misfolded proteins by increasing ER folding capacity and the up-regulation of the production of ER chaperones.<sup>51</sup> Basically, the erUPR is a signal transduction pathway consisting of three mediators which are located in the ER membrane: 1) The inositol requiring enzyme 1 (IRE-1), 2) the PKR-like ER kinase (PERK), and 3) the activating transcription factor 6 (ATF6). Under normal conditions these three sensors are bound by a chaperone called Grp78 (also known as immunoglobulin heavy chain-binding protein, BIP) and the erUPR is not activated.<sup>49</sup> Unfolded and misfolded proteins in the ER cause dissociation of Grp78 from these mediators. The chaperone assists in protein folding and the IRE-1 and PERK are activated by dimerization.<sup>46</sup> Under stress situations ATF6 move from the ER to the Golgi where it is activated (**Fig. I 4**).<sup>52</sup> Restoration of ER homeostasis and resolution of the stress situation are promoted via the activation of the erURP. Furthermore, the degradation

of unfolded and misfolded proteins is enhanced. This process is called the ER-associated degradation (ERAD). Basis for the ERAD is retro translocation. Misfolded proteins are dislocated from the ER into the cytosol. The valosin-containing protein (VCP) is an ATPase which is essential for this degradation and recruited to ER for this function.<sup>53-56</sup>

The first response to ER stress, activation of IRE-1, leads to splicing of X-box binding protein-1 (XBP-1) mRNA. The expression of ER chaperones and proteins involved in the ERAD are regulated by the spliced form of XBP-1.<sup>57,58</sup> Activation of IRE-1 can also result in the induction of apoptosis and inflammatory signaling. The cytosolic domain of IRE-1 can associate with the adaptor protein TNFR-associated factor (TRAF) 2 to activate the apoptosis signal-regulating kinase (ASK) 1 and cJunN terminal kinase (JNK) pathway.<sup>59,60</sup>

The second response pathway, the PERK pathway, mediates the translational attenuation through phosphorylation of the  $\alpha$  subunit of eukaryotic translation initiation factor (eIF)2.<sup>61</sup> Furthermore, signaling through the PERK pathway leads to an induction of activating transcription factor (ATF) 4 and genes involved in the antioxidant response and the redox control of the ER.<sup>62,63</sup> The pro-apoptotic transcription factor CCAAT/enhancer binding protein (C/EBP) homologous protein (CHOP) could also be induced by the PERK signaling. This results in a negative feedback of eIF2 $\alpha$  phosphorylation.<sup>64</sup>

The third response is via the translocation of ATF6 proteins to the Golgi. There, they are cleaved into active amino-terminal forms, which can regulate ER chaperone expression and bind to promoters containing ER stress elements (ERSE), UPR elements (UPRE) and cAMP response elements (CRE) in the nucleus. Thereby, the transcription of XBP-1 and many other ER UPR genes related to ERAD and protein folding are induced.<sup>65,66</sup>

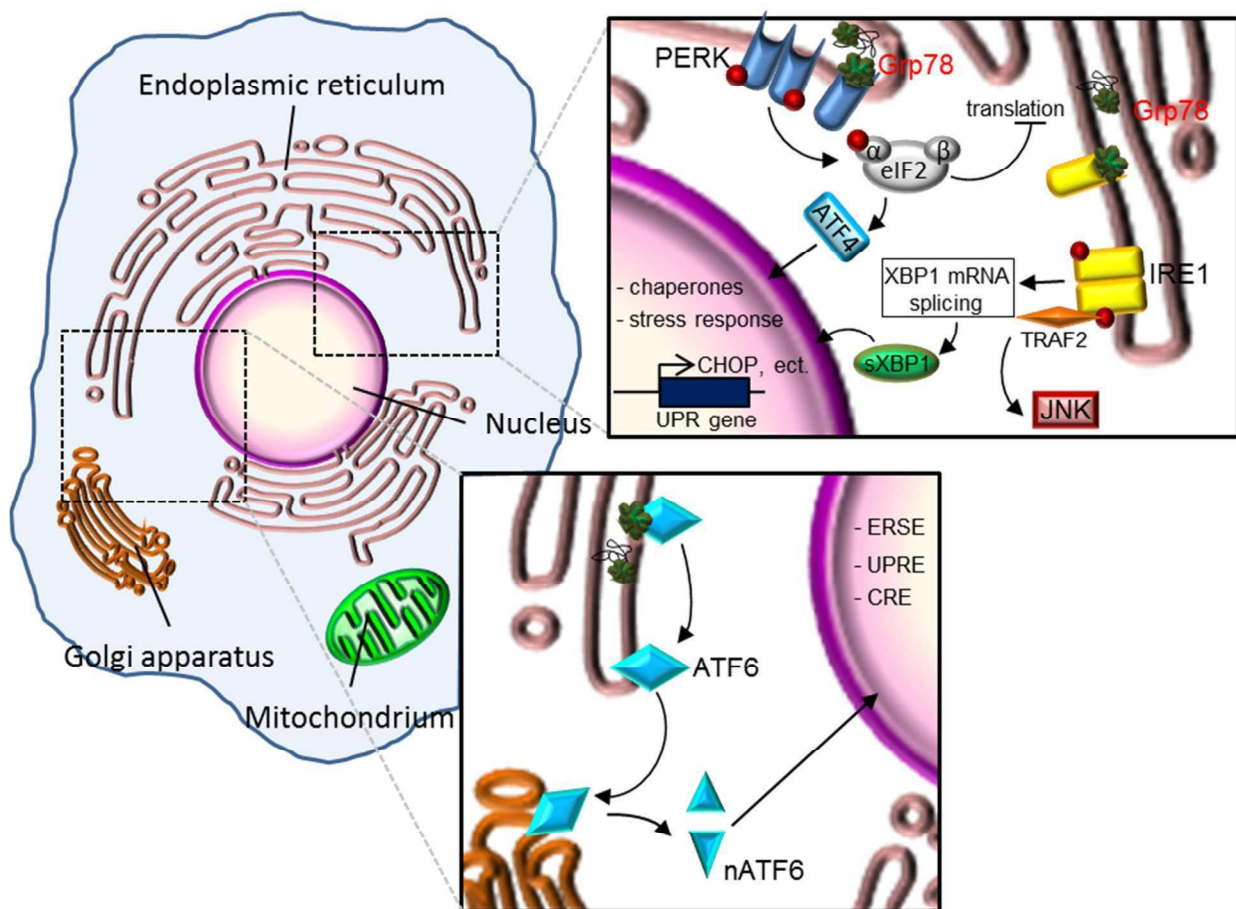


**Fig. 1 4: Schematic view of the endoplasmic reticulum unfolded protein response**

Under stress conditions unfolded and misfolded proteins in the ER result in dissociation of Grp78 from three mediators: IRE-1, PERK, and ATF6. This induces signaling cascades known as the erUPR. The consequence is an activation of kinases, attenuation of global protein translation and recruitment of transcription factors to UPR genes to start the cellular stress responses.

### erUPR and inflammation in obesity

It was speculated from recent data that ER-stress may be relevant to mediate certain pathological conditions, such as inflammation in obesity. Mouse studies have shown that there might be a direct link between ER-stress, obesity and the development of type 2 diabetes. In obese mice models (independent if obesity is dietary or caused by the genetic background) the levels of erUPR proteins are elevated. Furthermore, a suppression of insulin receptor signaling is mediated via IRE-1–dependent activation of JNK and leads to a metabolic dysregulation.<sup>50,67</sup>

Clinical human studies demonstrated that ER-stress might occur as a relevant pathophysiological process in adipose tissue of obese subjects. In adipose tissue of insulin-resistant individuals increased erUPR markers were shown. Weight loss is

able to reverse this situation.<sup>68,69</sup> Currently, an association between ER-stress and inflammation can only be hypothesized. A possible interaction can occur during the UPR through the downstream activation of JNK and the NFκB pathway<sup>70,71</sup> and the production of reactive oxygen species.<sup>72</sup> These mechanisms are considered to play also a central role in obesity-associated inflammation.<sup>73</sup> JNK up-regulates the expression of pro-inflammatory factors like TNFα, MCP-1 and IL-6 which are highly expressed under an obese condition.

However, if ER stress is prolonged during obesity, the erUPR activates pro-apoptotic pathways and the cells die.<sup>74</sup> This seems to be a potential trigger for the recruitment of macrophages into WAT.<sup>75</sup>

### Mitochondria and the mtUPR

Mitochondria are well known to be the “powerhouse” of the cell. In eukaryotic cells the mitochondrion is an organelle with a double membrane.<sup>76</sup> One of the major functions is the production of adenosinotriphosphate (ATP), which is essential for a variety of processes in the cell. Furthermore, mitochondria produce intracellular reactive oxygen species (ROS), store high amounts of calcium (Ca<sup>2+</sup>) and regulate apoptosis.<sup>77-79</sup> The inter-membrane space looks like cristae or long tubules and form inner boundary between the two membranes.<sup>80</sup> Both membranes consist of protein translocases for protein translocation or membrane integration. Two classes of translocases are known: the translocase of the outer mitochondrial membrane (TOM) and the translocase of the mitochondrial inner membrane (TIM).<sup>81,82</sup> The translocation occurs with unfolded proteins which are folded in the matrix of the mitochondria. Therefore the mitochondrial matrix contains a lot of chaperones which assist in folding of imported proteins. Among others, the predominant proteins with chaperone activity are Hsp70 and Hsp60/10 (Chaperonin 60/10).<sup>83,47,84</sup> If the environmental behavior is adversely affecting mitochondrial function, unfolded or misfolded proteins accumulate within the mitochondria. Upon such negative events within the mitochondrial matrix, the transcription of nuclear genes encoding mitochondrial stress proteins is up-regulated. A signaling pathway responding to mitochondrial stress has been described as the mitochondrial UPR (mtUPR).<sup>47</sup> Like the erUPR, the mtUPR is designed to restore cell homeostasis by increasing the capacity to clear misfolded proteins by increasing the production of chaperones.

Compared to erUPR, the mechanisms of the mtUPR are less well understood. There are studies postulating that the Clp protease (caseinolytic peptidase) generates peptides which might be the first signal in the cascade of the mtUPR.<sup>85</sup> This initiation results in an up-regulation of chaperones like chaperonin 60 (Cpn60). The activation occurs mainly through CHOP which is a transcription factor shared by erUPR and mtUPR.<sup>41,47</sup> Furthermore it could be shown that the dsRNA-activated protein kinase (PKR), which is active during mtUPR in intestinal epithelial cells, could link the mtUPR to the erUPR via the phosphorylation of eIF2 $\alpha$ .<sup>86</sup>

The first indication of mtUPR was given by Martinus *et al.*. In this study the deletion of mitochondrial DNA (mtDNA) induced a stress response and resulted in higher transcription of Cpn60 and Cpn10.<sup>87</sup> Furthermore, it was shown that a truncated form of the ornithine transcarbamylase (OTC $\Delta$ ), which accumulates in the mitochondrial matrix increases the expression of Cpn60, Cpn10 and also ClpP. Surprisingly, chaperones involved in the erUPR were unaffected.<sup>47</sup> The mtUPR results in an activation of the transcription factor CHOP. It could be shown that the CHOP element was required for the mtUPR as target genes have a corresponding binding region in their promoter. As CHOP transcription could also be activated in response to the erUPR, this leads to the assumption that CHOP can be induced separately in response to two different stress response pathways (**Fig. I 5**).<sup>88,41,89</sup>

### *Mitochondrial dysfunction in obesity*

Adipose tissue plays a central role in obesity as it acts as an endocrine organ and releases a lot of adipokines and cytokines. The levels of adiponectin in both, plasma and adipose tissue, were significantly lowered in obese mice. This finding was associated with a reduction of mitochondrial content and function in adipose tissue. This impaired mitochondrial function could also activate erUPR via JNK activation and the induction of ATF3.<sup>90</sup> It could also be shown that the mitochondrial function in adipose tissue (especially in BAT) is required for an adaptive thermogenesis, energy balance and body weight. As further studies have demonstrated that adult humans possess active BAT, mitochondrial dysfunction in this tissue was linked to impaired thermogenesis and disturbed energy expenditure. Therefore it leads to the development of obesity.<sup>91-93</sup>

Due to negative environmental factors, like high nutrient excess, changes of protein expression and the mtUPR signaling could be explained by metabolic dysregulation.<sup>89</sup> Animal experiments have shown that Cpn60 expression was significantly suppressed in rats under a high fat diet. Furthermore, the expression level of cytochrome c, peroxisome proliferator-activated receptor- $\gamma$  coactivator-1 $\alpha$  (PGC-1 $\alpha$ ) and the copy number of mtDNA was decreased. This is accompanied by impaired glucose tolerance.<sup>94</sup> A clinical human study could also show, that lower blood Cpn60 level were associated with an increased risk of type 2 diabetes.<sup>95</sup> Furthermore, mitochondrial stress and/or impairment of the mtUPR were also described to be involved in neurological diseases and sporadic diseases of aging.<sup>96,44</sup>

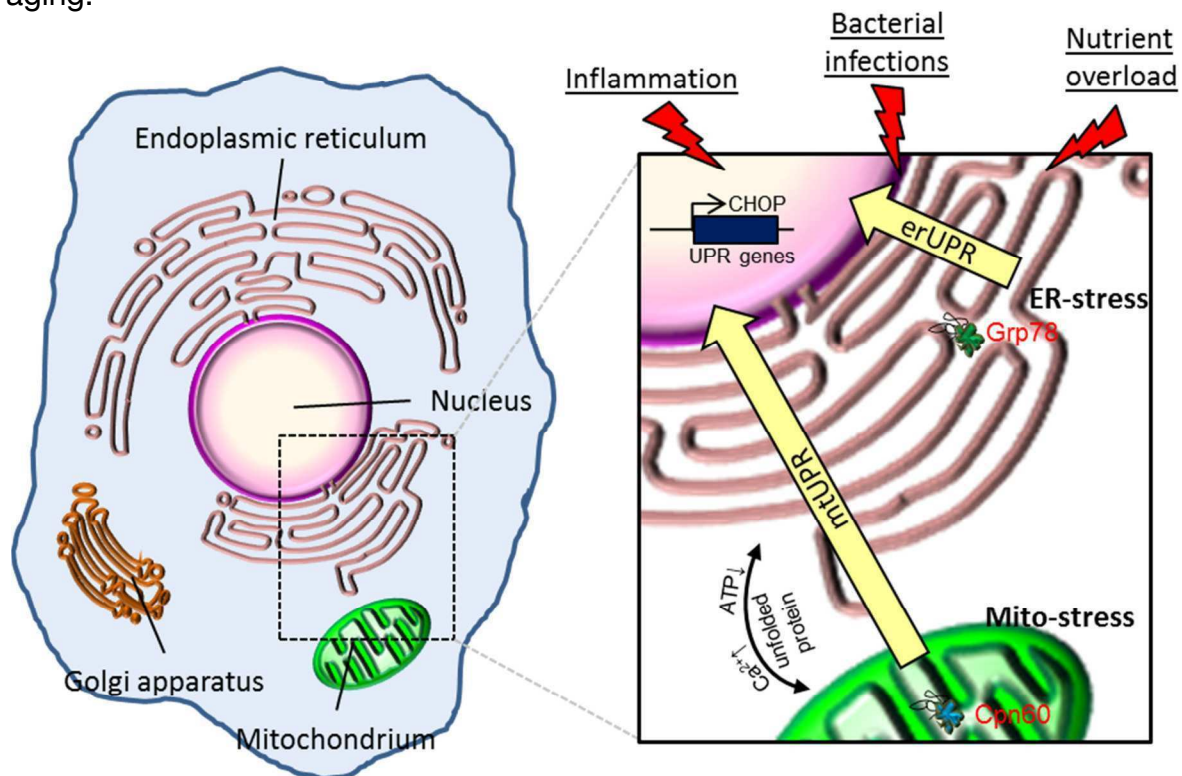


**Fig. I 5: Interaction of the ER and the mitochondria under harmful environmental stress**

Stress responses mediated by nutrient overload, inflammation and/or bacteria. Harmful environmental stresses increase unfolded and misfolded proteins in the mitochondrial matrix and the ER. This results in the activation of the mtUPR and/or erUPR, respectively. There seems to be a direct cross-talk between mitochondria and ER during stress.

## ***High fat diet and animal models***

As obesity is a condition increasing worldwide, intensive research is carried out in this area, especially in animals. Rodents are often used as models for obesity. The advantages for rodent models are the shorter generation times, easy breeding, lower cost and the similarities between rodent and human genetics.<sup>97</sup> There are models available for genetic-induced and diet-induced obese mice. A high fat diet (HFD) is often used as a model, with no genetic mutation. For HFD-induced obesity the C57BL/6J mice are often used, as they show close similarity to humans. For example, they exhibit abnormalities comparable to the metabolic syndrome in humans.<sup>98,99</sup> Using such HFD-induced obesity mice models is beneficial because manipulation of diet may rescue the obese phenotype. Furthermore, crossing of mice with genetically mutated mice, can provide information if the gene of interest is associated with obesity or not.<sup>100</sup>

### *Grp78<sup>+/-</sup> mice and Cpn60<sup>+/-</sup> mice*

The ER chaperone Grp78 is increased in obesity and has a distinct influence on the development of obesity related complications. Therefore, a mouse with targeted mutation of the Grp78 allele was created. The homozygous Grp78<sup>-/-</sup> mouse is embryonically lethal. Thus a Grp78<sup>+/-</sup> mice model was created and is viable and fertile.<sup>101</sup> Furthermore, it was shown that Grp78 heterozygosity attenuates HFD-induced obesity, prevents white adipose tissue inflammation and hyperinsulinemia and promotes adaptive UPR. An improving ER quality control, folding capacity and insulin signaling upon ER stress is the consequence.<sup>102</sup>

In view of the mtUPR the chaperone Cpn60 is interesting, as it was significantly suppressed in rats under high fat diet. The same results were shown in adipose tissue of ob/ob and db/db mice, both models for obesity.<sup>103,104</sup> A mouse model was established based on the findings, that a positive association of circulating Hsp60 concentrations with BMI, leptin, HOMA-IR, and blood pressure was shown.<sup>105</sup> The Cpn60<sup>-/-</sup> mice are embryo lethal.<sup>106</sup> Therefore, the Cpn60<sup>+/-</sup> mice was created (see dissertation of E. Berger, Biofunctionality, Munich, Germany). These mice model has a conditional knock out of the heat shock protein 1 (chaperonin) which is located on mouse chromosome 1.





## **Aim of the work**

As outlined before, obesity has negative effects on the development of various diseases. Clinical and experimental studies in obesity revealed that the erUPR may be relevant to mediate certain pathologic conditions like inflammation. The mtUPR signaling could also be explained by metabolic disorders. Whereas the correlation of UPR signaling and diseases like obesity and/or T2D was hypothesized, the underlying mechanisms are still unclear. There is little known, about the development of UPR during adipogenesis (a process, which is strongly related to the development of obesity), and how the development of obesity is influenced by the UPR signaling.

Hence, we want to investigate whether adipogenesis is a process which induces UPR or not. Therefore markers of the erUPR and the mtUPR were determined in murine 3T3-L1 cells, human SGBS cells, primary isolated human preadipocytes and also in adipose tissue of C57BL/6N mice of different ages.

Furthermore we want to understand, how the erUPR and the mtUPR influence the development of obesity. Thus the effect of high fat diet on the development of obesity was investigated in two different mouse models. For the understanding of erUPR and its influence on metabolic processes the Grp78<sup>+/-</sup> mice were used. On the other hand the Cpn60<sup>+/-</sup> mouse model was used to investigate the influence of the mtUPR on the development of obesity.



## **Material and Methods**

### ***Cell culture***

#### **3T3-L1 cell culture**

The mouse preadipocyte cell line 3T3-L1 (passage 4-20) (ATCC-Nr.: CL-173, ATCC, Wesel, Germany) were cultured as described previously<sup>107</sup> in a humidified 5% CO<sub>2</sub> atmosphere at 37°C. Cells were grown in 6, 12 or 24 well culture plates (Biochrom AG, Berlin, Germany). To obtain differentiated adipocytes, Dulbecco's modified Eagle's medium (Invitrogen, Darmstadt, Germany) containing 10% fetal calf serum (FCS) (PAA Laboratories GmbH, Pasching, Austria) and 1% penicillin and streptomycin (pen-strep) (Invitrogen, Darmstadt, Germany) was supplemented with 250 [nmol/l] dexamethasone (SigmaAldrich, Taufkirchen, Germany), 0.5 [mmol/l] isobutyl-methylxanthine (IBMX) (SERVA Electrophoresis GmbH, Heidelberg, Germany) and 66 [nmol/l] insulin (SigmaAldrich) to 80% confluent preadipocytes for the first 3 days. After induction, the medium of cells were replaced with Dulbecco's modified Eagle's medium containing 10% FCS and 1% pen-strep supplemented with 66 nmol/l insulin. The medium was refreshed twice weekly for additional 15 days.

#### **SGBS cell culture**

The primary human preadipocyte cell line SGBS (passage 2-7)<sup>108</sup> were cultured in a humidified 5% CO<sub>2</sub> atmosphere at 37°C. The cells were grown in T25 cell culture flasks or 6 well culture plates (BD Falcon, Heidelberg, Germany). Until confluence the cells were cultured in proliferation medium (PM) which is composed of Dulbecco's modified Eagle's medium-Ham's F-12 (1:1, vol/vol) (Invitrogen, Darmstadt, Germany) containing 10 FCS (Gibco-Invitrogen, FischerScientific, Germany), 33 µM biotin (Firma), 17 µM pantothenate (SigmaAldrich, Taufkirchen, Germany) and 1 pen-strep (Invitrogen, Darmstadt, Germany). To promote adipose differentiation the cells were induced with feeding medium (FM) (mixture of PM and MCDB-131 (Invitrogen, Darmstadt, Germany), 66 nM insulin, 1 nM triiodothyronine (SigmaAldrich), 10 [µg/ml] human transferrin (SigmaAldrich), and 0.1 µM cortisol

## Material and Methods

(SigmaAldrich) supplemented with the adipogenic inducers of differentiation IBMX (0.5 mM), dexamethasone (25 nM), and rosiglitazone (2  $\mu$ M) (Enzo Life Sciences, Lörrach, Germany). After 4 days of induction, the medium was replaced by FM, and the cells were fed twice weekly for a total culture time of 12 days.

### Primary human preadipocytes cell culture

Primary human preadipocytes were isolated as described previously.<sup>109</sup> A final concentration of 240,000 cells per 6-well plate was cultured in proliferation medium (DMEM/HamF12 (1:1 vol/vol), 6.6 mM Biotin, 17 mM pantothenate, 1% pen-strep, 2.5% FCS , 10 [mg/ml] insulin, 100 [ $\mu$ g/ml] EGF, 25 [ $\mu$ g/ml] FGF). To promote differentiation the cells were induced with induction medium (DMEM/HamF12 (1:1 vol/vol), 6.6 mM Biotin, 17 mM pantothenate and 1% pen-strep, 10 [mg/ml] insulin, 2  $\mu$ M T3, 0.1 mM cortisol and 1 [mg/ml] transferrin, 2 mM rosiglitazone, 25  $\mu$ M dexamethasone, 20 mM IBMX). After 3 days medium was changed to differentiation medium (DMEM/HamF12 (1:1 vol/vol), 6.6 mM Biotin, 17 mM pantothenate, 1% pen-strep, 10 [mg/ml] insulin, 2  $\mu$ M T3, 0.1 mM cortisol, 1 [mg/ml] transferrin) which was refreshed twice a week for additional 16 days.

## **Patients**

### Isolation of primary human preadipocytes

Subcutaneous adipose tissue was obtained from lipectomy or body-lift surgeries. Patients consent was obtained beforehand and the ethical committee of the Technical University Munich approved the protocol. The tissue samples were transported immediately from the operation room to the laboratory in DMEM:F12 medium containing 1% pen-strep. Primary human adipocytes were prepared as described previously.<sup>110</sup> Primary human preadipocytes were isolated according to van Harmelen et al. 2003.<sup>109</sup> For preadipocyte isolation the tissue samples from surgery were freed from connective tissue and visible blood vessels and minced with scissors. Minced samples were digested in Krebs-Ringer-Phosphate buffer (KRP, pH7.4) containing 200 [U/ml] collagenase (Biochrom, Berlin, Germany) and 4% BSA (Sigma, Munich, Germany) for 60 min at 37°C in a shaking water bath (>60 beats/min). Afterwards the samples were centrifuged for 10 min at 300 g and the supernatant was discarded. The residual pellet was suspended in erythrocyte lysis buffer and incubated at room temperature for 10 min. Afterwards the suspension was filtered through a nylon mesh with a pore size of 250 µm and through a cell strainer with 70 µm pore size. After a second centrifugation step for 10 min at 300 g the pellet was suspended in culture medium. The cells were plated out to T75 culture plates. On the first day of culture the medium was changed to PM4-Medium (DMEM/HamF12 (1:1 vol/vol), 6.6 mM Biotin, 17 mM pantothenate, 1% pen-strep, 2.5% FCS, 10 [mg/ml] insulin, 100 [µg/ml] EGF, 25 [µg/ml] FGF).

### Isolation of primary human adipocytes

For the isolation of primary human adipocytes the procedure was the same like for preadipocytes until the collagenase step. For adipocytes the minced samples were digested in Krebs-Ringer-Phosphate buffer (KRP, pH7.4) containing only 100 [U/ml] collagenase (Biochrom, Berlin, Germany) and 4% BSA (Sigma, Munich, Germany) for 60-90 min at 37°C in shaking water bath (60 beats/min). Afterwards the cells were first filtered through a nylon mesh with 2,000 µm pore size followed by a filtration through a nylon mesh with a pore size of 250 µm. Floating cells were washed three times with KRP supplemented with 0.1% BSA. Total fraction was

## Material and Methods

either incubated in DMEM:F12 medium with 1% pen-strep or used for further fractionation by cell size.<sup>36</sup> To reduce the cell stress level medium was changed after 30 min. To determine mean adipocyte diameter a total of 100 fat cells from the total fraction as well as from every fraction were determined by light microscopy to calculate fat cell weight and volume.

### Fractionation of human adipocytes

Isolated adipocytes (see above) were fractionated into a fraction I with small cells and a fraction IV with large cells, according to Skurk et al. 2007.<sup>36</sup> Thereby the floating properties of the cells were used. After filling a separation funnel with 50 ml KRP supplemented with 0.1% BSA and adding 20 ml cells the whole separation funnel was gently mixed. Afterwards the cells float for a distinct time (fraction I: collection of 30 ml cell suspension after 45 s). After the procedure for fraction I was repeated until no cells could be collected anymore cells with an intermediate size were discard after 15 s of floating. Fraction IV was defined as the remaining cells in the separation funnel. Ensure that after each step the separation funnel was filled again with KRP supplemented with 0.1% BSA.

## **Animals**

### Experimental setup

Conventionally raised Grp78<sup>+/-</sup> mice (generous gift from Amy Lee)<sup>101</sup> and Cpn60<sup>+/-</sup> mice (Institute of Biofunctionality, Munich, Germany) on C57BL/6 background as well as their wild type littermates were fed a high fat diet (Ssniff S5745-E722, Ssniff, Soest, Germany) for 8 weeks after a weaning period of 4 weeks. Mice fed a conventional diet (Ssniff S5745-E720, Ssniff, Soest, Germany) were used as controls. During the feeding period weight development, as well as body mass composition was measured. Food intake was analyzed by daily food mass measurement for 5 successive days during the fourth week of the HFD regimen. Mice were killed at age of 12 weeks. Animal use was approved by the institution in charge (approval no. 55.2-1-54-2531-130-09).

### Genotyping of the mouse

For genotyping the DNA was extracted from the tail tip. After cutting a piece of tail from the mouse, it was digested overnight in 190 µl tail-buffer (see Buffer and Solutions) complemented with 10 µl Proteinase K (10 mg/ml) at 65°C. To stop proteinase K activity the tails were incubated 10 min at 95°C. Now a PCR was performed.

#### Tail-buffer

242.3 mg Tris

Add H<sub>2</sub>O until 160 ml → pH 8.3

745.6 mg KCl (50 mM)

900 µl Nonidet P40

900 µl Tween 20 (0.45%)

20 g Gelatine

→ dissolve at 70°C

Polymerase chain reaction (PCR) for genotyping

Polymerase chain reaction (PCR) attends to amplify specific DNA sequences by using unique primers and an adequate temperature program. A PCR master mix which contains primers, polymerase and nucleotides is added to the DNA sample and placed in a thermocycler. Therein the sample undergoes a cyclic temperature program that is specific for the following steps: denaturation of the DNA double helix into single strands, annealing of the primers and elongation of the single strands to double strands.

Primer sequences were the following:

Grp78\_for 5'-gtt-gat-att-gga-ggt-ggg-cao-acc-aag-3'  
Grp78\_rev 5'-ttg-tta-ggg-gtc-gtt-cac-cta-ga-3'  
Cpn60\_for 5'-acc-aag-acc-ctg-tac-tct-taa-cc-3'  
Cpn60\_rev 5'-agt-cct-atg-gga-ctg-gat-gg-3'  
Control\_for 5'-gag-act-ctg-gct-act-cat-cc-3'  
Control\_rev 5'-cct-tca-gca-aga-gct-ggg-gac-3'

**Table M 1: Standard-PCR-MasterMix (for the Phire HotStart DNA Polymerase)**

Volume	Reagent	Concentration
4 µl	5x Phire buffer	1x
0.4 µl	dNTPs (10mM)	200 µM
1 µl	Grp78_for (Primer forward)	500 nM
1 µl	Grp78_rev (Primer reverse)	500 nM
0.5 µl	Control_for (Primer forward)	250 nM
0.5 µl	Control_rev (Primer reverse)	250 nM
0.2 µl	Phire polymerase	1 U
11.4 µl	PCR H <sub>2</sub> O	
1 µl	DNA	

Using this protocol the genotyping for the Grp78<sup>+/-</sup> mice was performed. Therefore a special PCR program was used.



98°C	30 sec		
98°C	5 sec	}	35 x
65°C	5 sec		
72°C	15 sec		
72°C	60 sec		

Afterwards, the PCR products were subjected to electrophoresis on 1% agarose gels to determine amplicon specificity.

**Table M 2: Standard-PCR-MasterMix (for the Taq DNA polymerase)**

Volume	Reagent	Final concentration
5 µl	5x Phire Buffer	1x
0.5 µl	dNTPs (10mM)	200 µM
1.5 µl	MgCl <sub>2</sub>	1.5 mM
0.5 µl	Cpn60_for (Primer forward)	500 nM
0.5 µl	Cpn60_rev (Primer reverse)	500 nM
0.5 µl	Control_for (Primer forward)	250 nM
0.5 µl	Control_rev (Primer reverse)	250 nM
0.125 µl	Taq Polymerase	0.625 U
14.9 µl	PCR H <sub>2</sub> O	
1 µl	DNA	

Using this protocol the genotyping for the Cpn60<sup>+/-</sup> mice was performed. The special PCR program for the Cpn60<sup>+/-</sup> mice genotyping was:

95°C	60 sec		
95°C	30 sec	}	35 x
60°C	20 sec		
68°C	45 sec		
68°C	5 min		

Afterwards the PCR products were subjected to electrophoresis on 1% agarose gels to determine amplicon specificity.

## Material and Methods

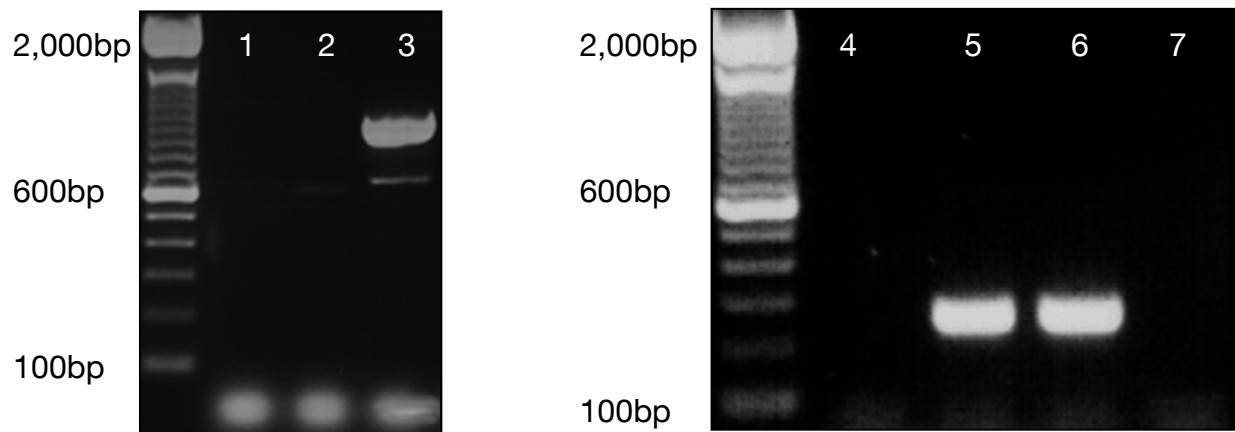


**Fig. M 1: Electrophoresis of the PCR products. The bands show the specific amplicons: 1+4- H<sub>2</sub>O control; 2-control band (~600bp); 3-Grp78<sup>+/-</sup> band (~900bp); 5+6-Cpn60<sup>+/-</sup> band (~400bp); 7-control band. The wt band is ~2,400bp and not visible.**

## Housing

Mice were housed under special pathogen free conditions in Makrolon cages (Tecniplast green line, type II long, 540 cm<sup>2</sup>) with sawdust straw and nesting material. Animals were kept on a 12 h light/dark cycle with a constant room temperature of 22 ± 1 C and a humidity of 55%. Cages were changed weekly. Food (ssniff®, M-Z autoclavable) and water were available *ad libitum*.

## Diets

For the feeding experiment the mice get a control diet and a high fat diet from SNIFF. The composition of the diets only differs in the fat content.

Table M 3: Composition of the different diets

Article Number (Ssniff)	Composition (%)	
	S5745-E720	S5745-E722
Category	Control	High-fat
Pellet size	10 mm	10 mm
$\gamma$ -radiation	25 kGy	25 kGy
ME Atwater (MJ/kg)	15,5	19,7
Protein	23	18
Fat	12	48
Carbohydrate	65	34
Protein	20,8	20,8
Fat	5,1	25,1
Fiber	5	5
Ashes	5,6	5,6
N-free extracts	60,1	40,6
Casein	24	24
Corn starch	47,8	27,8
Maltodextrin	5,6	5,6
Sucrose	5	5
Cellulose	5	5
Vitamin-Premix	1,20	1,20
Minerals/Trace	6	6
Soybean oil	5	5
Palm oil	-	20
EPAX 1050-TG	-	-
Palmitate C16:0 (mol%)	11,90	37,96
Stearate C18:0 (mol%)	2,91	3,85
Oleate C18:1 (mol%)	22,76	34,60
Linoleate C18:2 (mol%)	52,99	18,23
Linolenate C18:3 (mol%)	5,97	1,30
Arachidonate C20:4	-	-
EPA C20:5 (mol%)	-	-
DHA C22:6 (mol%)	-	-
Ratio n6/n3	8,88	13,97
Choline-Chloride	0,2	0,2
Butylhydroxytoluene	150	150
Tocopherol-Acetate	180	180

### Minispec NMR analysis

To determine the body composition of the mice a minispec TD-NMR analyzer (Bruker Optics; LF500H) was used. The mice were measured before, after 4 weeks and after 8 weeks (before sacrificing) of feeding. Therefore, the mice were placed in a red Plexiglas tube with vent holes, to restrain their mobility. The tube was inserted in the minispec for 3 minutes of measurement (figure 8). As the analysis based on the nuclear magnetic resonance (NMR) of the hydrogen atomic nuclei, the resonance absorption depends on the chemical environment and varies between different tissues. For this reason the minispec can distinguish lean mass and fat mass and calculate their amount.

### Indirect calorimetric measurement

The male mice were put in an open respirometric system (TSE; PhenoMaster, type I cages with 180 cm<sup>2</sup>) for at least 3 days. The normal 12 h light/dark cycle was kept in the system and food and water were available *ad libitum*. The principle of the indirect calorimetry is the measurement of O<sub>2</sub> consumption and CO<sub>2</sub> production over a time period to calculate the energy expenditure of the single mouse. Therefore, the normal Makrolon cages were connected to fresh air and the gas exchange was measured by a complex machine and the content of O<sub>2</sub> and CO<sub>2</sub> is quantified by an analyzer. The values of the gas content were calculated against a reference cage without a mouse.

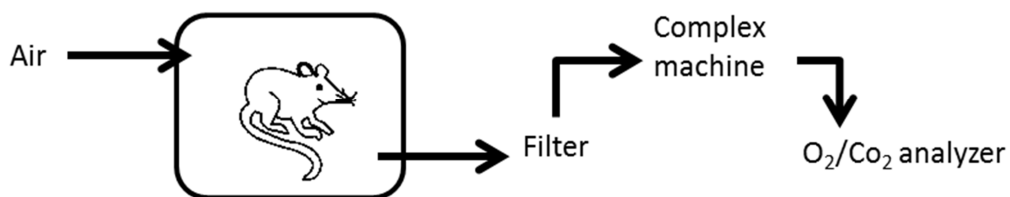


**Fig. M 2: Schema of the indirect calorimetry. A pump samples the air from the cage. O<sub>2</sub> consumption and CO<sub>2</sub> production is analyzed.**

### IP-GTT

After fastening the mice for 6 hours the weight of each mouse was determined for dose calculation of the 20% glucose solution. Cut a piece of the tail and measure the basal level of glucose in the blood with glucometer (0 min). Now the glucose solution was injected immediately intraperitoneally and after 15, 30, 60 and 120 min the glucose level of the blood was measured.



**Fig. M 3:** Intraperitoneal glucose injection. **The mouse was fixed in the neck and the glucose was injected between the papilla of the breast and the knee.**

### Sacrificing and sample collection

After fasting mice for 6 hours they were sacrificed in CO<sub>2</sub>. Dead was controlled by checking reflex stimulation. From killed animal's blood, the whole intestine, liver, kidney, spleen, muscle and the epididymal fat depot was collected. The blood was immediately centrifuged and plasma was frozen in liquid nitrogen. The other organs were frozen in liquid nitrogen.

### Bomb-calorimetric measurement

To determine the energy which is assimilated in the gut the following formula was used.

$$E_{\text{ass}} = E_{\text{in}} - E_{\text{feces}}$$

## Material and Methods

$E_{in}$  is the energy which enter the mice (food uptake per day x energy of the food) and  $E_{feces}$  is the energy of the feces (feces per day x energy of the feces). To measure this energy a bomb calorimeter with a direct calorimetric was used. Thereby, the samples were combusted under high pressure and with a surplus of oxygen. The heat will be absorbed and  $\Delta T$  will be measured. The measurement gives the heating value (J/g) of the sample.

For the combustion feces as well as food samples were dried at 60°C for 72 h. To ensure homogeneity of the samples, they were grinded with a bebble mill. Afterwards 1g of the sample was compressed to a pellet. The exact weight was type to the calorimeter and the measurement starts.

### Paraffin embedding

After sacrificing sample tissue was collected. A small piece of tissue was immediately fixed in 4% neutral buffered formalin (Sigma Aldrich, Steinheim, Germany). After 24 h the tissue was overlaid with 70% ethanol until the paraffin embedding.

### Hematoxylin-Eosin (HE)-staining

Tissue samples embedded in paraffin were cut into slices with a thickness of 5  $\mu$ m and were dried overnight. Immediately before staining slides were incubated for 10 min at 60°C. The staining was carried out automatically (Leica ST5020 staining machine) with 16 different steps. After removing of the paraffin, Hemalaun is responsible for nuclear staining and Eosin stains the surrounding tissue. The slides were then covered and pictures were taken with a bright field microscope.

**Table M 4: HE staining protocol**

<b>Step</b>	<b>Reagent</b>	<b>Period [min]</b>	<b>Step</b>	<b>Reagent</b>	<b>Period [min]</b>
<b>1</b>	Xylol	3	<b>9</b>	Eosin	2
<b>2</b>	Xylol	3	<b>10</b>	Ethanol 70%	1
<b>3</b>	Ethanol 100%	2	<b>11</b>	Ethanol 80%	1
<b>4</b>	Ethanol 96%	2	<b>12</b>	Ethanol 100%	1
<b>5</b>	Ethanol 70%	1	<b>13</b>	Ethanol 100%	1.5
<b>6</b>	Water	1	<b>14</b>	Xylol/alcohol	1.5
<b>7</b>	Hemalaun	4	<b>15</b>	Xylol	2
<b>8</b>	Water	2	<b>16</b>	Xylol	2

## ***Adipocyte differentiation, fat storage and adipocyte size***

### *GPDH (glycerol-3-phosphate dehydrogenase) measurements*

GPDH-activity was performed by an enzymatic kinetically assay according to an established protocol as described previously <sup>111</sup>. For the measurement of the protein content of the cultures, trichloroacetic acid precipitation was used to avoid lipid interference, according to a modification of the method of Lowry, 1951.<sup>112</sup>

### *DAPI Staining*

Because of its specific binding to the minor groove of DNA, 4', 6-Diamindin-2-phenylindol (DAPI) is especially suitable for visualizing nuclei. Blue fluorescent complexes can be detected at a wavelength of 340 nm.

Cells were washed with PBS and ice-cold methanol was given to each well for 10 min at 4°C to fix the cells at the bottom of the plate. After fixation cells were washed twice with PBS and 400 µl blocking solution (10% goat serum in PBS) was added for 30 min at room temperature. After washing with PBS three times, 200 µl of DAPI working solution was added for 5 minutes in the dark. Cells were then washed twice with PBS. 1 ml PBS was left to prevent cells from drying.

### *Oil-Red-O staining in cell culture*

For Oil-Red-O staining of lipid droplets the cells were first washed with PBS (Biochrom AG, Berlin, Germany) and fixed with 3.7% formaldehyde (Carl Roth GmbH, Karlsruhe, Germany) for 1 h. After fixation each well was rinsed with PBS and stained with Oil-Red-O working solution for 1 h. After staining the cells were overlay with 87% glycerol (Merck, Darmstadt, Germany) or water and stored at 4°C.

#### Oil-Red-O

##### *Stock solution:*

0.5 g Oil Red O  
(SigmaAldrich)  
100ml 99% isopropanol  
(Carl Roth GmbH)

##### *Working Solution:*

3 parts stock solution  
2 parts DI water  
→ filter working solution

Oil-Red-O staining of liver

The Oil-Red-O staining could be used for staining of neutral lipids (e.g. triglycerides). For this staining only cryosections are possible, as paraffin replaces the lipids. Therefore also formalin-fixed tissue embedded in O.C.T. (for Optimal Cutting Temperature) afterwards can be used. For staining the cryosections were fixed 1 h on glass slides in 10% formalin. Afterwards the slides were rinsed one time with tap water, two times with dH<sub>2</sub>O and one time with 60% isopropanol. The staining with Oil-Red-O working solution for 1 h followed. After rinsing the slides one time with 60% isopropanol they were counterstained with hematoxylin for 1 min. At the end the slides were rinsed well with tap water and mounted in pre-warmed glycerin jelly.

Determination of adipocyte size in adipose tissue

The adipocyte size was determined using the software ImageJ and Adobe® Photoshop®. The pictures of HE stained adipose tissue were opened in ImageJ. There the green channel (grey value) was used for further processes (Image→colour→split channel). The so called grey valued picture was opened in Photoshop settings for the best graduation curve were saved and used for all grey valued pictures. The saved picture was then open in ImageJ again and a specific threshold was adjusted (Image→adjust→threshold→apply). Afterward the noise was removed (Process→noise→remove outliers) and the picture was saved. This “threshold-inverted” picture was now opened in Photoshop again and the borders of adipocytes were drawn with the line tool until adipocytes are fully closed. The last step in the process for determination of adipocyte size was the measurement. Therefore the image was opened in ImageJ. The picture should have the exact scale (setting with line the same size like the scale bar, clicking Analyse→set scale→know distance→Unit (µm)) settings accepted. Afterwards, as a readout the area and the perimeter should be set (Analyse→set measurements→area, perimeter). Now to measure the cells the *wand tool* was used and immediately after clicking on the cells an extra sheet with the area and the perimeter pops up. This could be saved as an excel sheet for further evaluation.



### Triglyceride measurement in plasma samples

The triglyceride measurement was performed with plasma samples of the mice using triglycerides liquicolor<sup>mono</sup> (HUMAN, Wiesbaden, Germany) according to manufacturer's instructions.

### Triglyceride measurement in liver tissue

After isolation the liver have to be well prepared for the triglyceride measurement. Therefore, fresh or frozen tissue was homogenized with a tube pestle and 500 µl of 0.9% NaCl was added. Afterwards the solution was incubated for 10 min at RT shaking with 450 rpm. To extract triglycerides 200 µl of the homogenate were mixed with 500 µl of a 0.5 M ethanolic KOH. This mixture was incubated for 30 min at 71°C shaking with 450 rpm. The last step was adding 1 ml of 0.15 M MgSO<sub>4</sub> to the solution and vortex before centrifuging it for 10 min at 13,000 g. The measurement was the same like in plasma samples (see there). For the calculation not only the dilution factor but also the protein content should be included.

## **ELISA**

### Adipokine-ELISA

Adiponectin, leptin and IL-6 (murine/human) concentrations in cell culture supernatants were determined using the appropriate ELISA kits (R&D Europe, Abington, UK) according to the manufacturer's instructions.

### Insulin-ELISA

Insulin levels in the murine plasma were determined using an Ultra-Sensitive Mouse Insulin ELISA Kit (Crystal Chem Inc., Cat-No.:#90080, Downers Grove, IL, USA) according to the manufacturer's instructions.

## **Protein expression**

### Protein isolation (cell culture)

Cells were washed twice with ice-cold PBS. RIPA lysis buffer (50 mM Tris-HCl pH 8, 150 mM NaCl, 1% NP-40, 0.5% sodium deoxycholate, 0.2% SDS) containing protease inhibitors and 1 mM phenylmethylsulfonylfluorid (PMSF) was added to the cells. The cells were then scraped off and disaggregated with an insulin syringe. After centrifugation at 10,000 g at 4°C for 10 min the supernatant was immediately frozen at –80°C until analysis.

### Protein isolation (tissue samples)

After preparation small tissue pieces (10-50mg) were immediately frozen in liquid nitrogen. For protein isolation the tissue was crushed with a tube mortar on ice and 150-200 µl RIPA lysis buffer were added to the powder. The suspension was vortexed and an incubation for at least 30 min on ice followed. After this the suspension was vortexed again. After centrifugation at 10,000 g at 4°C for 10 min the supernatant was immediately frozen at –80°C until analysis.

### Bicinchoninic acid (BCA) method

The protein content was determined using BCA Protein Assay Kit including BSA protein standard (Thermo Fischer Scientific, Bonn, Germany). We performed the assay according to the manufacturer's instructions.

### Western blot

Protein isolated from cell culture or tissue samples (see protein isolation) were add to Laemmli buffer (TrisCl (12.5 ml), 10% SDS (8 ml), glycerol (7.9 g), DTT (7.7 mg), bromphenol (0.5%) (1.25 ml), H<sub>2</sub>O (50 ml)) and was denatured (95°C, 10 min). 20 µg of protein were subjected to 10%-15% (v/v)-acrylamide gels depending on the molecular weight of the protein of interest.

Sodium-dodecyl-sulfate polyacrylamide gel electrophoresis (SDS-PAGE) was performed at 15 mA until the bromophenol blue dye reached the bottom of the gel. Proteins were blotted on PVDF membranes (ZEFA-Laborservice, Harthausen, Germany) and the presence of proteins on the membrane was detected by staining with 0.5% (w/v) Ponceau S in 1% (v/v) acetic acid for 1 min. After blocking the

membrane for 1 h with a blocking solution containing 5% dry milk in TBST the membranes were incubate for 1 h at RT or overnight at 4°C with the primary antibody for the protein of interest. The membranes were washed 3 times for 10 min with TBST and then the secondary antibody was incubated for 1 h. After binding of this secondary antibody the membrane was washed again (3 times for 10 min) and the proteins were detected using an enhanced chemiluminescence light-detecting kit (ECL) as recommended by the manufacturer (GE, Arlington Heights, IL). Anti-BIP, anti-p-eIF2 $\alpha$ , anti-VCP, anti-Hsp60(Cpn60) and anti-p-cJun (all from Cell signalling Technology, Beverly, MA) and anti-GADD153(CHOP), anti-PKR, anti-JNK1/3 (all from Santa Cruz Biotechnology, Europe) were used with the appropriate HRP-conjugated secondary antibodies, goat anti-rabbit, goat anti-mouse, rabbit anti-goat (all from Dianova, Hamburg, Germany) to detect the respective protein.

10x TBS (Tris Buffer Saline):

12.1 g Tris

40 g NaCl

Add H<sub>2</sub>O ad 500 ml

TBS-T (Tris Buffer Saline-Tween):

100 ml 10x TBS

1 ml Tween20

Add H<sub>2</sub>O ad 1 l

Semi-Dry-Blotting Buffer:

3.03 g Tris

14.4 g Glycin

200 ml Methanol

Add H<sub>2</sub>O ad 1 l

### **Statistical analysis**

For statistical computations GraphPad Prism 5 was used. Results for cell culture and mouse studies were obtained by at least three independent experiments if not stated otherwise. All data are presented as means  $\pm$  SE. Data comparing treatment vs. corresponding control group were analyzed using unpaired t tests and between several groups by one-way or two-way analysis of variance (ANOVA) followed by an appropriate multiple comparison procedure. If data were not normally distributed non-parametrical tests were used. Differences between groups were considered significant if P-values were  $<0.05$ .

To analyze differences in housekeeping proteins also three independent biological replicates were performed. For densitometric analyses day 0 was set to 100% as reference. Afterwards one sample t-test was performed. Un-normalized data were analyzed by unpaired t-test. This test compares the means of two unmatched groups, assuming that the values follow a Gaussian distribution.

For the analysis of UPR markers one-way analysis of variance (ANOVA) was used. One-way ANOVA compares means of three or more unmatched groups. To identify which of the means are different Turkey multiple comparison test was used. This test compares differences between each pair (for example day 0 and day 8) with appropriate adjustment of multiple testing.

To measure if the mice have an impaired glucose tolerance a glucose tolerance test (GTT) was performed. For the area under the curve (AUC) the total peak area was used with a baseline of the starved value (time=0 min).

## Results

### ***In vitro assessment of UPR markers during adipogenic differentiation***

#### *Qualitative assessment of housekeeping proteins in adipocytes of different sizes*

To characterize UPR signaling in an expanding tissue it was necessary to validate constancy of housekeeper proteins as the volume expansion of adipocytes during differentiation might be a problem in adipose tissue research in view of adequate protein controls. As gene expression studies in adipocytes already reported high variation of typical housekeeping genes in fat cells under different treatment conditions,<sup>113</sup> we wanted to address this important issue on protein level. Therefore, we performed western blot analysis to follow the development of selected HKs ( $\beta$ -actin,  $\alpha$ -tubulin, GAPDH, histone 3 (H3) and HPRT) and Coomassie staining during adipose differentiation in human SGBS cells and murine 3T3-L1 cells, but also in primary isolated human preadipocytes (experiments by Simone Matthä).<sup>114</sup>

SGBS cells are used as an alternative to primary isolated human preadipocytes. They exhibit very similar biochemical and physiological properties compared to mature adipocytes.<sup>108</sup> A closer look in the development of HK proteins, showed that GAPDH and  $\alpha$ -tubulin levels significantly decreased by  $56.50 \pm 15.32 \%$  and  $58.72 \pm 11.37 \%$ , respectively at day 16 compared to the undifferentiated stage (Figure 1A and C). H3 and HPRT fluctuated considerably during the differentiation process (Figure 1D and E) and also  $\beta$ -actin showed a high variation (Figure 1B). One must consider that the western blot of H3 presumably shows an artefact on day 14. Coomassie-stained protein bands were the most robust read-out for normalizing protein amounts on the membrane (Figure 1F).<sup>114</sup>

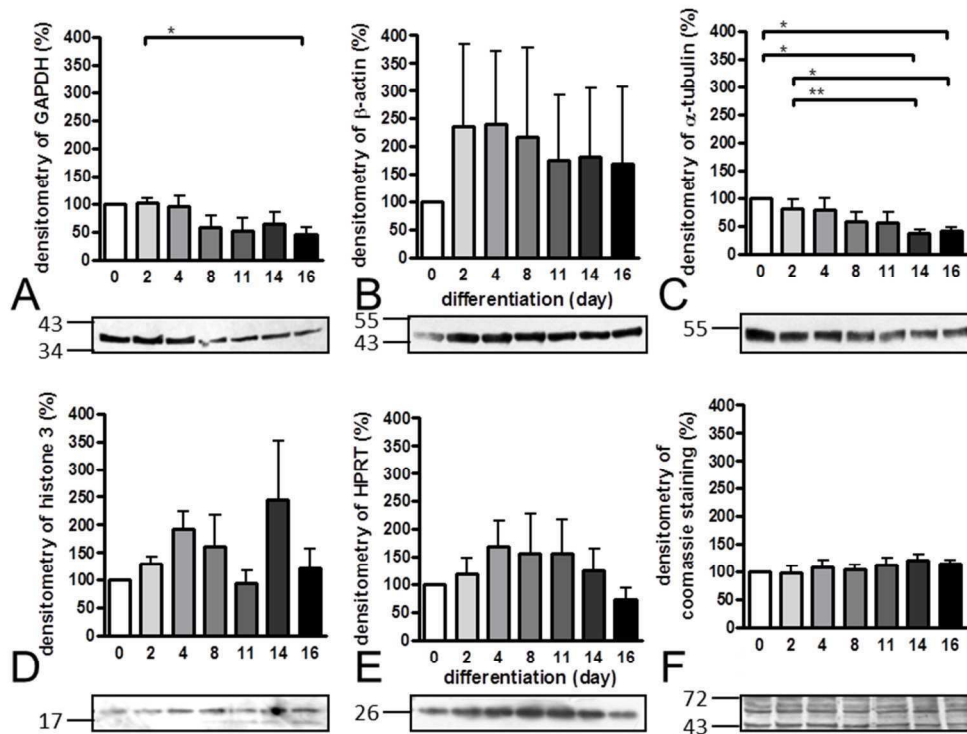


**Figure 1: Course of HKs in differentiated SGBS cells**

During differentiation protein was harvested at the time points indicated and western blot analysis was performed for GAPDH (A),  $\beta$ -actin (B),  $\alpha$ -tubulin (C), histone 3 (D), HPRT (E), and Coomassie staining (55 - 30 kDa) (F). Data are shown as relative changes compared to the protein level on day 0. Each column is the mean  $\pm$  SD of 3 independent experiments. One western blot is shown below. Statistical analysis was performed by one sample t-test and unpaired t-test (\*p $\leq$ 0.05; \*\*p $\leq$ 0.01).

Another common preadipocyte cell line which is used to study obesity is the murine cell line 3T3-L1. Compared to SGBS cells, 3T3-L1 cells are permanently cultured in FBS-containing media. Therefore it was not surprising that they also showed substantial changes in the commonly used loading controls. In contrast to the human system, GAPDH showed the highest variation with constantly increasing levels up to  $2,134 \pm 1,584\%$  at day 17 (p = 0.34) (Figure 2A). In contrast,  $\beta$ -actin and  $\alpha$ -tubulin significantly decreased during differentiation ( $53.46 \pm 20.27\%$  and  $66.24 \pm 4.20\%$ ) with the lowest levels at the end of the culture period (Figure 2B and C). H3 and HPRT varied significantly, but without a clear tendency (Figure 2D and E). Only Coomassie-staining revealed a stable pattern reflecting equal loading on the membrane (Figure 2F).<sup>114</sup>

In conclusion, there are many differences between the human preadipocyte models (primary isolated human preadipocytes and SGBS) and 3T3-L1 which are discussed in the work of Matthae S et al. 2013.<sup>114</sup>

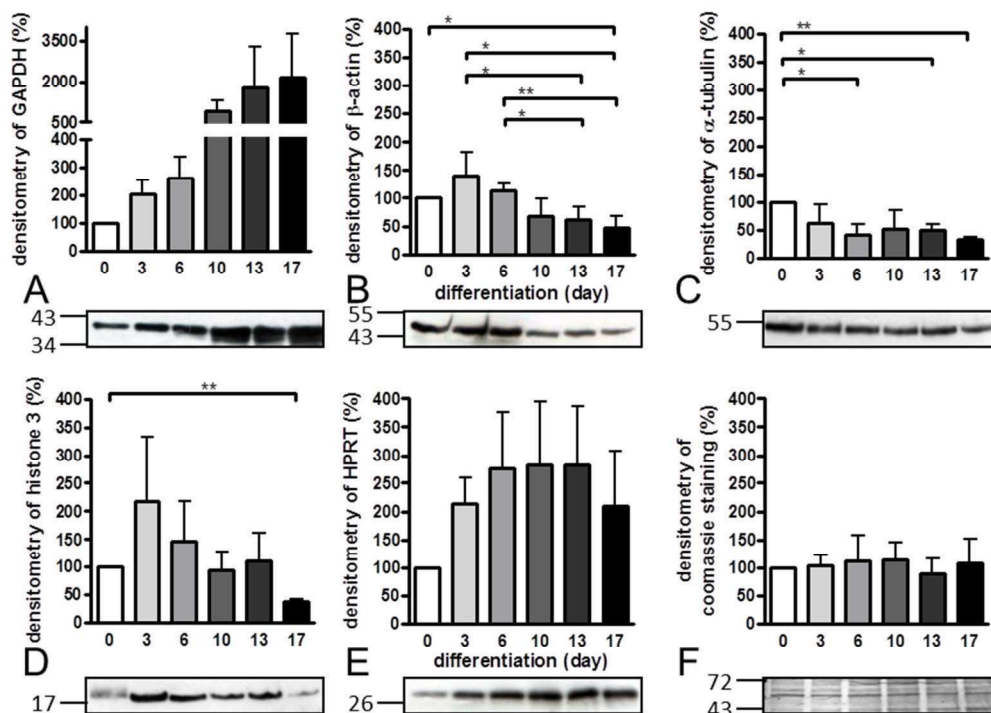


**Figure 2: Course of HKs in differentiated murine 3T3-L1 cells**

Murine fibroblast-like 3T3-L1 cells were differentiated and protein was harvested at the time points indicated and western blot analysis was performed for GAPDH (A),  $\beta$ -actin (B),  $\alpha$ -tubulin (C), histone 3 (D), HPRT (E), and Coomassie staining (55 - 33 kDa) (F). Data are shown as relative changes compared to the protein level at day 0. Each column is the mean  $\pm$  SD of 3 independent experiments. One western blot is shown below. Statistical analysis was performed by one sample t-test and unpaired t-test (\* $p \leq 0.05$ ; \*\* $p \leq 0.01$ ).

UPR markers during differentiation of primary isolated human preadipocytes as well as SGBS cells

To investigate whether the adipogenic differentiation is a stress situation for the cell we differentiated primary isolated human preadipocytes and human SGBS cells. Differentiation was followed until a complete adipose phenotype emerged in the cells. Complete differentiation was verified by Oil-Red-O staining and the measurement of GPDH (glycerol-3-phosphate dehydrogenase) activity which steadily increased during the differentiation period (not shown). Secretion of typical adipokines (adiponektin and leptin) paralleled the differentiation process. As shown before, primary isolated human preadipocytes as well as SGBS cells developed a slightly different secretion pattern with a tardy increase of leptin in the latter cell type. The release of the pro-inflammatory cytokine IL-6 steadily declined in human preadipocytes and SGBS cells during the differentiation period (Figure 3).

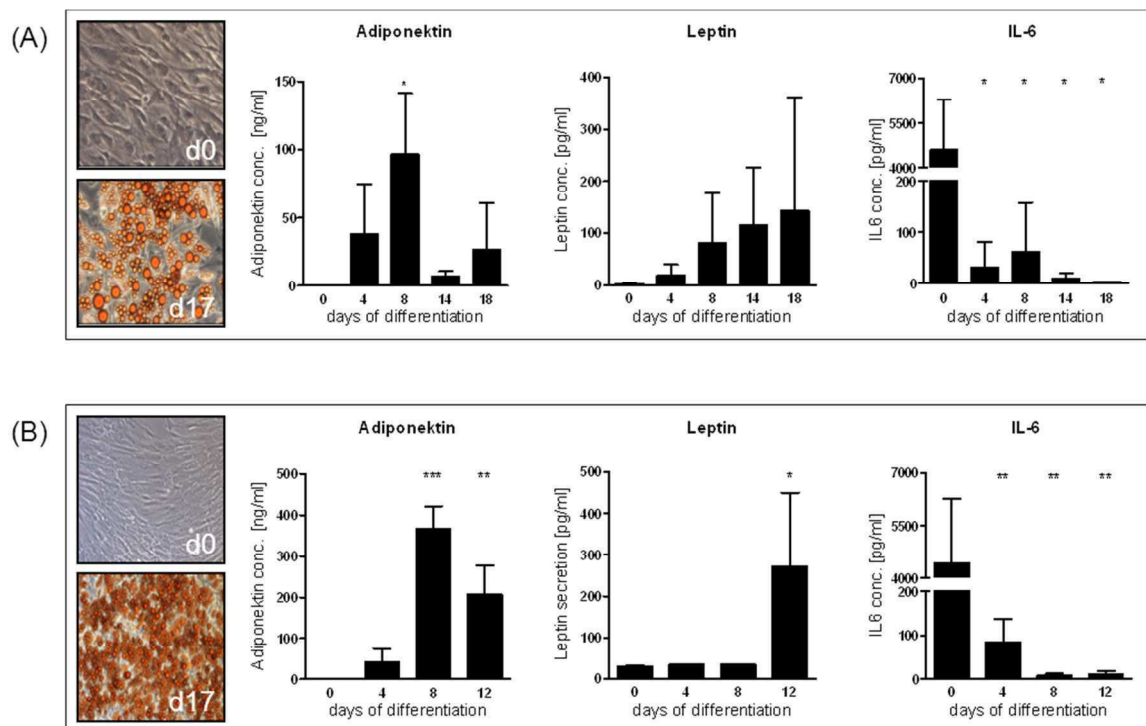


**Figure 3: Secretion of adipokines during differentiation in different preadipocyte models**

The upper panel (A) shows the development of primary isolated human preadipocytes (d=0) into adipocytes (d=17) as well as the adipokine secretion. In the lower panel (B) the development of SGBS preadipocytes (d=0) into adipocytes (d=17) as well as their adipokine secretion is shown. For visualization of differentiation cells were stained with Oil-red-O on the last day of culture. Adiponektin, leptin as well as IL-6 were measured by ELISA. Each bar represents mean  $\pm$  SD. Statistical analysis was performed by one-way ANOVA (\* $p \leq 0.05$ ; \*\* $p \leq 0.01$ ; \*\*\* $p \leq 0.001$  compared to day 0; n=3).



Furthermore we wanted to investigate typical makers for the erUPR pathways (Grp78, p-eIF2 $\alpha$  and CHOP), which indicate the activation stage commonly observed during the ER-stress response. We decided to use these factors because Grp78 is the major chaperone located in the ER, which activates the erUPR (by dissociating from three UPR transducers PERK, IRE and ATF6). eIF2 $\alpha$  and its phosphorylation were used to get insight whether the erUPR was activated via the PERK pathway, which is often associated with diabetes.<sup>115</sup> Additionally, we decided to measure CHOP expression for pro-apoptotic activation. These three markers were semi-quantitatively measured by western blot analysis during adipose differentiation, to test if this process has an influence on the cell stress level. For Grp78 and p-eIF2 $\alpha$  calnexin was used as a loading control. To correct the intensity of CHOP, a Coomassie staining was used, as we found out that this was the most robust loading control for human preadipocytes. In primary human preadipocytes, Grp78 significantly decreased during the course of differentiation by  $96.13 \pm 50.95\%$  on day 8 compared to  $4.47 \pm 7.72\%$  on day 0. In parallel, the level of eIF2 $\alpha$  phosphorylation decreased continuously after day 3 with maximal reduction after 16 days of differentiation ( $10.86 \pm 11.23\%$  and  $-65.61 \pm 15.92\%$ , respectively). CHOP increased during differentiation by  $61.69 \pm 60.51\%$  on day 16. A similar picture could be observed in SGBS cells. Here, Grp78 decreased steadily during the course of differentiation with significant reductions from day 8 onwards with lowest levels of  $-173.2 \pm 5.83\%$  at day 16. Phosphorylation of eIF2 $\alpha$  also decreased during differentiation by  $145.0 \pm 12.73\%$  on day 16. In SGBS preadipocytes CHOP was already present at baseline ( $174.4 \pm 302.0\%$ ) and did not show a significant change at any time point (Figure 4).

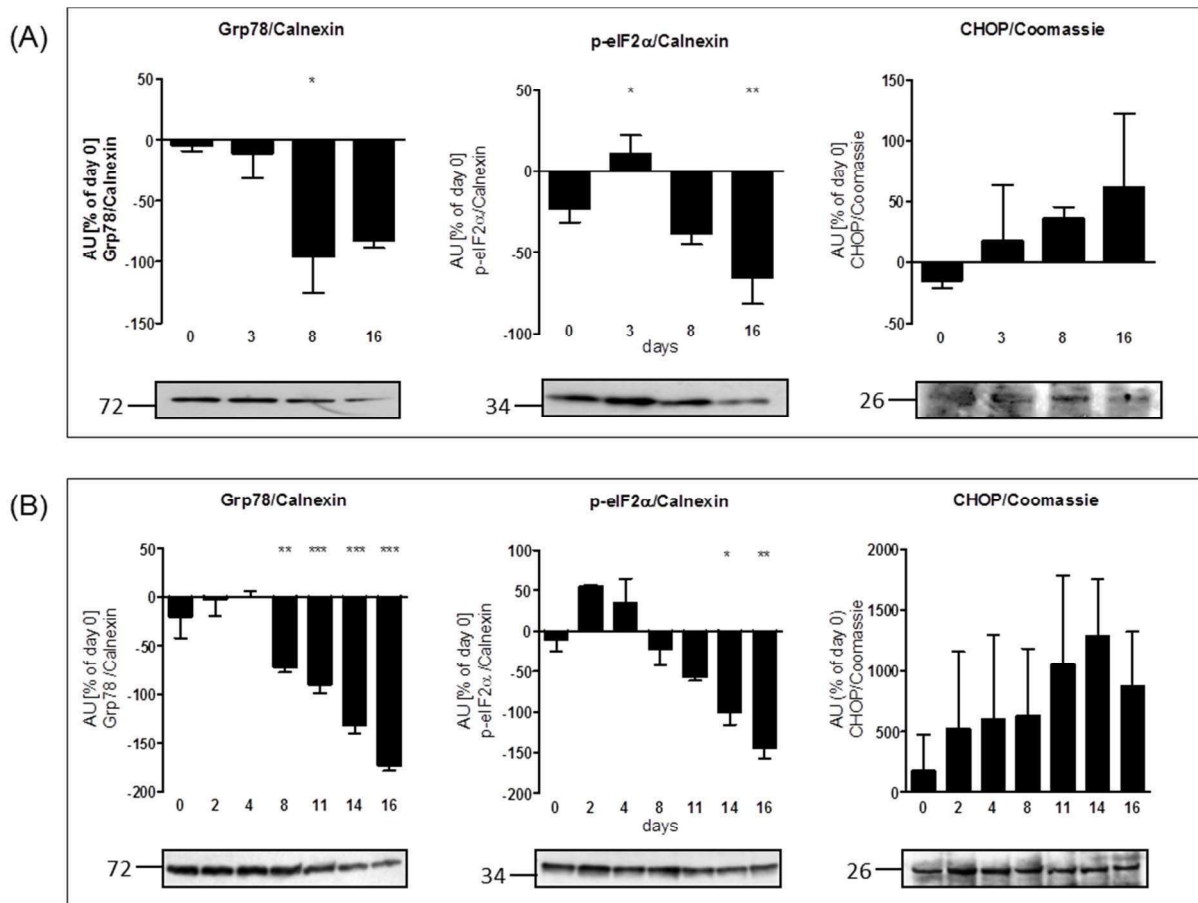


**Figure 4: Markers of erUPR during the course of differentiation in primary isolated human preadipocytes (A) and SGBS cells (B)**

For western blot analysis 20 µg of total protein lysate was used. At different time points of adipogenesis markers for erUPR Grp78, p-eIF2α and CHOP were detected. Calnexin (as an ubiquitous marker of the ER) was used as an internal control for Grp78 and p-eIF2α. Coomassie staining of the membrane was used as internal control for CHOP. Intensities of western blots are shown as auxiliary units in % compared to day 0 of three independent experiments. Only one out of three western blots is shown below. Control values were adjusted to one experiment. Statistical analysis was performed by one-way ANOVA (\*p<0.05; \*\*p<0.01; \*\*\*p<0.001 compared to day 0; n=3).

To unravel the role of mtUPR in adipogenic differentiation, Cpn60 as well as protein levels of PKR were measured during the process of differentiation. Cpn60 is considered as a target gene in the mtUPR, because it assists in folding and is up-regulated by the presence of unfolded proteins in the mitochondrial matrix.<sup>47</sup> The double-stranded RNA-activated protein kinase (PKR) seems to be also relevant in the activation of the mtUPR. It has been shown that PKR is involved in a broad variety of cellular stress responses. Additionally it has been described that PKR participates in ER-stress signaling as well as it is up-regulated under obese situations.<sup>116,117</sup> As Cpn60 is not only located in the mitochondria and PKR as well is located in the cytosol, we used Coomassie staining as an internal loading control.

During differentiation of primary isolated human preadipocytes Cpn60 increased constantly with maximal levels of  $163.4 \pm 97.43\%$  compared to baseline at day 0 ( $7.69 \pm 62.34\%$ ). The protein level of PKR declined (reaching significance at day 8 – 16 by  $116.7 \pm 38.86\%$  and  $74.98 \pm 24.04\%$ , respectively) during the differentiation process. In human SGBS cells the mitochondrial protein Cpn60 increased from almost undetectable levels at day 0 ( $20.20 \pm 34.98\%$ ) to a very high level at day 16 of differentiation ( $10,463 \pm 3,738\%$ ). PKR increased during induction of differentiation but thereafter decreased to almost undetectable levels ( $63.90 \pm 113.0\%$ ) (Figure 5).

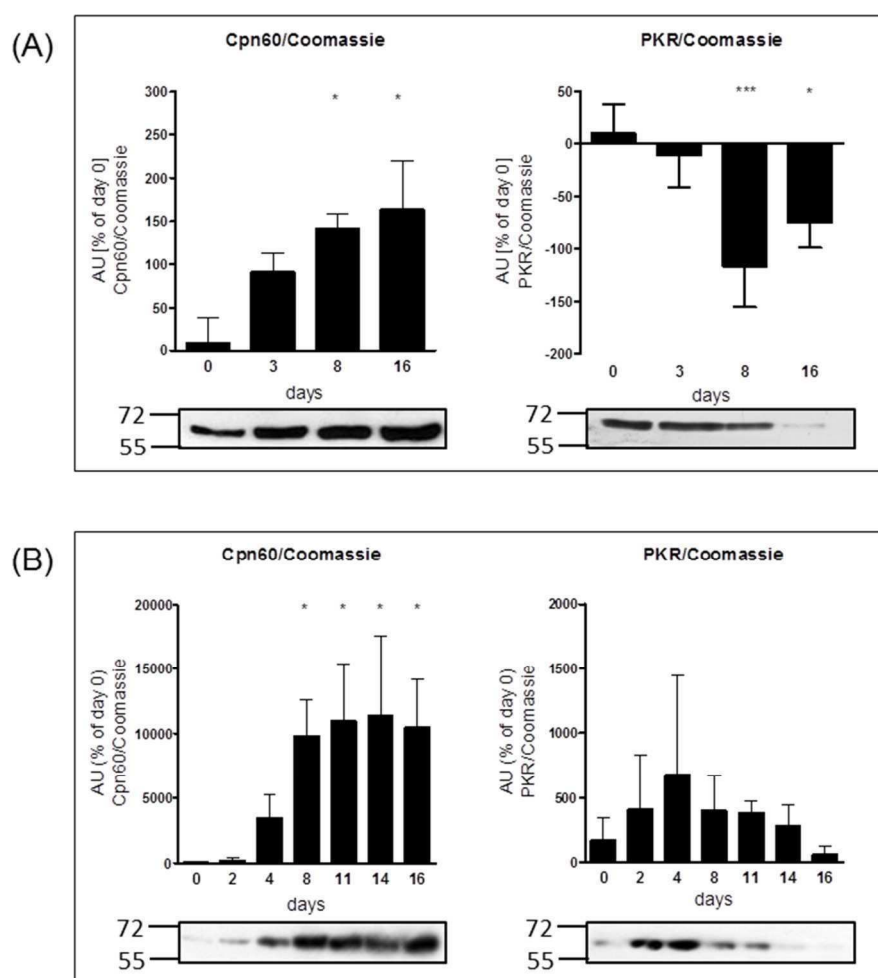


**Figure 5: Markers of mtURP during differentiation in primary isolated human preadipocytes (A) and SGBS cells (B)**

Total protein was collected at different time point of differentiation and Cpn60 as well as PKR levels were determined. Coomassie staining of the membrane was used as internal control. The intensities of the western blots were shown as auxiliary units in % compared to day 0 from three independent experiments. Only one out of three western blots is shown below. Control values were adjusted to one experiment. Statistical analysis was performed by one-way ANOVA (\* $p \leq 0.05$ ; \*\*\* $p \leq 0.001$  compared to day 0;  $n=3$ ).

As during erUPR also the ER associated degradation (ERAD) could be activated, we investigated if VCP, a transporter protein involved in ERAD, is affected by differentiation of human adipocytes. VCP is located in the ER and therefore we used calnexin as a protein loading control. In primary isolated human preadipocytes VCP increased during the course of differentiation by  $124.2 \pm 121.2\%$  on day 16 whereas it could already be detected at the beginning of differentiation in SGBS with levels of  $10.29 \pm 13.03\%$ . In these SGBS cells the VCP protein is always present at a high level (Figure 6).

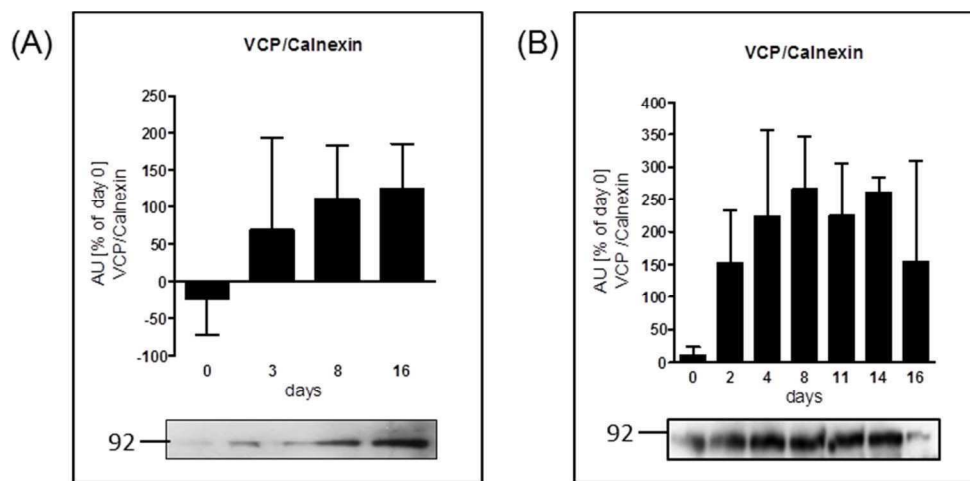


**Figure 6: The ERAD marker VCP during the course of differentiation in primary isolated human preadipocytes (A) and SGBS cells (B)**

For western blot analysis 20  $\mu$ g of total protein lysate was used. At different time points of adipogenesis VCP levels were determined. Calnexin (as a ubiquitous marker of the ER) was used as internal control. Intensities of western blots are shown as auxiliary units in % compared to day 0 of three independent experiments. Only one out of three western blots is shown below. Control values were adjusted to one experiment. Statistical analysis was performed by one-way ANOVA (\* $p \leq 0.05$ ; \*\* $p \leq 0.01$ ; \*\*\* $p \leq 0.001$  compared to day 0;  $n=3$ ).

c-jun amino-terminal kinase (JNK) is involved in pro-inflammatory pathways which are activated by cytokines. As it was shown that JNK activation is elevated in obesity<sup>69</sup>, we were interested in measuring the protein levels of JNK1/3 and the phosphorylation of cJun as a downstream target of JNK during differentiation. As both proteins are located in the cytosol we did Coomassie staining to correct for the protein load.

In primary human preadipocytes, JNK1/3 levels slightly decreased until day 16 of differentiation by  $39.12 \pm 27.82\%$ . On the other hand, p-cJun increased during the

first 8 days of differentiation and remained stable for the rest of differentiation until day 16 (with  $89.67 \pm 89.05\%$  and  $61.61 \pm 90.76\%$ , respectively). SGBS cells showed a constant decline in JNK1/3 protein levels during differentiation with significant reductions by  $69.99 \pm 2.41\%$  at day 11, while p-cJun levels were unaffected at the same time ( $22.61 \pm 24.68\%$  at day 0 and  $3.73 \pm 19.37\%$  at day 16) (Figure 7).

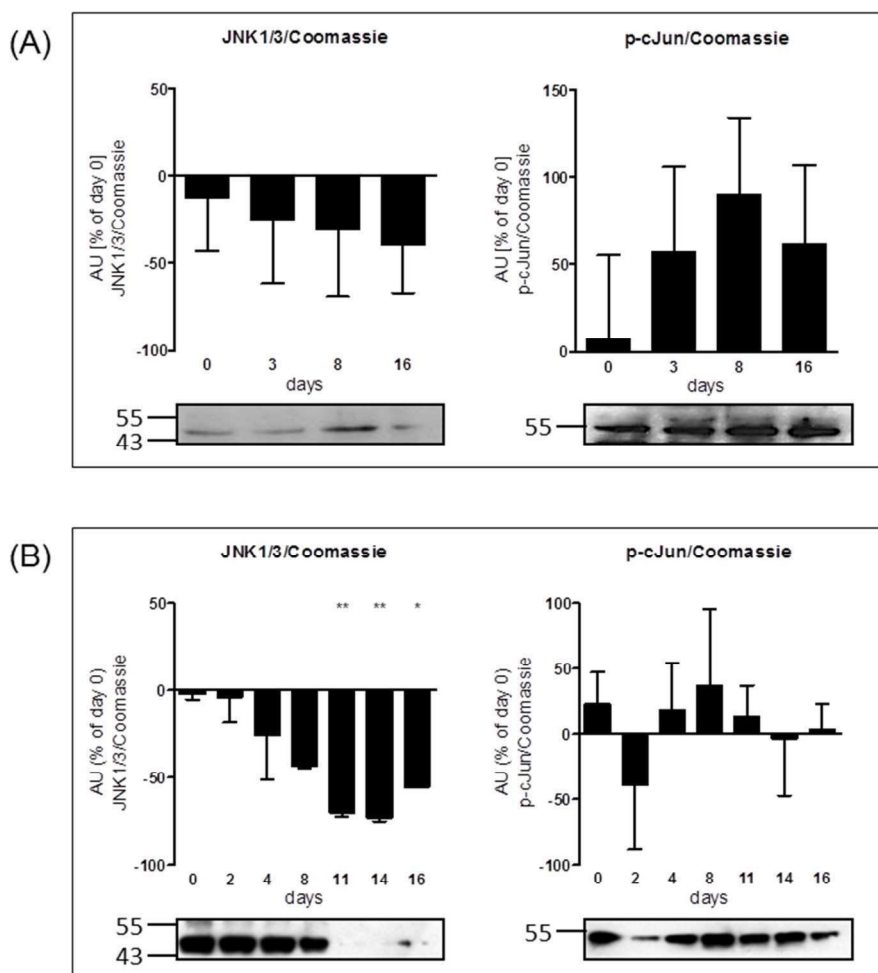


**Figure 7: The course of JNK-activation during adipogenic differentiation in different preadipocyte models**

At different time points during adipogenesis total protein was collected from primary isolated human preadipocytes (A) and SGBS cells (B) for western blot analysis to measure the inflammatory markers JNK1/3 and its downstream protein p-cJun. Coomassie staining of the membrane was used as internal control. The intensities of the western blots were shown as auxiliary units in % of day 0 of three independent experiments. Only one western blot is shown below. Control values were adjusted to one out of three representative experiments. Statistical analysis was performed by one-way ANOVA (\* $p \leq 0.05$ ; \*\* $p \leq 0.01$  compared to day 0;  $n=3$ ).

### UPR markers during differentiation of murine 3T3-L1 cells

As the *in vivo* experiments were planned in different mouse models, we wanted to test whether murine cells react in a same way during differentiation like the human cell models. Therefore we choose 3T3-L1 cells for differentiation experiments. Differentiation was followed until a complete adipose phenotype emerged in the cells. Complete differentiation was also verified by Oil-Red-O staining and the measurement of GPDH activity which steadily increased during the differentiation period (not shown). Secretion of typical adipokines (adiponectin and leptin) increased during differentiation. It is noteworthy that human (primary isolated human preadipocytes and SGBS) and murine 3T3-L1 cells differed in the absolute amount of secreted IL-6, which is considered as a pro-inflammatory adipokine. Whereas IL-6 release steadily declined in human preadipocytes and SGBS cells during the differentiation period, it continuously increased in 3T3-L1 cells during differentiation (Figure 8).

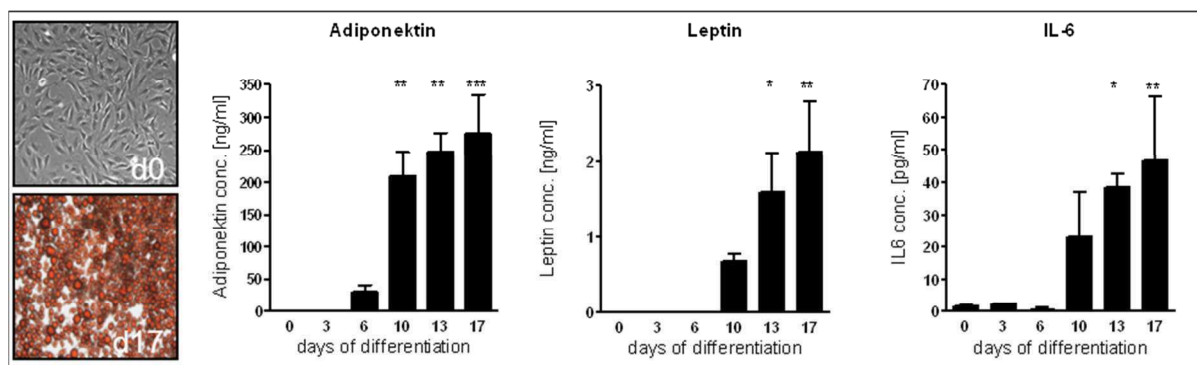


**Figure 8: Secretion of adipokines during differentiation in murine 3T3-L1 cells**

The pictures show the development of 3T3-L1 preadipocytes (d=0) into adipocytes (d=17). At the last day of culture the cells were stained with Oil-red-O. Adiponectin, leptin and IL-6 secretion were measured by ELISA. Each bar represents mean  $\pm$  SD. Statistical analysis was performed by one-way ANOVA (\* $p \leq 0.05$ ; \*\* $p \leq 0.01$ ; \*\*\* $p \leq 0.001$  compared to day 0;  $n=3$ ).

Makers for erUPR (Grp78, p-eIF2 $\alpha$  and CHOP) showed a different pattern in their protein levels during differentiation of 3T3-L1 compared to the human cell models. Again, calnexin was used as a loading control for Grp78 and p-eIF2 $\alpha$ . For CHOP we performed Coomassie staining. The murine 3T3-L1 cells responded to the adipogenic stimulation with an increase in Grp78 levels by  $166.9 \pm 125.8\%$  at day 17. In contrast, p-eIF2 $\alpha$  decreased by  $412.5 \pm 18.04\%$  at day 17, whereas CHOP increased dramatically from undetectable levels at the beginning of adipose

differentiation ( $-0.83 \pm 1.43\%$ ) up to  $340.9 \pm 102.7\%$  at day 17. So it followed the change of Grp78 during the differentiation (Figure 9).

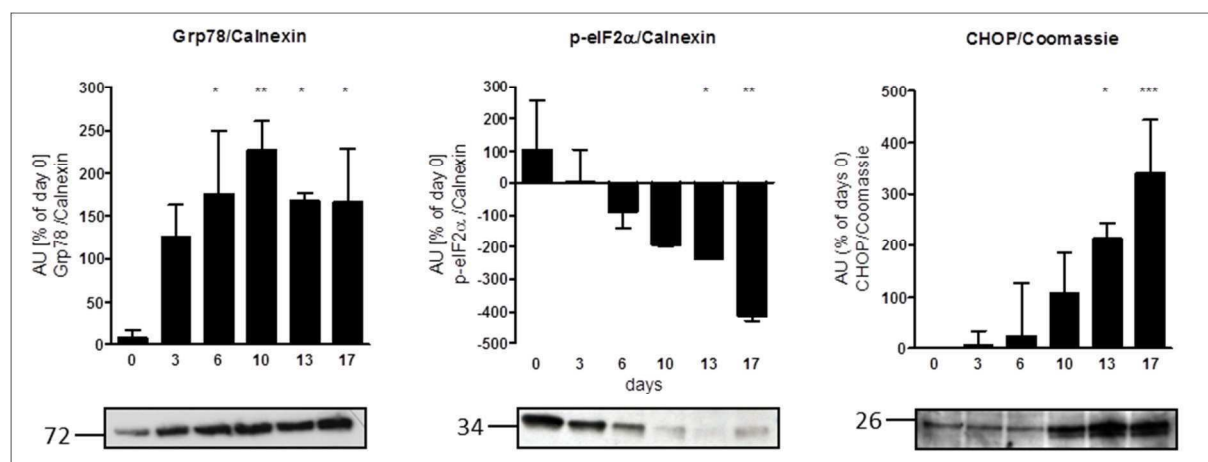


**Figure 9: erUPR marker during the course of differentiation in 3T3-L1 cells**

For western blot analysis 20  $\mu$ g of total protein lysate was used. At different time points of adipogenesis markers for erUPR Grp78, p-eIF2 $\alpha$  and CHOP were detected. Calnexin (as an ubiquitous marker of the ER) and a Coomassie staining of the membrane were used as internal controls. Intensities of western blots are shown as auxiliary units in % compared to day 0 of three independent experiments. Only one western blot is shown below. Control values were adjusted to one out of three representative experiments. Statistical analysis was performed by one-way ANOVA (\* $p \leq 0.05$ ; \*\* $p \leq 0.01$  compared to day 0;  $n=3$ ).

To further study the role of mtUPR during murine adipogenic differentiation, we measured protein levels of Cpn60 as well as protein levels of PKR during the process of differentiation. Protein level of Cpn60 increased during the course of differentiation reaching significance by  $910.3 \pm 395.8\%$  at the end of differentiation. PKR seems to be unaffected by the differentiation process in 3T3-L1 cells. The protein levels of PKR is more or less the same at day 0 compared to day 17 ( $-12.47 \pm 10.95\%$  and  $-25.69 \pm 16.45\%$ , respectively) (Figure 10).

The ERAD protein VCP also differed in its levels during differentiation between human and murine cells. As VCP is located in the ER, calnexin was used as loading control. Whereas VCP levels increased during human adipogenic differentiation it only increased until day 6 of differentiation in 3T1-L1 cells to levels of  $147.2 \pm 3.94\%$ . Afterwards VCP rapidly declined until significance at day 17 ( $-262.6 \pm 14.14\%$ ) (Figure 11).

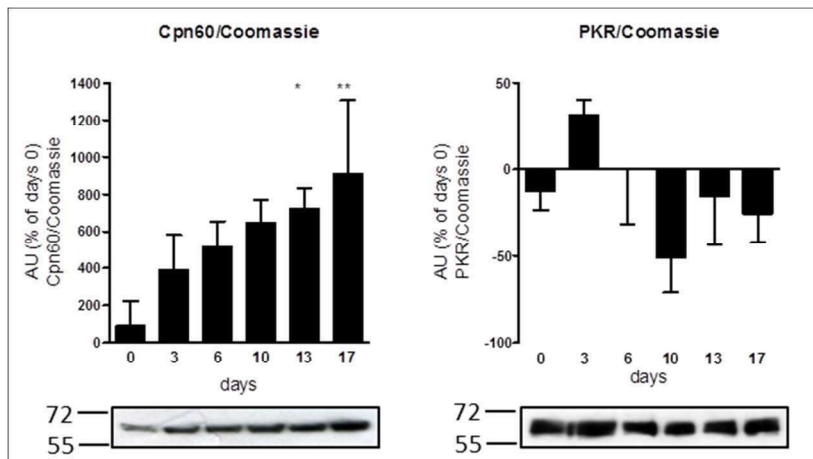


**Figure 10: mtUPR marker during differentiation in 3T3-L1 cells**

At different time points during adipogenesis total protein was collected and Cpn60 as well as PKR levels were determined. The integrated densities of the bands from Coomassie staining were used as internal control. The intensities of the western blots were shown as auxiliary units in % of day 0 of three independent experiments. Only one out of three western blots is shown below. Control values were adjusted to one experiment. Statistical analysis was performed by one-way ANOVA (\* $p \leq 0.05$ ; \*\* $p \leq 0.01$  compared to day 0;  $n=3$ ).

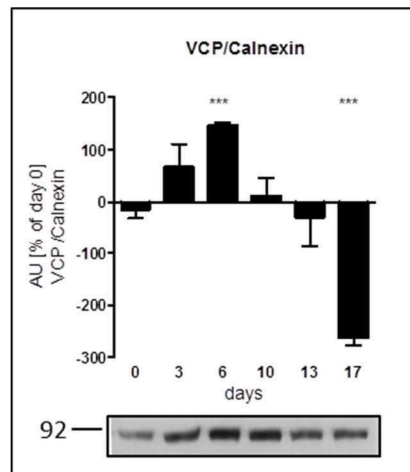


**Figure 11: VCP levels during differentiation of murine 3T3-L1 cells**

At different time points of adipogenesis VCP levels (as a marker for the ERAD pathway) were measured. Calnexin was used as internal control. Intensities of western blots are shown as auxiliary units in % compared to day 0 of three independent experiments. Only one western blot is shown below. Control values were adjusted to one out of three representative experiments. Statistical analysis was performed by one-way ANOVA (\* $p \leq 0.05$ ; \*\* $p \leq 0.01$  compared to day 0;  $n=3$ ).



The pro-inflammatory marker JNK and the phosphorylation of cJun exhibited a different pattern in 3T3-L1 as compared to the human models. Levels of JNK1/3 showed no significant changes between day 0 and day 17 of differentiation ( $-21.50 \pm 30.41\%$  and  $5.50 \pm 0.71\%$ , respectively), whereas cJun phosphorylation revealed a clear activation pattern ( $p < 0.05$ ) throughout the differentiation process (Figure 12) with highest levels of  $1,262.4 \pm 485.9\%$  at day 13 of differentiation.

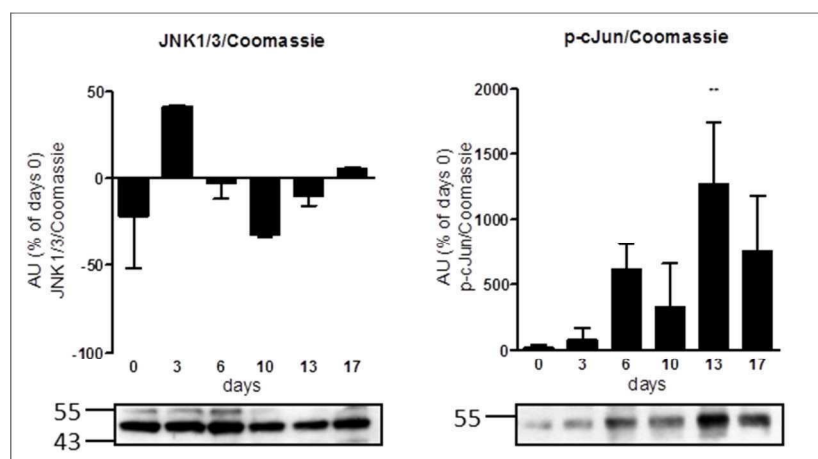


**Figure 12: Course of JNK activation during adipogenesis of 3T3-L1 cells**

At different time points during adipogenesis total protein was collected from 3T3-L1 cells to measure the inflammatory markers JNK1/3 and its downstream protein p-cJun. Coomassie staining of the membrane was used as internal control. The intensities of the western blots were shown as auxiliary units in % of day 0 of three independent experiments. Control values were adjusted to one representative experiment (\* $p \leq 0.05$ ; \*\* $p \leq 0.01$ ; \*\*\* $p \leq 0.001$  compared to day 0;  $n=3$ ).

**Assessment of UPR markers in primary isolated mature adipocytes and in clinical samples from a tissue bio bank**

As previous data have shown there is a difference between human and murine cell models, we were interested to test if we could confirm the human results with primary isolated mature adipocytes. Therefore, we measured levels of Grp78, Cpn60 and JNK1/3 in adipocytes from four individuals fractionated according to cell volume (Table 1).

**Table 1: Characteristics of four individual tissue donors and their fractionated adipocytes**

Male /female	1/3
Age, years	30.50 ± 7.26 (25-43)
BMI, kg/m <sup>2</sup>	28.77 ± 4.33
Mean adipocyte volume (pl)	653.2 ± 439.5
Fraction I adi volume (pl)	445.6 ± 305.7
Fraction IV adi volume (pl)	860.8 ± 454.9

Interestingly, levels of Grp78 were comparable between small (fraction I) and large (fraction IV) adipocytes. Although Cpn60 level seem to be higher in small adipocytes there is no statistical significance. The protein level of JNK1/3 was significantly higher in large adipocytes (p=0.047) (Figure 13A). Levels in the fourth fraction were 1.3 fold higher compared to fraction I. To assess erUPR markers in relation to adipocyte size, adipose tissue (AT) samples from men with normal glucose tolerance (NGT) or type 2 diabetes (T2D) were investigated. Age- and BMI-matched male subjects were divided into NGT and T2D subgroups (n=25 per group). The mean adipocyte volume was higher in patients with T2D compared to the NGT group (1,000 ± 215.0 pl vs. 802.0 ± 198.0 pl, p=0.003). In addition, AT macrophage infiltration was significantly higher in the T2D compared to the NGT group (4.54 ± 1.87% vs. 1.58 ± 0.72%, p<0.0001) (Table 2).

**Table 2: Characteristics of NGT and T2D subjects (N=25)**

	<u>NGT (25)</u>	<u>T2D (25)</u>	<u>p-value</u>
Age, years	49.28 ± 3.09 (45-59)	49.24 ± 3.13 (45-51)	p=0.96
BMI, kg/m <sup>2</sup>	47.86 ± 7.89	47.77 ± 7.75	p=0.96
Mean adipocyte volume (pl)	802.0 ± 198.0	1,000 ± 215.0	**p=0.003
Macrophage infiltration (%)	1.58 ± 0.72	4.54 ± 1.87	***p<0.0001

Furthermore, we found a close correlation between mean adipocyte volume and BMI (Figure 13B). The correlation coefficient is  $r=0.7282$ ;  $p \leq 0.0001$  for the NGT group and  $r=0.7723$ ,  $p \leq 0.0001$  for the T2D group. Regarding erUPR markers, we measured levels of Grp78 and JNK1/3 in the adipose tissue samples. Protein level of Grp78 was significantly higher (2.1 fold) in AT of T2D patients compared to NGT patients ( $p=0.031$ ), whereas no difference was observed for JNK1/3 expression (Figure 13C). Only in the NGT group, we found a negative correlation between adipocyte size and Grp78 (Figure 13D) ( $r=-0.4093$ ;  $p=0.0211$ ). On the other hand, JNK1/3 showed a positive correlation with mean adipocyte size in the T2D group ( $r=0.3940$ ;  $p=0.0256$ ) (Figure 13E).

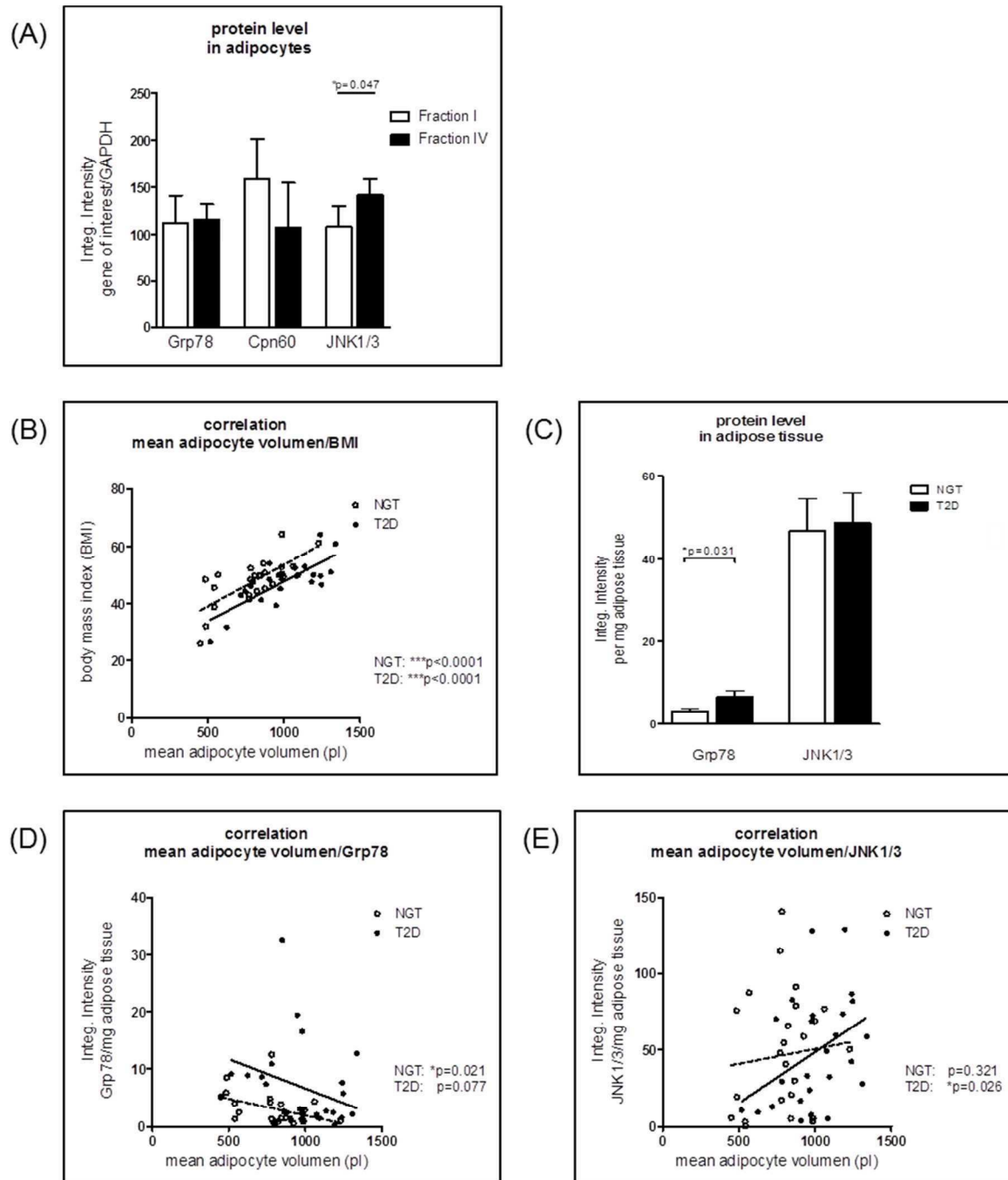


**Figure 13: UPR marker proteins in primary isolated fat cells of different sizes and in adipose tissue from needle biopsies**

Adipocytes were isolated and fractionated into small and large cells from 4 individuals (table 1). The expression levels for Grp78, Cpn60 and JNK1/3 in small and large adipocytes are shown in panel A (\* $p<0.05$ ; \*\* $p<0.01$ ; \*\*\* $p<0.001$ ;  $n=4$ ).

Furthermore, adipose tissue from of healthy obese (NGT) and type 2 diabetic obese (T2D) individuals ( $n=25/25$ ) was collected by needle biopsies. The characteristics of the study group are given in table 2. Biopsies were used for the measurement of cell size, immune cell infiltration and for western blot analysis. Correlations between BMI and mean adipocyte volume in NGT and T2D subjects were calculated (B). Levels of Grp78 and JNK1/3 were measured in adipose tissue of the study group (C). After the determination of the mean adipocyte volume it was correlated with Grp78 (D) and JNK1/3 (E). Statistical analysis was performed by one-tailed Pearson correlation.

## Measurement of UPR markers in different mouse models

### Development of adipose tissue in C57BL/6N mice of different ages

As the *in vitro* data could show there is a difference between stress response during differentiation in human and murine cells, we investigated the stress response in adipose tissue during growth in C57BL/6N wild type mice. Epididymal adipose tissue from C57BL/6N wild type mice of different age were used to examine the development of fat cell size over time. As expected the amount of adipose tissue is very low in 2 week old mice. This corresponds to a very small mean fat cell size. In contrast, adipocytes of 12 week old mice showed a constantly increasing cell size causing growth of fat pads (Figure 15). To determine the distribution of fat cell size tissue sections were photographed, adipocytes were counted and the size was calculated. Fat cells from 2 week old mice showed a small fat cell size of  $0.76 \pm 0.46 \times 10^3 \mu\text{m}^2$ . In contrast, fat cells of 6 and 10 week old mice were markedly larger with  $1.55 \pm 0.85 \times 10^3 \mu\text{m}^2$  and  $2.32 \pm 1.28 \times 10^3 \mu\text{m}^2$ , respectively. 12 week old mice showed the highest fat cell sizes ( $5.21 \pm 2.92 \times 10^3 \mu\text{m}^2$ ). There is a clear shift in cell size from week 2 to week 12 (Figure 14).

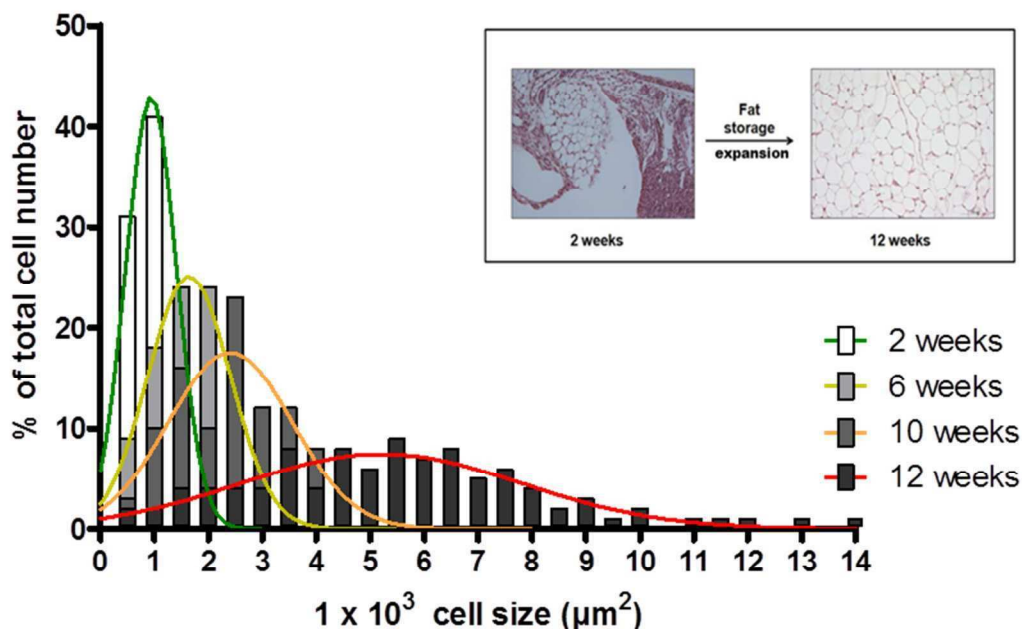


**Figure 14: Distribution of adipocyte sizes in epididymal adipose tissue from C57BL/6N mice of different age and HE staining of epididymal adipose tissue from C57BL/6N wild type mice**

Distributions of fat cell sizes ( $\mu\text{m}^2$ ) in mice aged 2 (green), 6 (yellow), 10 (orange), and 12 weeks (red) are demonstrated. For HE-staining the adipose tissue was cut into slices with a thickness of 5  $\mu\text{m}$ . The left picture represents the epididymal fat pad of 2 week old mice. In contrast, the right side shows adipose tissue of 12 week old mice. Magnification 200x.

## Results

As we wanted to investigate whether aging and growth process of adipose tissue somehow induce the UPR we performed western blot analysis with the epididymal adipose tissue of C57BL/6N wild type mice. Coomassie staining was used as internal control, because in the whole tissue lysate one cannot assign the signal to a specific cell. As the protein level of all investigated markers was very low at an age of 4 weeks we compared the changes to the protein levels at 6 weeks. The marker for erUPR Grp78 slightly decreased during the development from week 6 until week 12. Cpn60, as a marker for mtUPR clearly increased at week 12 compared to week 6. As Grp78 levels declined we also investigated VCP as a protein involved in ERAD pathways. VCP could not show a clear tendency, because it almost disappeared in week 8 and afterwards increased again until week 12 to base level (Figure 15).

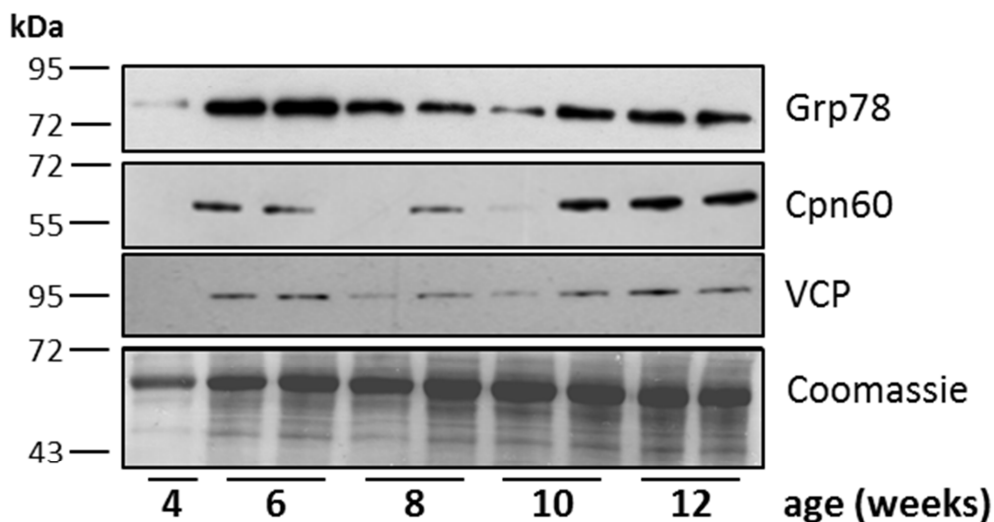


**Figure 15: UPR markers in epididymal adipose tissue of C57BL/6N mice of different age**

Total protein lysate extracted from adipose tissue to measure cell stress marker proteins by western blot. Grp78, Cpn60 and VCP protein levels were determined. Coomassie was used as internal control. Western blot analysis was performed with 2 different mice at each time point except at 4 weeks of C57BL/6N mice.

### Grp78<sup>+/-</sup> mice – a basal characterization under a high fat diet

To evaluate the relevance of Grp78 mediated erUPR for diet induced obesity (DIO), we subjected Grp78<sup>+/-</sup> mice to a high fat diet for 8 weeks. In principle, Grp78<sup>+/-</sup> mice do not show an obvious phenotype under normal conditions. Further work could show that DIO is improved and pathways involved in the erUPR are activated in Grp78<sup>+/-</sup> mice under a high fat diet.

#### **Development of weight and body composition**

To check, if the Grp78<sup>+/-</sup> mice are protected against DIO, we measured the weight of each mouse twice a week. Interestingly, weight development showed no difference between Grp78<sup>+/-</sup> mice and their wild type littermates (wt). Wt mice showed a significantly higher body weight after 1 week of feeding, whereas there was no significant difference in body weight for the Grp78<sup>+/-</sup> mice until 4 weeks of feeding.

As every group had a different weight at the beginning of the feeding experiment ( $12.78 \pm 2.14\text{g}$  for wt-Ctrl,  $14.52 \pm 1.95\text{g}$  for wt-HFD,  $13.95 \pm 2.57\text{g}$  for Grp78<sup>+/-</sup>-Ctrl and  $13.77 \pm 2.35\text{g}$  for Grp78<sup>+/-</sup>-HFD), the total weight gain was also important to be investigated. Therefore we assessed the total weight gain of each mouse in the feeding trial. The total weight gain showed only a significant difference between Grp78<sup>+/-</sup>-Ctrl ( $6.07\text{g} \pm 2.56\text{g}$ ) and Grp78<sup>+/-</sup>-HFD ( $10.84\text{g} \pm 3.45\text{g}$ ) and not between wt-Ctrl ( $7.23\text{g} \pm 2.78\text{g}$ ) and wt-HFD ( $9.61\text{g} \pm 2.81\text{g}$ ) (Figure 16).

To investigate whether body composition is different between the genotypes under different diets a minispec NMR-analysis was performed beforehand, after 4 weeks and after 8 weeks of the feeding trial. At the beginning and after 4 weeks of feeding there were no obvious differences between the genotypes. The development of body lean mass and body fat mass is comparable in Grp78<sup>+/-</sup> mice and their wt littermates. Control wt mice ( $2.39\text{g} \pm 0.46\text{g}$ ) as well as Grp78<sup>+/-</sup>-Ctrl mice ( $2.22\text{g} \pm 0.38\text{g}$ ) showed almost the same body fat mass after 8 weeks of feeding. Only the body fat mass of the wt-HFD group ( $3.58\text{g} \pm 1.00\text{g}$ ) is significantly higher compared to wt-Ctrl mice and higher than the body fat mass of the Grp78<sup>+/-</sup>-HFD group ( $3.16\text{g} \pm 1.20\text{g}$ ) after 8 weeks of feeding (Figure 16).

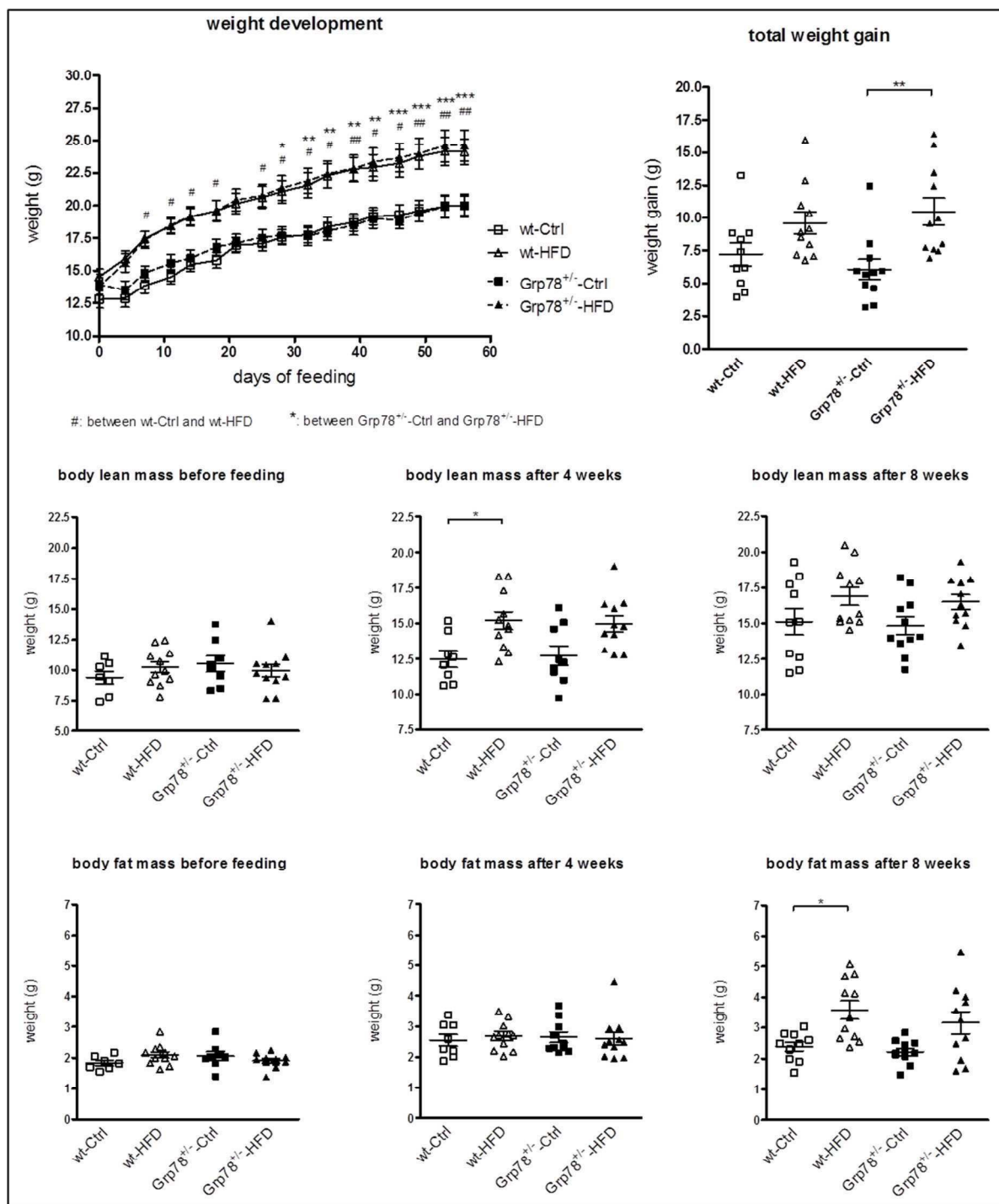


**Figure 16: Weight development after eight weeks feeding trial as well as lean-/ fat-mass development of Grp78<sup>+/-</sup> mice fed with a control and a high fat diet**

Grp78<sup>+/-</sup> mice and their wt littermates received a control or high fat diet for 8 weeks (n≥10 per group). The weight was determined twice a week. Also the total weight gain was calculated. Using NMR technology the lean-/fat mass of the mice were determined before feeding (4weeks old), after 4 weeks of feeding (8weeks old) and after 8 weeks of feeding (12 weeks old).

Statistical analysis was performed by repeated measures two-way ANOVA and one-way ANOVA followed by turkey's test (\*p≤0.05, \*\*p≤0.01, \*\*\*p≤0.001).



### Assimilation of food during the feeding

To test where the changes in body composition come from, we measured food intake, excretion of feces and the assimilation in the gut during the 4<sup>th</sup> week and in the 8<sup>th</sup> week of the feeding experiment. During the 4<sup>th</sup> week of the feeding trial an obvious difference in the food uptake between the control diet and the high fat diet could be observed. This difference disappeared during the 8<sup>th</sup> week of feeding. The excretion of feces is more or less the same over the whole feeding period. Already during the 4<sup>th</sup> week of feeding the mice under high fat diet had a significantly higher assimilation coefficient ( $p < 0.0001$ ) compared to mice fed the control diet. Meaning, those mice under high fat diet assimilated more energy in the gut than those under control diet. In the 8<sup>th</sup> week we observed a lower assimilation coefficient in the Grp78<sup>+/-</sup>-HFD group compared to the wt-HFD group ( $p < 0.05$ ) whereas the difference between the diets persisted (Figure 17).

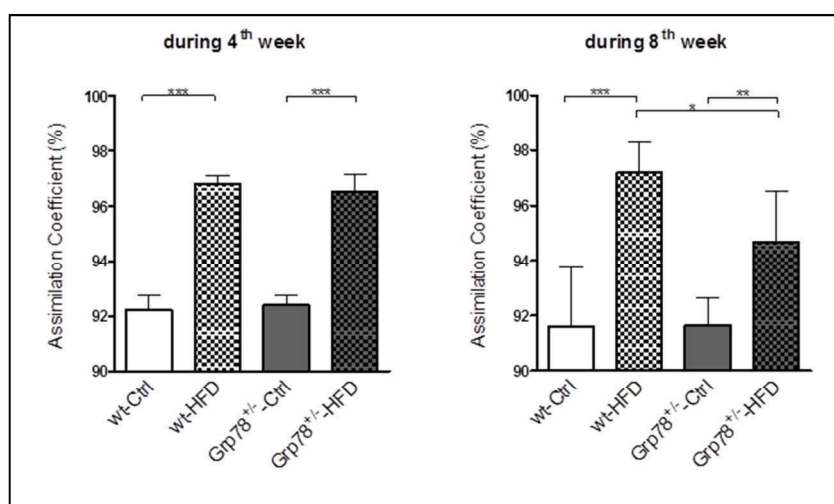


**Figure 17: Assimilation coefficient of Grp78<sup>+/-</sup> mice at different time points during the feeding trial**

During the 4<sup>th</sup> and the 8<sup>th</sup> week of fed Grp78<sup>+/-</sup> mice and their wt littermates a control or high fat diet, the assimilation coefficient was determined. Statistical analysis was performed by one-way ANOVA followed by turkey's test, (\* $p \leq 0.05$ , \*\* $p \leq 0.01$ , \*\*\* $p \leq 0.001$ ).

Furthermore, we also measured the resting metabolic rate (RMR) during the 8<sup>th</sup> week of the feeding trial. Here we could not find any difference between the genotypes in the amount of daily energy expended by the mice. The amount of energy expended in the night differed between the genotypes. Whereas there is a correlation between

the energy expenditure and the weight of mouse in the wt group, this correlation disappeared in the Grp78<sup>+/-</sup> group.

### **Metabolic characteristics and organ development**

To test whether the diets or the genotype have an effect on the glucose sensitivity, a glucose tolerance test (GTT) was performed 3 days before sacrificing. Surprisingly, no significant difference between the groups could be observed.

Additionally, we investigated plasma levels for glucose, insulin and triglycerides after a fasting period of 6 h for the insulin sensitivity and triglyceride metabolism. The plasma glucose as well as the plasma insulin level could give evidence whether the mice develop insulin resistance or not. There are no significant differences between the four groups for plasma glucose as well as for plasma insulin level. Furthermore, we calculated the HOMA-IR, a surrogate parameter for the insulin resistance. Plasma insulin levels as well as the HOMA-IR were elevated in the high fat diet groups independent of the genotype. These results correlated with an elevation of the area under the curve of the glucose tolerance test. The triglycerides in plasma seemed to be unaffected by the diet and were similar between wt and Grp78<sup>+/-</sup> mice (Figure 18).

The question whether the genotype and/or the different diets exert an effect on the development of several organs has to be answered. After a feeding trial of 8 weeks, we sacrificed the mice at an age of 12 weeks. The weight of high fat diet fed mice was significantly higher compared to their controls, with a difference of  $24.13 \pm 3.32\text{g}$  to  $20.01 \pm 2.78\text{g}$  and  $24.61 \pm 4.10\text{g}$  to  $20.17 \pm 2.42\text{g}$  in the wt and Grp78<sup>+/-</sup> group, respectively. Neither the epididymal fat (EP fat) nor the mesenteric fat (Mes fat) showed significant differences in their weight after the feeding process. Furthermore, we isolated the liver as well as the spleen and the whole intestine. All these organs showed a similar phenotype, except the caecum which is significantly heavier in the control group compared to the high fat diet group independent of the genotype (Table 3).

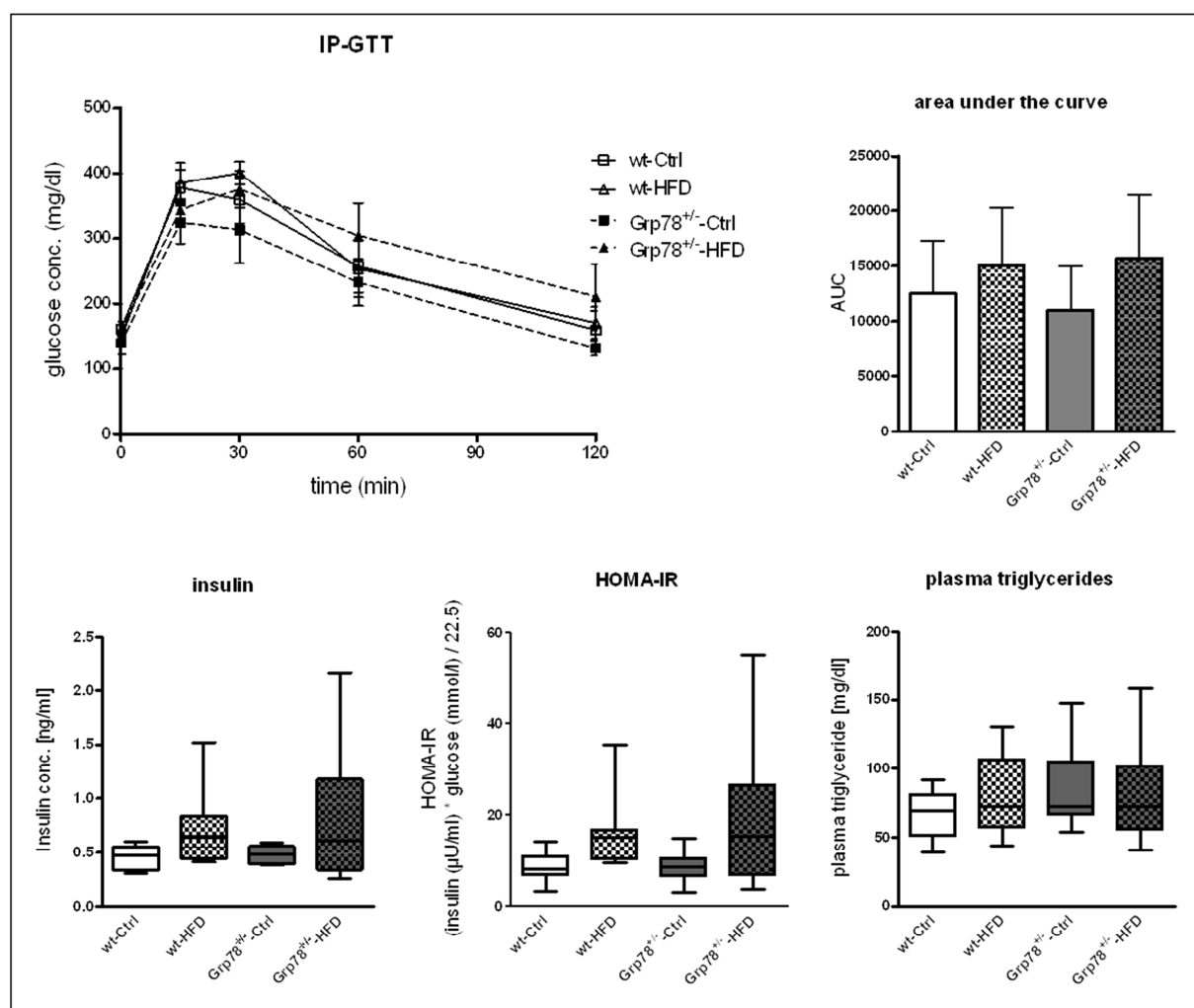


**Figure 18: Glucose tolerance test, insulin levels, and HOMA-IR as well as plasma triglycerides of Grp78<sup>+/-</sup> mice after 8 weeks fed a control and a high fat diet**

After 7 weeks of feeding a glucose tolerance test of Grp78<sup>+/-</sup> mice and their wt littermates (only males, n $\geq$ 5) was performed (repeated measures two-way ANOVA: \*p<0.05, \*\*p<0.01, \*\*\*p<0.001).

After sacrificing, plasma insulin levels as well as plasma triglyceride levels were determined (n $\geq$ 10 per group). Furthermore the HOMA-IR was estimated from glucose and insulin plasma levels after death. Statistical analysis was performed by one-way ANOVA followed by turkey's test.

**Table 3: Weight of several organs of the Grp78<sup>+/-</sup> mice**

	wt-Ctrl	wt-HFD	Grp78 <sup>+/-</sup> -Ctrl	Grp78 <sup>+/-</sup> -HFD
<b>EP-fat depot</b> (% of body weight)	0.99 $\pm$ 0.31	1.31 $\pm$ 0.76	0.96 $\pm$ 0.27	1.46 $\pm$ 1.06
<b>Mes-fat depot</b> (% of body weight)	0.37 $\pm$ 0.11	0.52 $\pm$ 0.24	0.43 $\pm$ 0.08	0.51 $\pm$ 0.33
<b>Liver</b> (% of body weight)	3.90 $\pm$ 0.19	3.70 $\pm$ 0.32	3.95 $\pm$ 0.45	3.89 $\pm$ 0.32
<b>Spleen</b> (% of body weight)	0.32 $\pm$ 0.06	0.34 $\pm$ 0.06	0.31 $\pm$ 0.04	0.35 $\pm$ 0.04
<b>Caecum</b> (% of body weight)	0.92 $\pm$ 0.16	0.70 $\pm$ 0.15*	0.96 $\pm$ 0.20	0.68 $\pm$ 0.13**

\*-between the diet, #-between the genotype (\*p<0.05, \*\*p<0.01)

### Morphology and characterization of liver and adipose tissue

In obesity the liver pathology as well as the adipose tissue pathology has crucial relevance to classify and constitute the level of a disease. Therefore it is relevant if liver of Grp78<sup>+/-</sup> mice stores more lipids and react with different UPR activation compared to the wt littermates. We measured triglyceride levels in the liver and several cell stress markers using western blot. The triglyceride levels in the liver were significantly elevated in wt-HFD mice (144.95 ± 94.84 mg/g) compared to the wt-Ctrl group (68.25 ± 35.6 mg/g). The high variation is an evidence for responders and non-responders in the wt-HFD group. There was no considerable difference between the Grp78<sup>+/-</sup>-HFD group and the control group. The Oil-Red-O staining could also confirm these changes (Figure 19).

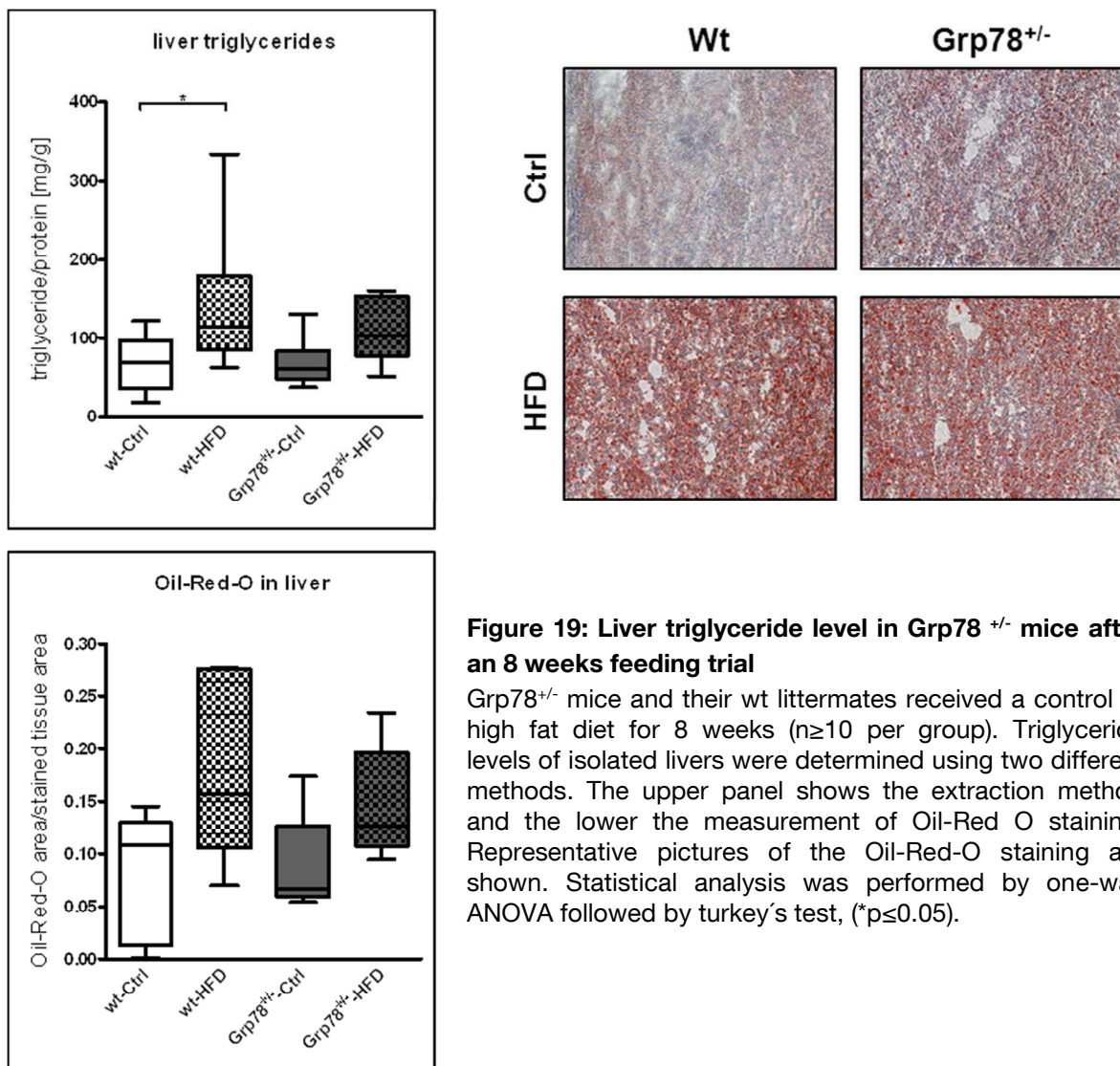


**Figure 19: Liver triglyceride level in Grp78<sup>+/-</sup> mice after an 8 weeks feeding trial**

Grp78<sup>+/-</sup> mice and their wt littermates received a control or high fat diet for 8 weeks (n≥10 per group). Triglyceride levels of isolated livers were determined using two different methods. The upper panel shows the extraction method and the lower the measurement of Oil-Red O staining. Representative pictures of the Oil-Red-O staining are shown. Statistical analysis was performed by one-way ANOVA followed by turkey's test, (\*p≤0.05).

Protein expression levels of several markers were investigated to get a hint of activated UPR in livers of the Grp78<sup>+/-</sup> mice. After the feeding period of 8 weeks, the animals were sacrificed at an age of 12 weeks. Protein levels of Grp78 as a typical marker for the erUPR was measured by western blot. For tissue samples, Coomassie staining was used as internal loading control. Grp78 seemed to be unaffected regardless genotype or diet. Only the high fat diet of the Grp78<sup>+/-</sup> mice resulted in an increase of Grp78 level (1.3 fold;  $p \leq 0.05$ ) compared to the wt-HFD group. Furthermore protein levels of Cpn60 as well as protein levels of PKR were measured. Both are considered to be involved in the mtUPR. Cpn60 levels as well as PKR levels did not differ between the feeding groups and the genotype. Only in the wt group the protein level of Cpn60 showed a difference between control and high fat fed mice. The wt-Ctrl mice had 1.5 fold higher Cpn60 levels than the wt-HFD group ( $p \leq 0.05$ ). To test whether there is a difference in the ERAD signaling, we investigated the protein levels of VCP. Surprisingly, there is a significant elevation (2.4 fold,  $p \leq 0.01$ ) of VCP protein level in Grp78<sup>+/-</sup> mice fed with the control diet compared to the wt-Ctrl mice (Figure 20).

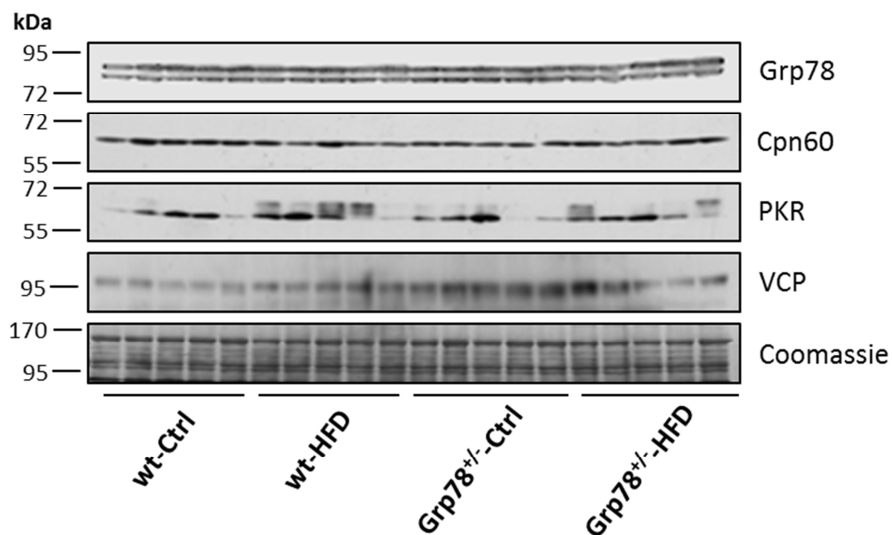
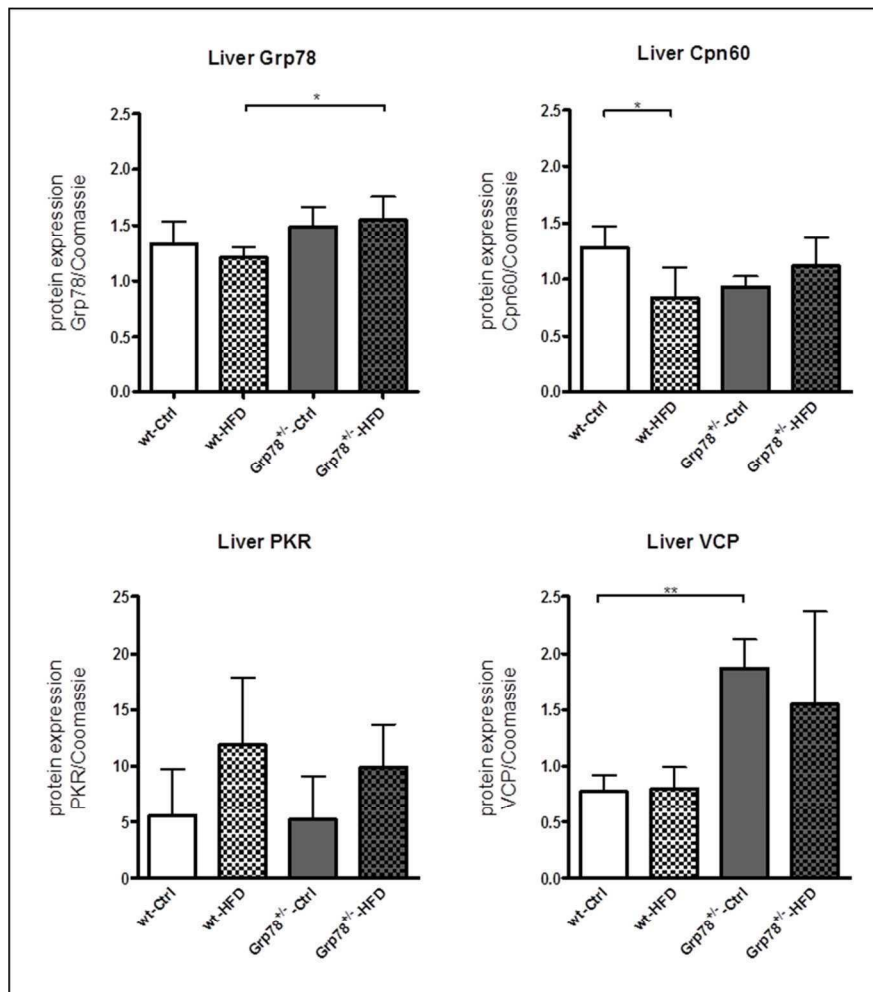


**Figure 20: UPR markers in liver of Grp78<sup>+/-</sup> mice fed either a control or a high fat diet**

For western blot analysis 20  $\mu$ g of total protein lysate was used. For each animal group the UPR markers Grp78, p-eIF2 $\alpha$ , Cpn60, PKR and VCP were detected (n=5 mice/group). Proteins were normalized to Coomassie staining of the membrane. Intensities of western blots are shown as relative protein expression (protein of interest/Coomassie) of n=5 animals. Statistical analysis was performed by one-way ANOVA followed by Bonferroni's multiple comparison test (\*p $\leq$ 0.05, \*\*p $\leq$ 0.01).

With regard to adipose tissue, we isolated epididymal fat of Grp78<sup>+/-</sup> mice as well as their wt littermates. Several mouse studies revealed that there might be a direct link between cellular stress, obesity and the development of type 2 diabetes (irrespective whether obesity has a genetic or a diet-induced background).<sup>50</sup> Therefore it is important if the size of adipocytes change and how the adipose tissue response to the different diets of our feeding experiment. In figure 21 adipocyte size and the distribution of the fat cell size is shown in the four different groups of animals. The fat cell size in the isolated epididymal fat pad is different not only between the genotype but also between the different diets. The fat cell size of the wt-Ctrl group ( $1,626 \pm 758.9\mu\text{m}^2$ ) is significantly smaller than the fat cell size of the wt-HFD group ( $2,309 \pm 1,138\mu\text{m}^2$ ) and bigger than the Grp78<sup>+/-</sup>-Ctrl group ( $1,375 \pm 746.4\mu\text{m}^2$ ). The fat cells of the Grp78<sup>+/-</sup>-HFD mice ( $3,070 \pm 1,884\mu\text{m}^2$ ) were bigger than the fat cells of the Grp78<sup>+/-</sup>-Ctrl group and also bigger than the fat cells of the wt-HFD group.

The distribution of the fat cell size showed that Grp78<sup>+/-</sup> mice under control diet have more small adipocytes compared to their wt littermates. Under high fat diet this effect disappeared, because there are a few cells between  $4 \times 10^3 \mu\text{m}^2$  and  $9 \times 10^3 \mu\text{m}^2$  in the epididymal adipose tissue of the Grp78<sup>+/-</sup>-HFD mice and this is not the case for the wt-HFD mice. For each group a representative HE stained picture is shown (Figure 21).

One can see in figure 21 that there were differences in the adipocyte size of epididymal fat between the genotypes and the diet they received. Therefore we used tissue sample of the epididymal fat pad to perform western blot analysis.

In white adipose tissue (WAT) we could observe the difference in Grp78 level under control diet. In the Grp78<sup>+/-</sup>-Ctrl mice we found half as much of the protein like in the wt-Ctrl mice (0.5 fold;  $p \leq 0.001$ ). Surprisingly, the high fat diet induces the protein expression of Grp78 in the Grp78<sup>+/-</sup>-HFD group compared to the Grp78<sup>+/-</sup>-Ctrl group. The level of Grp78 was 1.5 fold higher in the Grp78<sup>+/-</sup>-HFD group compared to the Grp78<sup>+/-</sup>-Ctrl group ( $p \leq 0.05$ ). Interestingly, the level of Cpn60 and PKR showed no differences independent of the genotype or the feeding regimen. Only VCP levels were significantly reduced in the Grp78<sup>+/-</sup>-Ctrl group compared to wt-Ctrl mice ( $0.07 \pm 0.05$  vs.  $0.53 \pm 0.37$ , respectively) ( $p \leq 0.05$ ) (Figure 22).

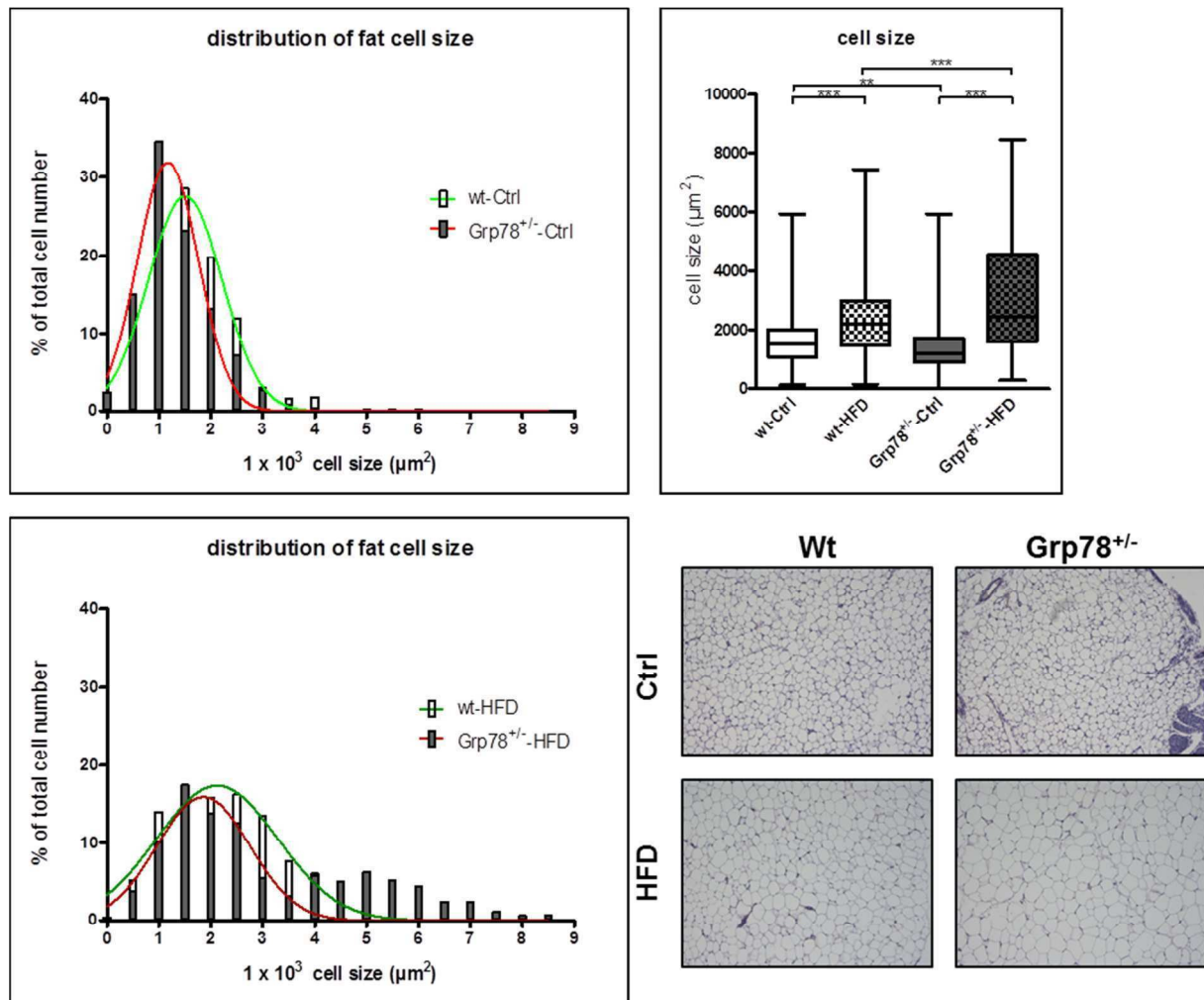


**Figure 21: Fat cell size and the distribution of fat cell size of Grp78<sup>+/-</sup> mice after 8 weeks fed with high fat diet or control diet**

After 8 weeks of feeding the animals were sacrificed and the epididymal fat depot was dissected. Paraffin slides for HE staining were prepared and the cell size was measured (n=500 per group and genotype). Afterwards the distribution of adipocytes was determined in % of the total cell number. Statistical analysis was performed by one-way ANOVA followed by turkey's test (\*\*p≤0.01, \*\*\*p≤0.001).



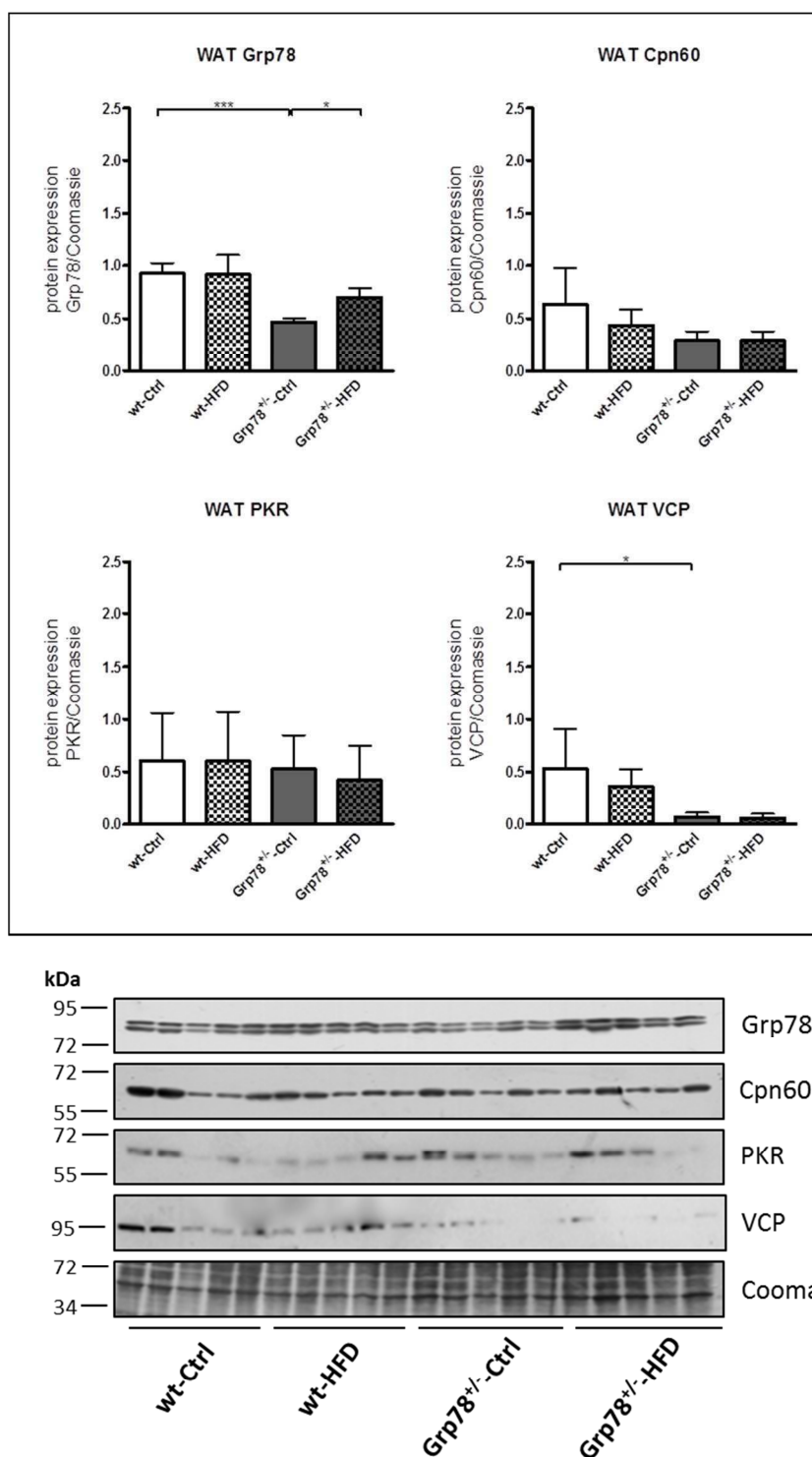


**Figure 22: UPR markers in WAT of *Grp78*<sup>+/-</sup> mice fed a control and a high fat diet**

For western blot analysis 20  $\mu$ g of total protein lysate was used. For each animal group the Grp78, p-eIF2 $\alpha$ , Cpn60, PKR and VCP were detected (n=5 mice/group). Coomassie staining of the membrane was used as internal control. Intensities of western blots are shown as relative protein levels (protein of interest/Coomassie) of n=5 animals. Statistical analysis was performed by one-way ANOVA followed by Bonferroni's multiple comparison test, (\*p $\leq$ 0.05, \*\*\*p $\leq$ 0.001).

### *Cpn60<sup>+/-</sup> mice – A basal characterization under a high fat diet*

As our *in vitro* data revealed Cpn60 is also highly enhanced during adipogenesis, we evaluate the relevance in Cpn60<sup>+/-</sup> mice. Therefore, we fed Cpn60<sup>+/-</sup> mice and their littermates to a high fat diet or a control diet for 8 weeks. Cpn60<sup>+/-</sup> mice did not show an obvious phenotype under normal conditions. Feeding them a high fat diet might therefore elicit a special response or a special phenotype due to the challenge of nutrition.

#### **Development of weight and body composition**

Regarding the weight development and total weight gain we could show that the HFD has a significant effect in the wt group and not in the Cpn60<sup>+/-</sup> group. As the wt-Ctrl mice gained  $8.52 \pm 2.51$ g and the wt-HFD mice gain  $12.46 \pm 3.35$ g ( $p \leq 0.05$ ), the Cpn60<sup>+/-</sup> group gain  $7.99 \pm 3.35$ g and  $11.88 \pm 3.82$ g, respectively. Interestingly, only Cpn60<sup>+/-</sup> mice show a significantly higher body weight at the end of the feeding experiment.

The body composition also differed between the genotypes. So we could show that wt-HFD mice had already a significantly higher fat mass ( $4.96 \pm 2.16$ g) compared to the wt-Ctrl mice ( $1.93 \pm 1.00$ g) ( $p \leq 0.05$ ) after receiving a HFD or a control diet for 4 weeks. For the Cpn60<sup>+/-</sup> group we could not observe this until week 8 of feeding, where the wt-HFD mice as well as the Cpn60<sup>+/-</sup>-HFD mice had significantly more fat mass compared to their control mice. The lean mass is the same between the different groups at each time point (Figure 23).

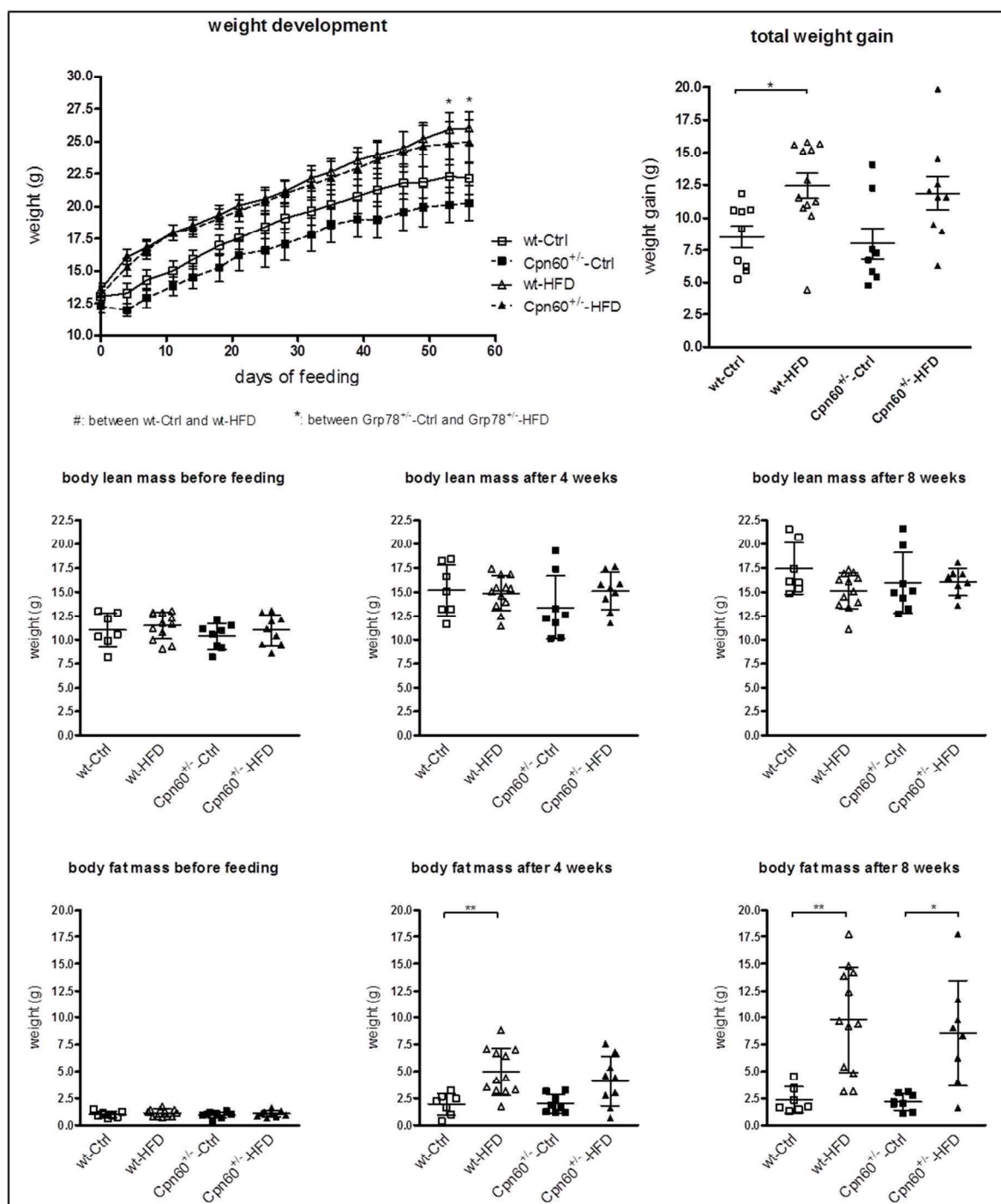


**Figure 23: Weight development, weight gain and the lean-/ fat-mass development of Cpn60<sup>+/-</sup> mice fed a control and a high fat diet**

For weight development each mouse in each group were weighed twice a week ( $n \geq 8$  per group). The weight was determined twice a week. Also the total weight gain was calculated. Lean and fat mass of the mice were measured before feeding (4 weeks old), after 4 weeks of feeding (8 weeks old) and after 8 weeks of feeding (12 weeks old).

Statistical analysis was performed by repeated measures two-way ANOVA and one-way ANOVA followed by turkey's test (\* $p \leq 0.05$ , \*\* $p \leq 0.01$ , \*\*\* $p \leq 0.001$ ).

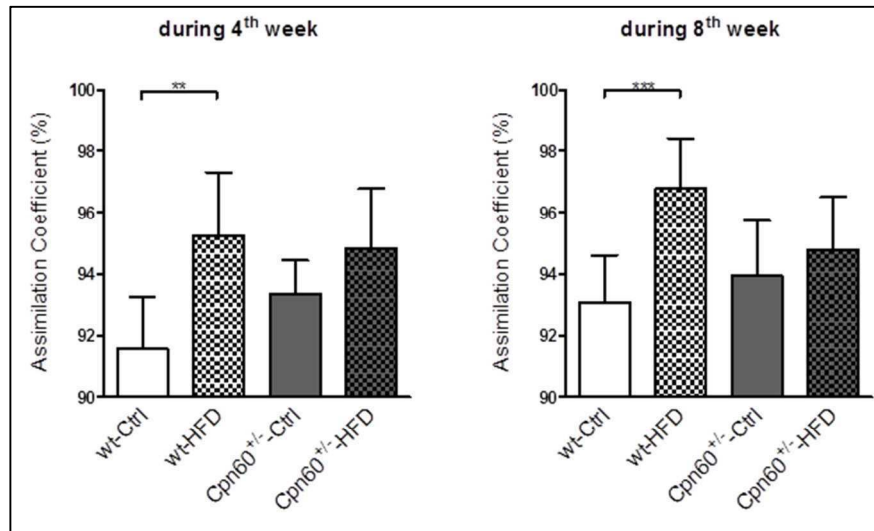


**Figure 24: Assimilation coefficient of Cpn60<sup>+/-</sup> mice during the 4<sup>th</sup> and the 8<sup>th</sup> week of feeding**

After 3 and 7 weeks of feeding the assimilation coefficient was estimated from food uptake data and excreted feces. The assimilation coefficient was computed ( $n \geq 8$  per group). Statistical analysis was performed by one-way ANOVA followed by turkey's test, (\*\* $p \leq 0.01$ , \*\*\* $p \leq 0.001$ ).

### Assimilation of food during feeding

For the assimilation coefficient in the 4<sup>th</sup> and 8<sup>th</sup> week of feeding, we measured food intake and the excretion of feces in all groups ( $n \geq 8$  in each group). For both genotypes we could not find any significant difference in food uptake or excretion of feces neither in the 4<sup>th</sup> week nor in the 8<sup>th</sup> week fed mice with a high fat diet or a control diet. Surprisingly, the assimilation coefficient was already higher ( $p \leq 0.01$ ) in wt-HFD mice ( $95.22 \pm 2.08\%$ ) than in wt-Ctrl mice ( $91.56 \pm 1.72\%$ ). Cpn60<sup>+/-</sup>-Ctrl mice and Cpn60<sup>+/-</sup>-HFD mice showed assimilation coefficients of  $94.81 \pm 1.96\%$  and  $93.38 \pm 1.06\%$ , respectively. In the 8<sup>th</sup> week of feeding this difference persisted, whereas the assimilation coefficient of the wt group raised up to  $96.76 \pm 1.64\%$  for the wt-HFD mice and  $93.10 \pm 1.50\%$  for the wt-Ctrl mice ( $p \leq 0.001$ ). The assimilation coefficient in the Cpn60<sup>+/-</sup> group was the same as in the 4<sup>th</sup> week with  $94.76 \pm 1.74\%$  for the Cpn60<sup>+/-</sup>-HFD mice and  $93.93 \pm 1.79\%$  for the Cpn60<sup>+/-</sup>-Ctrl mice (Figure 24).

Furthermore we also measured the resting metabolic rate (RMR) during the 8<sup>th</sup> week of the feeding trial. Here we could not find any difference between the genotypes in the amount of energy expended by the mice neither at day nor at night. A correlation between the energy expenditure and the weight of mouse could be observed ( $r=0.7233$ ;  $p=0.0002$ ). Only the oxygen consumption under the resting state is

significantly higher in the Cpn60<sup>+/-</sup>-HFD group ( $103.0 \pm 8.77$  ml O<sub>2</sub>/h) compared to the wt-HFD group ( $82.13 \pm 10.64$  ml O<sub>2</sub>/h).

### **Metabolic characteristics and organ development of Cpn60<sup>+/-</sup> mice**

The intraperitoneal glucose tolerance test (GTT) was performed 3 days before sacrificing. Figure 26 shows that mice fed with a high fat diet had higher glucose levels with a diminished decrease after 15 min. Ctrl mice showed a rapid decrease of blood glucose after 15 min. This could be measured by the area under the curve of the blood glucose levels which is higher in the HFD-groups.

Plasma insulin levels were elevated in high fat diet fed mice and with significant differences between Cpn60<sup>+/-</sup>-Ctrl mice ( $0.41 \pm 0.23$  ng/ml) and Cpn60<sup>+/-</sup>-HFD mice ( $1.44 \pm 0.91$  ng/ml) ( $p \leq 0.05$ ). Cpn60<sup>+/-</sup>-HFD mice showed high variation which is an evidence for responders and non-responders in this group. The estimated HOMA-IR, a surrogate parameter for insulin resistance, was also significant between Cpn60<sup>+/-</sup>-Ctrl ( $9.71 \pm 4.37$ ) and Cpn60<sup>+/-</sup>-HFD mice ( $31.09 \pm 23.99$ ) ( $p \leq 0.05$ ). The HOMA-IR of wt-Ctrl mice ( $18.51 \pm 8.19$ ) is almost 2 fold higher compared to Cpn60<sup>+/-</sup>-Ctrl mice, even though it is not significant. Additionally, we determined triglyceride levels in plasma. The triglyceride level significantly increased in mice fed a high fat diet independent of their genotype. Surprisingly, Cpn60<sup>+/-</sup>-HFD mice ( $151.7 \pm 8.52$  mg/dl) had significantly higher triglyceride levels than wt-HFD mice ( $137.7 \pm 6.52$  mg/dl) ( $p \leq 0.05$ ) (Figure 25).

The weight of the HFD fed mice in the Cpn60<sup>+/-</sup> group was significantly higher compared to their control group, with  $25.62 \pm 4.26$  g and  $20.25 \pm 3.79$  g, respectively. Both fat depots, the EP fat and the Mes fat were significantly heavier in the high fat diet group independent of their genotype ( $p \leq 0.05$ ). The liver as well as the spleen differed neither between the genotype nor between the diets. In this experiment the caecum is also significantly heavier in the control group of the wt mice ( $p \leq 0.001$ ) and in the control group of Cpn60<sup>+/-</sup> mice ( $p \leq 0.001$ ) than in the high fat diet fed groups (Table 4).

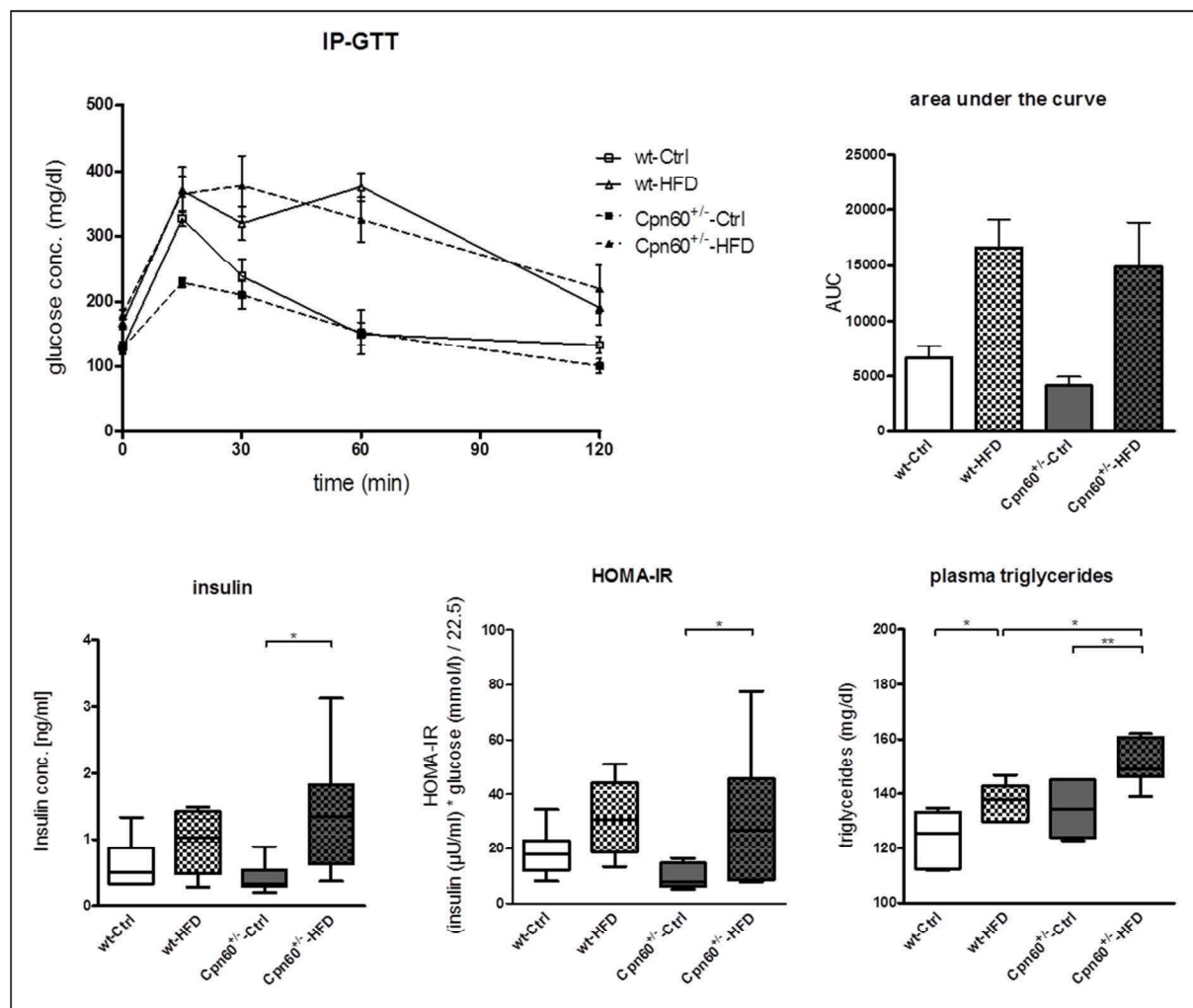


**Figure 25: Glucose tolerance test, insulin levels, and HOMA-IR as well as plasma triglycerides of Cpn60<sup>+/-</sup> mice fed a high fat diet or a control diet**

After 7 weeks of feeding a glucose tolerance test was performed in Cpn60<sup>+/-</sup> mice and their wt littermates (only males, n≥5, n=2 for Cpn60<sup>+/-</sup>-Ctrl). After sacrificing, plasma insulin levels as well as plasma triglyceride levels were determined (n≥8 per group). Statistical analysis was performed by one-way ANOVA followed by turkey's test, (\*p≤0.05, \*\*p≤0.01).

**Table 4: Organ weights of Cpn60<sup>+/-</sup> mice**

	Wt-Ctrl	Wt-HFD	Cpn60 <sup>+/-</sup> Ctrl	Cpn60 <sup>+/-</sup> HFD
<b>EP-fat depot</b> (% of body weight)	1.39 ± 0.44	3.14 ± 1.55**	1.06 ± 1.26	2.88 ± 1.44*
<b>Mes-fat depot</b> (% of body weight)	0.41 ± 0.16	0.88 ± 0.35**	0.32 ± 0.52	0.93 ± 0.28**
<b>Liver</b> (% of body weight)	4.16 ± 0.34	3.79 ± 0.33	4.08 ± 0.39	3.90 ± 0.13
<b>Spleen</b> (% of body weight)	0.28 ± 0.04	0.28 ± 0.07	0.34 ± 0.04	0.30 ± 0.05
<b>Caecum</b> (% of body weight)	1.04 ± 0.19	0.67 ± 0.12***	1.23 ± 0.24	0.64 ± 0.25***

\*-between the diet, #-between the genotype (\*p<0.05, \*\*p<0.01, \*\*\*p<0.001)

## Morphology and characterization of liver and adipose tissue

Regarding the storage of lipids in the liver and the stress response due to the different diets, we measured triglyceride levels on the one hand and on the other hand we performed western blot analysis of liver samples. We could show, that triglyceride levels in the wt-HFD group are significantly elevated compared to their control group ( $p \leq 0.001$ ). The levels vary between  $127.9 \pm 14.02 \text{ mg/g}$  for the wt-Ctrl mice,  $188.3 \pm 15.46 \text{ mg/g}$  for the wt-HFD mice,  $148.7 \pm 16.85 \text{ mg/g}$  for the Cpn60<sup>+/-</sup>-Ctrl mice and  $165.4 \pm 19.77 \text{ mg/g}$  for the Cpn60<sup>+/-</sup>-HFD mice. Triglycerides in the Cpn60<sup>+/-</sup>-HFD group seemed to be not that elevated and were significantly reduced compared to the wt-HFD animals in the Oil-Red-O method ( $p \leq 0.05$ ) (Figure 26).

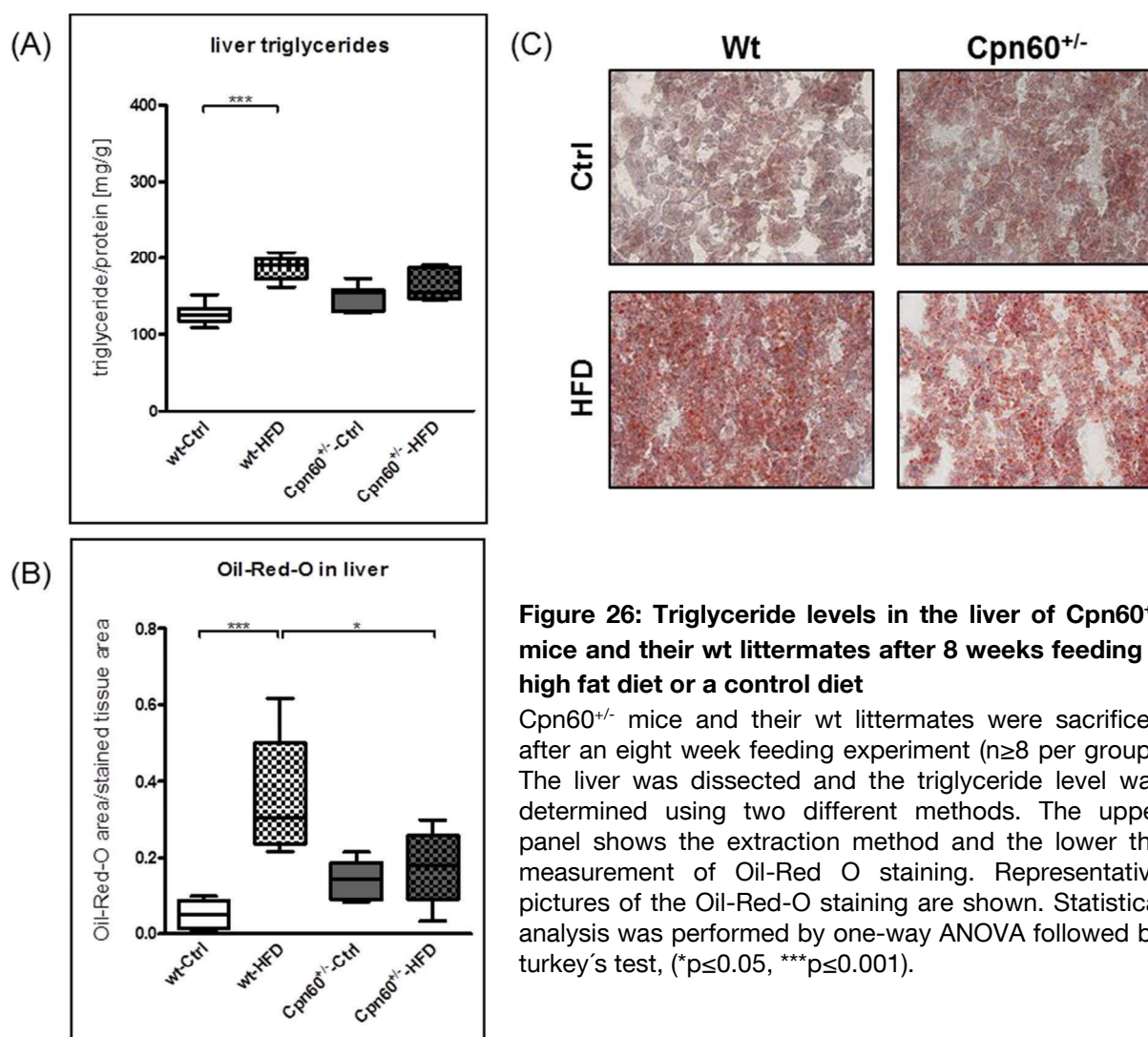


**Figure 26: Triglyceride levels in the liver of Cpn60<sup>+/-</sup> mice and their wt littermates after 8 weeks feeding a high fat diet or a control diet**

Cpn60<sup>+/-</sup> mice and their wt littermates were sacrificed after an eight week feeding experiment ( $n \geq 8$  per group). The liver was dissected and the triglyceride level was determined using two different methods. The upper panel shows the extraction method and the lower the measurement of Oil-Red O staining. Representative pictures of the Oil-Red-O staining are shown. Statistical analysis was performed by one-way ANOVA followed by turkey's test, ( $*p \leq 0.05$ ,  $***p \leq 0.001$ ).

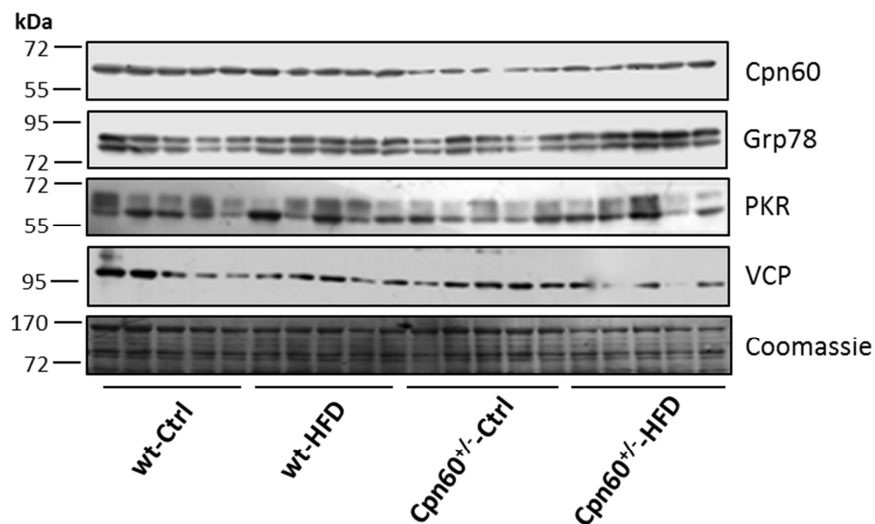
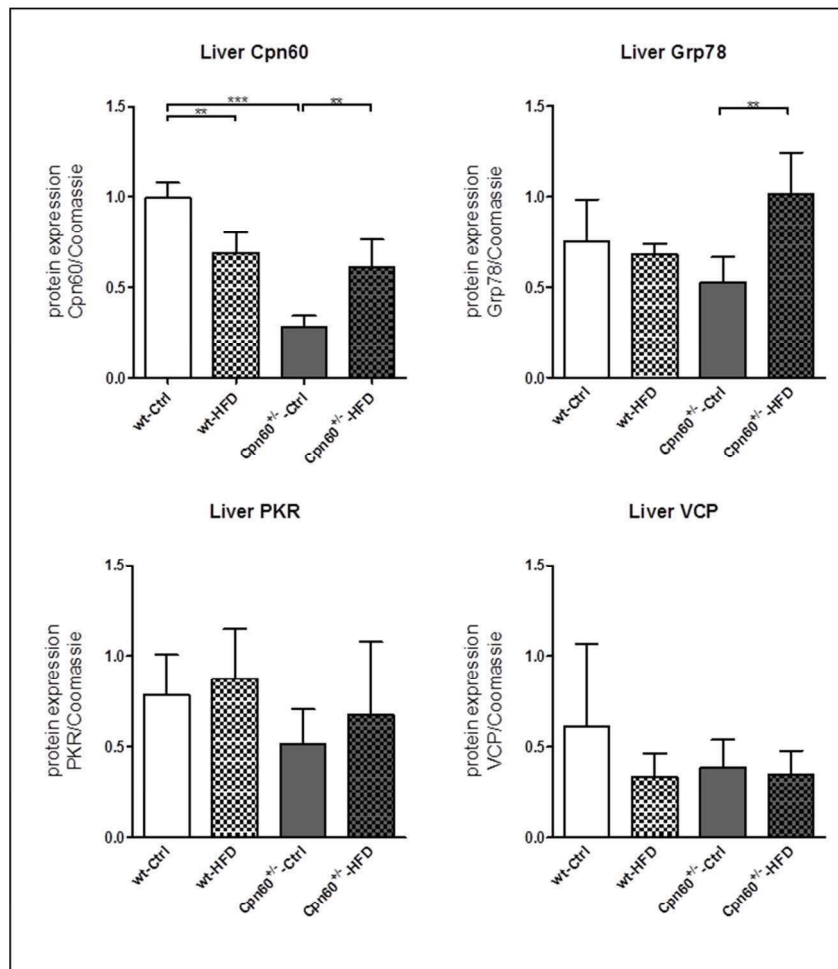


**Figure 27: Protein levels of UPR markers in liver of Cpn60<sup>+/-</sup> mice after a feeding trial of 8 weeks** 20 µg of total liver protein was used for western blot analysis. For western blot analysis 20 µg of total protein lysate was used. For each animal group the UPR markers Grp78, p-eIF2α, Cpn60, PKR and VCP were detected (n=5 mice/group). Coomassie staining of the membrane was used as internal control. Intensities of western blots are shown as relative protein levels (protein of interest/Coomassie) of n=5 animals. Statistical analysis was performed by one-way ANOVA followed by Bonferroni's multiple comparison test, (\*\*p≤0.01, \*\*\*p≤0.001)



After 8 weeks of feeding we sacrificed the mice at an age of 12 weeks and liver samples were used for western blot analyses. The protein level of Cpn60 in the liver clearly showed the heterozygous knock out of Cpn60 in the Cpn60<sup>+/-</sup>-Ctrl animals compared to the wt-Ctrl mice, with relative protein levels of  $0.28 \pm 0.06$  and  $0.99 \pm 0.08$ , respectively ( $p \leq 0.001$ ). Interestingly, the Cpn60 level was reduced in wt-HFD mice ( $0.69 \pm 0.11$ ) compared to the wt-Ctrl mice ( $p \leq 0.01$ ), whereas it was increased in Cpn60<sup>+/-</sup>-HFD animals ( $0.61 \pm 0.16$ ) compared to Cpn60<sup>+/-</sup>-Ctrl mice by 217% ( $p \leq 0.01$ ). Grp78 levels were significantly increased in Cpn60<sup>+/-</sup> mice under a high fat diet compared to their control animals, with levels of  $1.02 \pm 0.23$  and  $0.53 \pm 0.14$  ( $p \leq 0.01$ ), respectively. Protein levels of PKR and VCP seemed to be unaffected regardless of genotype or diet (Figure 27).

Figure 28 shows the adipocyte size and the distribution of fat cell size of the four different groups. The distribution of the fat cell size in the animals which received a control diet showed that Cpn60<sup>+/-</sup>-Ctrl mice have smaller adipocytes than mice from the wt-Ctrl group. Surprisingly, this effect disappears if mice were fed with a high fat diet. The adipocytes of the wt-HFD group ( $3,019 \pm 1,496 \mu\text{m}^2$ ) are significantly bigger than the adipocytes of the wt-Ctrl group ( $1,776 \pm 890.2 \mu\text{m}^2$ ) ( $p \leq 0.001$ ). The same was observed for adipocytes from Cpn60<sup>+/-</sup>-HFD mice ( $3,050 \pm 1,696 \mu\text{m}^2$ ) compared to their control group ( $1,552 \pm 779.9 \mu\text{m}^2$ ) ( $p \leq 0.001$ ). The only difference between the genotypes existed between the wt-Ctrl group and the Cpn60<sup>+/-</sup>-Ctrl animals, because the Cpn60<sup>+/-</sup>-Ctrl animals have significantly smaller adipocytes than the wt-Ctrl mice ( $p \leq 0.05$ ). For each group a representative HE stained picture is shown (Figure 28).

In white adipose tissue (WAT) we could show a difference in all of the proteins we measured using western blot. In the heterozygous genotype (Cpn60<sup>+/-</sup>-Ctrl) we found a drastic reduction of Cpn60 by 84% ( $p \leq 0.01$ ) compared to wt-Ctrl mice. Also Grp78 was different between the genotypes but only when they were fed with a high fat diet. Grp78 decreased in the Cpn60<sup>+/-</sup>-HFD group (relative protein level of  $0.69 \pm 0.14$ ) compared to the wt-HFD mice (relative protein level of  $1.15 \pm 0.07$ ). PKR and VCP differed between the genotypes but only in the control diet groups. In Cpn60<sup>+/-</sup>-Ctrl mice we found a reduction of PKR by 89% ( $p \leq 0.01$ ) compared to wt-Ctrl mice. Relative protein level of VCP was significantly increased in Cpn60<sup>+/-</sup>-Ctrl mice ( $4.74 \pm 2.66$ ) compared to the wt-Ctrl group ( $0.20 \pm 0.45$ ) ( $p \leq 0.01$ ) (Figure 29).

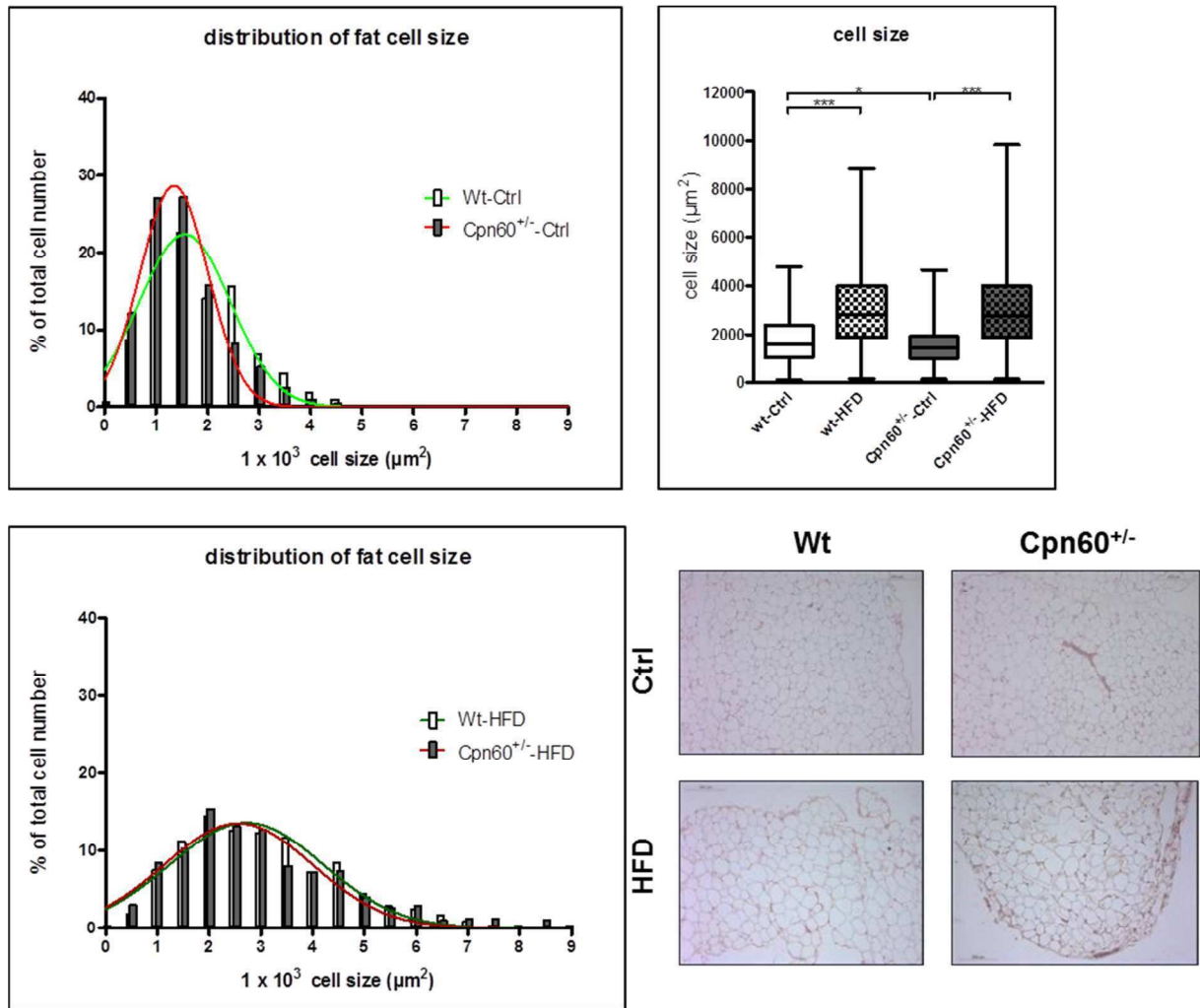


**Figure 28: Fat cell size and the distribution of fat cell size of Cpn60<sup>+/-</sup> mice after an eight week feeding experiment**

The mice were sacrificed after 8 weeks of feeding a high fat or control diet. The epididymal fat depot was dissected. Paraffin slides for HE staining were prepared and the cell size was measured (n=500 per group and genotype). Afterwards the distribution of cell sizes of adipocytes was determined in % of the total cell number. Statistical analysis was performed by one-way ANOVA followed by turkey's test, (\*p≤0.05, \*\*\*p≤0.001).

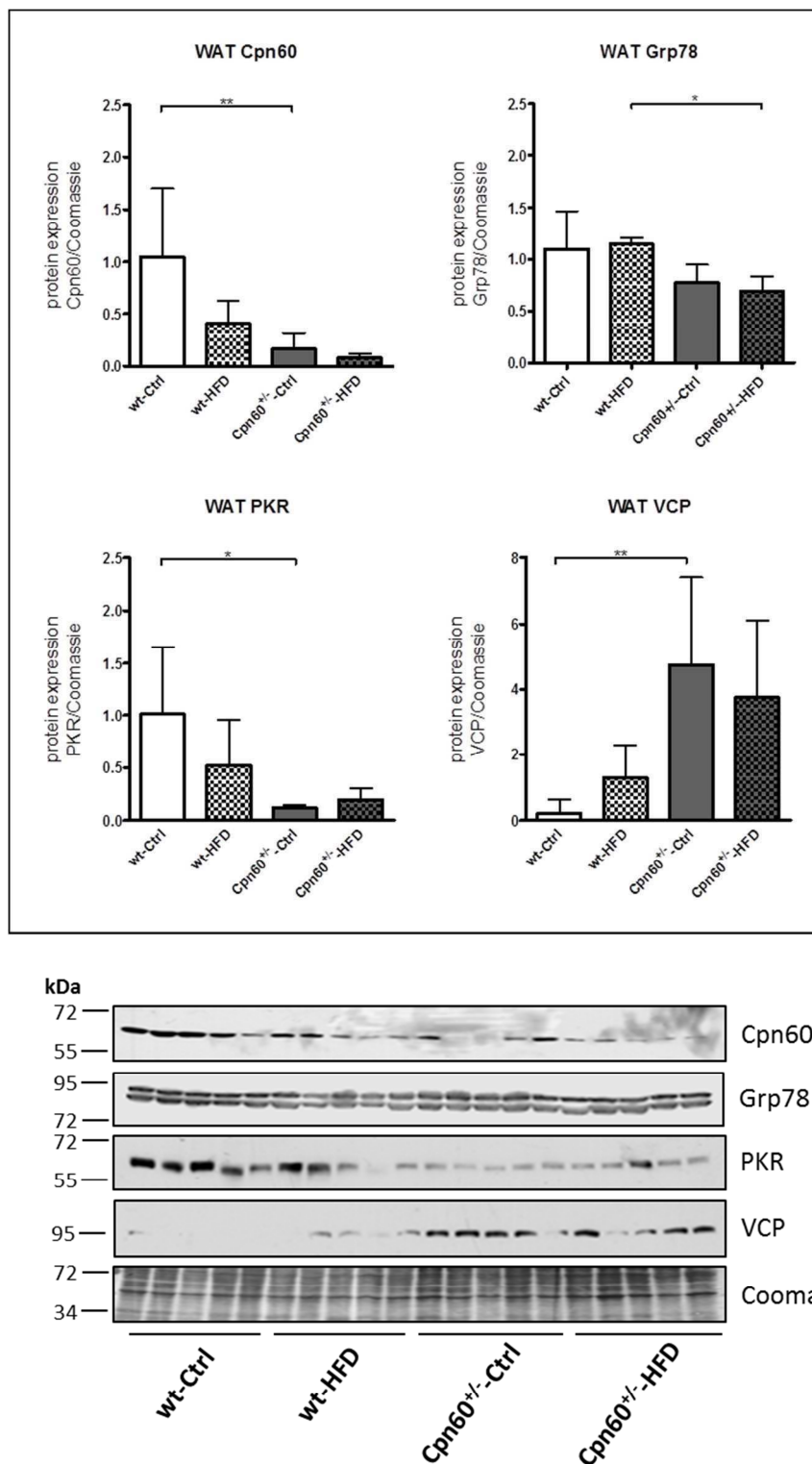


**Figure 29: UPR markers in WAT of Cpn60<sup>+/-</sup> mice fed a high fat diet for 8 weeks**

Western blot analysis was performed using 20  $\mu$ g of total protein lysate. For western blot analysis 20  $\mu$ g of total protein lysate was used. For each animal group the UPR markers Grp78, p-eIF2 $\alpha$ , Cpn60, PKR and VCP were detected (n=5 mice/group). Coomassie staining of the membrane was used as internal control. Intensities of western blots are shown as relative protein expression (protein of interest/Coomassie) of n=5 animals. Statistical analysis was performed by one-way ANOVA followed by Bonferroni's multiple comparison test, (\*p $\leq$ 0.05, \*\*p $\leq$ 0.01, \*\*\*p $\leq$ 0.001).



## Discussion

### ***UPR during adipogenic differentiation***

#### *Markers of the UPR vary during the process of adipogenic differentiation*

Recent reports suggested that obesity and related metabolic complications are associated with ER-stress in adipose tissue,<sup>118,69</sup> which may also contribute to local inflammation. We therefore investigated the development of signaling markers activated upon the erUPR during adipose differentiation in two established human models (SGBS and primary preadipocytes) and compared these results with the murine 3T3-L1 model, which is widely used for mechanistic studies. All cell models showed more or less the same secretion pattern of adipokines. Adiponektin was not detectable in preadipocytes, only after induction (day 4) it increased. This is in line with further studies as adiponektin is highly expressed and secreted by mature adipocytes and preadipocytes which differentiate into adipocytes.<sup>119,120</sup> During obesity and even further in insulin resistance and type 2 diabetes the expression and secretion of adiponektin is reduced.<sup>121</sup>

To investigate the development of signaling markers activated upon the erUPR we performed western blot analysis. In all cell models investigated in this work, we performed Coomassie staining as it was found to be a sensitive and stable internal control for protein studies during adipogenesis.<sup>114</sup> The interpretation of the results from primary isolated human preadipocytes is not simple, as the cells are derived from different donors. Thus, it is possible that multiple experiments result in heterogeneous outcomes, as the cells are of different genetic background. To overcome this problem more experiments should be done. How many depends on the factor which is investigated and the result of the power-calculation.

Our results demonstrate that neither preadipocytes nor SGBS cells induce classical markers of the erUPR like Grp78 or p-eIF2 $\alpha$  during the *in vitro* differentiation process. The levels of these markers were even continuously reduced throughout the differentiation process which was more pronounced in SGBS cells compared to freshly prepared human preadipocytes. One can assume that with a higher amount of experiments for the preadipocytes more significant results with less variation could be shown. Interestingly, the data obtained in 3T3-L1 cells show a different

pattern for these erUPR markers with constantly increasing levels of Grp78, whereas p-eIF2 $\alpha$  significantly decreased. Phosphorylation of eIF2 $\alpha$  was known to have a repressing effect on PPAR $\gamma$  and C/EBP $\alpha$  expression, thereby exerting an inhibitory signal to the differentiation cascade.<sup>122,123</sup> A reduced expression and phosphorylation of these factor could therefore promote adipogenic differentiation.

An important aspect of adipose cellularity is adipocyte hypertrophy which is probably closer associated with various comorbidities than adipose tissue mass per se. A hypertrophic type of obesity is strongly associated with the development of insulin resistance<sup>124</sup> and large fat cells significantly predict the risk for future diabetes in men and women.<sup>125,126</sup> Therefore, we measured cell size and markers of the UPR in the AT of subjects with or without type 2 diabetes mellitus. As already reported before<sup>125</sup>, fat cell size was increased in the subjects with diabetes. This increase in adipocyte volume was associated with higher macrophage infiltration in adipose tissue (Table 2). Taken together adipose tissue of patients with type 2 diabetes mellitus reveals a profile towards inflammation. Up-regulation of Grp78 in AT of T2D subjects could not be explained by larger adipocytes but rather as an effect of other cells located in the adipose tissue. Nevertheless, a larger number of samples should be evaluated to confirm the data.

Not only an erUPR could be activated by obesity but also the mitochondrial function is disturbed by negative environmental effects. The mtUPR could restore the cell homeostasis like the erUPR and increase the production of chaperones like Cpn60. Our data indicate that also the mtUPR is somehow activated by the differentiation process. In all cell models investigated Cpn60 increased during the course of differentiation. These findings are in line with results from other groups as Cpn60 and Cpn60 responsiveness is a basic functional property of adipocytes.<sup>127,128</sup> The double-stranded RNA-activated protein kinase (PKR) is also relevant in the activation of the mtUPR.<sup>86</sup> Additionally, it has been described that PKR participates in erUPR as well as it is up-regulated under obese situations.<sup>116,117</sup> But in none of the cell models PKR levels increased during differentiation. The levels of this marker were even continuously reduced throughout the differentiation process in freshly prepared human preadipocytes. As always, three independent western blots were combined in densitometric measurement, sometimes the western blot which is shown below differs from the graph, like in Figure 5. The bands in the western blot

of PKR in primary isolated human preadipocytes are very intensive at day 0, day 3 and day 8. At day 16 the band almost disappeared. As the graph indicates, even on day 8 no PKR should be seen. This is because the other experiments show a different pattern for PKR, and the densitometric analysis displays the arithmetic mean.

Another downstream transcription factor of the erUPR and the mtUPR is C/EBP homologous protein (CHOP). Transcription of CHOP is considered to mediate apoptosis.<sup>129</sup> Other studies have shown that ER stress is also involved in pancreatic  $\beta$ -cell apoptosis. This was mediated through CHOP which can be induced in the PERK, as well as in the ATF6 pathway during the erUPR.<sup>130</sup> In our experiments we could show that CHOP tended to increase throughout the differentiation process in all cell models investigated. CHOP was shown before to be activated upon erUPR as well as mtUPR.<sup>41,64</sup> As Grp78 was not induced during adipogenesis in the human cell models, the induction of CHOP indicates an activation by mtUPR. In all cells lines investigated we could show an induction of Cpn60, which confirms this assumption.

Concluding the experiments for the UPR markers each western blot shows the total amount of protein whereas the densitometric measurement, which combined three independent western blots only show a tendency how the protein changes during the course of differentiation. Therefore a statement about the protein amount in the cells cannot be made with this analysis. In these experiments the western blot only shows if there is protein on day 0 and how it changes (increase or decrease) during adipogenesis.

### ERAD and inflammation are important during the process of adipogenic differentiation

In our differentiation experiments we could show, that the process called ERAD (endoplasmic reticulum associated degradation), which is activated downstream of the UPR, seems to be relevant in regard of adipocyte size and the development of diseases like diabetes. Unfolded or misfolded proteins which are retained in the ER were eliminated/de-translocated by ERAD. Therefore, it is not surprising, that an activated ERAD is closely related to the pathogenesis of many diseases<sup>131</sup>, like diabetes in Akita insulin mutant mice.<sup>132</sup>

We measured VCP (valosin-containing protein), a cytosolic ATPase associated with various cellular activities and essential for de-translocation of misfolded proteins during ERAD.<sup>55</sup> VCP is activated in primary isolated preadipocytes as well as in SGBS cells during differentiation. 3T3-L1 cells showed a different pattern for VCP. During the induction period (day 0 to day 3) and until day 6 of differentiation VCP increased. Afterwards it almost disappeared. The induction of VCP in the human cell models could indicate that without activating UPR by Grp78, the human cell line deals with the increased protein load in the ER for maintaining the homeostasis of the cell.<sup>133</sup> Therefore, the fact that the cells do not undergo apoptosis by induction of CHOP might argue that they stay alive by ERAD.

Nevertheless, figure 6 also shows high standard variation, which occurs because we combined three independent western blots for the densitometric analysis. For primary isolated preadipocytes the western blots differed even more from the graph as the western blot of the SGBS cells. This is the case as there are more influencing factors from human donors (age and gender). For SGBS cells the western blot shows a high signal and therefore it is difficult to give a reliable interpretation of it. Figure 11 shows the results for VCP in 3T3-L1. The western blot which is shown is one out of three where a signal for VCP on day 13 and day 17 could be detected. The other two western blots (not shown) show no signal of VCP from day 10 onto day 17.

To see whether adipogenic conversion is associated with inflammation we measured JNK, which is usually activated during the UPR.<sup>134</sup> The mitogen-activated-protein (MAP)-kinase was shown to regulate, among others, the expression of the NFkB-activating cytokine IL-6.<sup>135</sup> This predominantly pro-inflammatory immune mediator seems to be directly involved in the regulation of the ER-stress response.<sup>136</sup> JNK was also reported to cause an impairment of insulin signaling and may thereby act as a link between adipose tissue inflammation and insulin resistance.<sup>70</sup> Our results in human cells showed that JNK tended to decrease during differentiation and reach significance from day 11 on at least in SGBS-cells. This decline was paralleled by a reduction of IL-6 in the culture medium and might argue for the reduced inflammatory activity observed in differentiating adipocytes. Other studies have shown that reduced expression of JNK protected adipocytes from insulin resistance.<sup>137</sup> Interestingly, an increased JNK activity was not associated with



elevated IL-6 levels in 3T3-L1. The western blot of p-cJun (Figure 7B), a downstream target of JNK, shows high variation over the time and therefore no clear development could be realized. It is only possible to conclude that there is no significant change in the protein level of p-cJun during differentiation.<sup>138</sup>

As we found a difference between human and murine cell models in JNK levels, we investigated JNK levels in primary isolated mature adipocytes as well as in AT samples from men with NGT or T2D. In mature adipocytes and in clinical samples of AT from subjects with or without T2D higher leukocyte infiltration might argue for a higher inflammatory level in AT of T2D subjects. Interestingly, JNK levels of the AT were comparable between the two groups. There was no association of leukocyte infiltration with fat cell size in healthy controls, whereas there was a significant correlation in T2D subjects. We confirmed these results in primary human adipocytes and were able to show that JNK is increased in hypertrophied adipocytes.

In conclusion, we hypothesize that adipogenic differentiation and hypertrophy are not necessarily associated with elevated markers of erUPR in humans. The changes of these markers observed may be more likely a result of consecutive adaptations to the requirements of cell homeostasis. Nevertheless, it seems that factors from the UPR and pro-inflammatory markers like IL-6 are closely related, although it is unknown what is cause and consequence. Adipocyte size was usually higher in diabetic subjects and might therefore be responsible for the inflammatory state but less likely for the activation of erUPR. It might be speculated that not only adipocytes but also other cells (macrophages/leukocytes) act as a source of chronic adipose tissue inflammation via activation of erUPR. Therefore, disturbances in cellular integrity of adipose tissue may be responsible for the pro-inflammatory state observed in hypertrophic obesity.

### ***UPR in different mouse models***

#### ***Characteristics of adipose tissue in C57BL/6N mice of different ages***

Obesity is a disease with an expansion of the adipose tissue. The WAT comprises about 90% of this organ. Two major mechanisms can take place to facilitate the

storage of excess energy. On the one hand, adipose tissue growth may be caused by an increased lipid load per adipocyte (hypertrophy) and/or on the other hand by an increased number of adipocytes (hyperplasia). Hyperplasia appears early in lifetime, whereas hypertrophy is characterized by a late lifetime.<sup>139</sup> Rodent models are often used for research in several diseases as they are established and easy to feed with a high fat diet to become obese. For the characteristic analysis we use the epididymal adipose tissue of C57BL/6N mice of different age. The epididymal fat depot as well as the fat cell size of this depot increased from week 2 to week 12 in C57BL/6N mice. In humans has also be proposed that fat cell size increases with age, although there is no agreement in which period of life time hypertrophy and/or hyperplasia occur.<sup>140,141</sup> However, Spalding *et al.* could show, that hyperplasia only occurs during childhood, whereas the number of adipocytes stays constant and 10% of them are renewed annually at all adult ages.<sup>33</sup> Nevertheless, hypertrophy appears to be also a risk factor for metabolic diseases as it could be shown that an increase in adipocyte size is linked to insulin resistance.<sup>125</sup> Furthermore, it is suggested, that obesity and growth of fat cell size is a stimulus for stress response at a cellular level, like erUPR or mtUPR. We could confirm the findings of our *in vitro* experiments in C57BL/6N mice as we could show that Grp78 slightly decreased during development from 6 to 12 weeks. This effect was less prominent than in the human cell culture models, but it was clearly different from the 3T3-L1 cell line. This result accentuates the difference between murine cell line and *in vivo* mouse tissue. An increase during development could be confirmed for the mitochondrial chaperone Cpn60. This result shows no difference between the murine cell culture model and mouse tissue. The human cell lines responded in the same way for Cpn60. VCP did not show a clear tendency as it almost disappeared in week 8 and increased again until week 12. In this case hypertrophy might be the reason for these findings as VCP increase at that time point (12 weeks old) when the number of adipocytes didn't further increase.<sup>139</sup> The cells have to deal with an increase lipid load and therefore a lot of proteins have to be synthesized. More VCP is necessary for the cell to deal with the increased protein load in the ER for maintaining homeostasis.

In our experiment to assess the development of UPR markers in adipose tissue of C57BL/6N mice with different age (Figure 15) the interpretation of the western blots

are disputable. Only one mouse was used for the four week control, as mice are very small and have nearly no epididymal adipose tissue (less than 1% of total body weight). Also the protein levels of all investigated markers were very low at the age of four weeks. For week 6, 8, 10 and 12 two mice were used to perform western blot analyses with the epididymal adipose tissue. It is noticeable that sometimes the results of two single mice are contradictory (Figure 15). One example might be the level of Cpn60 in 8 week old mice. In one mouse Cpn60 could be detected and in the other one not. Therefore, one has to conclude that in this experiment the number of mice might be too low to provide a firm conclusion about the course of the protein level during the development. More C57BL/6N mice (biological replicates) would be needed to provide a reliable interpretation to the question if and how the protein level of UPR markers in adipose tissue of C57BL/6N mice changes with growing age. Furthermore one can assume that there is a high heterogeneity in C57BL/6N mice. Nevertheless in 6 and 12 week old mice there is a good signal on the western blot, which could indicate the increase of UPR markers in adipose tissue of C57BL/6N mice. As seen in the Coomassie staining of the western blot there is also a difference in the amount of proteins over the different age of the mice, especially week 4 compared to the others. It could be that epigenetic changes play a role in view of the protein profile in our mice. To analyze this, the number of mice investigated must be higher to provide a firm conclusion about the epigenetic influence. Nevertheless it could be shown before that Coomassie staining is a sensitive and stable internal control for protein studies during developmental analysis in adipocytes.<sup>114</sup>

To conclude this we can state that the results of the UPR *in vivo* in C57BL/6N mice are not comparable to murine 3T3-L1 but rather to the *in vitro* human cell culture models. With this knowledge, it is doubtful if results from the 3T3-L1 cell line could give a hint how the erUPR proceed in humans. Furthermore, our experiments show that mice trials are a good method to learn and understand more about the UPR as there are similarities between mice and human results.

Age and duration of high fat feeding is an important factor for protection of obesity in Grp78<sup>+/-</sup> mice

In a work from 2010, Risheng and colleagues showed that “Grp78 heterozygosity promotes adaptive unfolded protein response and attenuates diet-induced obesity and insulin resistance”.<sup>102</sup> As the Grp78<sup>-/-</sup> mouse is embryo lethal,<sup>101</sup> they use the Grp78<sup>+/-</sup> mouse for their experiments. Therein, Grp78<sup>+/-</sup> mice were fed with a high fat diet from week 10 until week 30. They could show that Grp78<sup>+/-</sup> mice had significantly lower body weight than the <sup>+/+</sup> siblings. This effect comes from lower fat mass and smaller body size. Furthermore, the O<sub>2</sub> consumption and the CO<sub>2</sub> production were elevated in Grp78<sup>+/-</sup> mice. In regard of the metabolic profile, Grp78<sup>+/-</sup> mice had lower blood glucose and blood insulin level. There were less lipid droplets in the liver and the WAT was not as inflamed in Grp78<sup>+/-</sup> mice under HFD in comparison to the <sup>+/+</sup> siblings under HFD. In this work they argued that the partial loss of Grp78 could mimic low chronic ER stress and promote adaptive erUPR.<sup>102</sup>

As we wanted to know whether the described results also occur in the early life of Grp78<sup>+/-</sup> mice, we tried to confirm these findings in Grp78<sup>+/-</sup> mice at an age of 12 weeks. We fed Grp78<sup>+/-</sup> mice and their <sup>+/+</sup> littermates a high fat diet from weeks 4 to 12. Consequently, we fed the mice only 8 weeks (in contrast to 20 weeks in the work of Risheng and colleagues<sup>102</sup>) and we also combined with female mice as we could not observe any differences between genders. The composition of the diet in regard of fat by calories was similar to the work of Risheng and colleagues.<sup>102</sup>

In our experiment we could not confirm the lower body weight or the differences in the body composition of the Grp78<sup>+/-</sup>-HFD group. The reason could be that the duration of HFD was only 8 weeks in our experiment. Comparing the results the body weight was not significantly different until week 14 in the published work. Concerning the energy expenditure we could only observe a trend that mice in the Grp78<sup>+/-</sup>-HFD group behave differently than wt-HFD mice. In regard of the metabolic profile, we did not see any difference between Grp78<sup>+/-</sup> mice and wt mice independent of the diet. The reason could be the duration of the exposure to the HFD, the amount and type of fatty acid in the diet. All these factors may have significant effects on adipose tissue metabolism.<sup>142</sup> Furthermore, we assessed the liver and WAT morphology. There was no significant difference in the liver after 8 weeks of feeding. In this context the duration of the feeding might be important as

well, as macrophage infiltration (accompanied by severe inflammation) and metabolic changes first occurs in adipose tissue and then shifts towards the liver.<sup>143</sup> The distribution of the fat cell size showed that Grp78<sup>+/-</sup> mice under control diet have smaller adipocytes compared to their wt littermates. This effect disappeared under high fat diet, because there were a few cells between  $4 \times 10^3 \mu\text{m}^2$  and  $9 \times 10^3 \mu\text{m}^2$  in the epididymal adipose tissue of the Grp78<sup>+/-</sup>-HFD mice. In the work of Risheng *et al.* the authors postulate a compensatory adaptive response to counteract the critical level of Grp78 in maintaining ER homeostasis. They discussed the up-regulation of ERAD, which improved ER homeostasis and attenuated inflammation.<sup>102</sup> In liver tissue we could confirm this hypothesis as VCP is significantly increased in Grp78<sup>+/-</sup> mice. This increase is independent of the diet. Compared to further findings, the heterozygous knock out of Grp78 does not change that much in liver tissue. We could also show that Grp78<sup>+/-</sup>-HFD mice have lower amounts of triglycerides in the liver compared to wt-HFD mice. This finding is in agreement with other studies, in which reduced steatosis in the liver could be observed in Grp78<sup>+/-</sup>-HFD mice.<sup>102</sup> There is no obvious difference in adipocyte size or morphology between the two genotypes, neither under Ctrl nor HFD. We could show that in Grp78<sup>+/-</sup>-HFD mice, Grp78 level in the adipose tissue was nearly comparable to the wt-HFD mice. This finding suggests a translational block or some other posttranscriptional regulation. We could not confirm an increase in VCP in WAT. It is most likely that other yet unknown pathways may contribute to this situation. For example, Risheng Ye *et al.* postulated a potential link between mitochondrial function, energy expenditure and chaperone proteins. A recent study could link ER to the mitochondria.<sup>144</sup> We could confirm the results of other studies, that mitochondrial heat shock proteins, especially Cpn60, are reduced under HFD. Furthermore, we found the same results in liver tissue.<sup>145,103</sup> The heterozygous knock out of Grp78 have no compensatory effect on it.

In Figure 20 and Figure 22 the results of UPR markers in liver and in WAT of Grp78<sup>+/-</sup> is shown. Although there are 5 biological replicates in each group of mice it is noticeable that the signal in each group is highly fluctuating. Also the quality of the western blot is not always the same. It might be that background disturbs the signal which comes from the protein of interest. The VCP western blot of the Grp78<sup>+/-</sup> mice (Figure 22) has some dark clouds in the background of some protein bands. For the

interpretation of VCP in Grp78<sup>+/-</sup> mice one have to keep in mind, that this could be the reason why there is a big difference between wt-HFD mice and Grp78<sup>+/-</sup>-HFD mice. Nevertheless, the heterogeneity in the groups is still a problem. In our experiments we combined male and female mice. Furthermore we used mice with an age of 12 weeks. It could be that some of them are still in adolescence and some are already adult. Furthermore, the reaction to a HFD might be different in each mouse during adolescence. It is known that HFD in adolescent mice result in spatial memory impairment and changes in hippocampal morphology.<sup>146</sup> Therefore we have two factors of influence which might play a role for the protein of interest. We combined all this group variation as we perform densitometric measurement of all 5 mice investigated. The big heterogeneity might be prevented, if older mice (15-20 weeks) of the same sex will be used and the number of biological replicates will be increased.

In conclusion, we can state that duration of the feeding trial and age of the mice are important factors for the interpretation of results. Attenuation of diet-induced obesity and insulin resistance which was shown by Risheng *et al.* appears only in older mice with longer high fat diet feeding duration.

### Cpn60<sup>+/-</sup> mice establish a mild phenotype under normal conditions

In the field of obesity research also the mtUPR is very interesting. It was shown that the mitochondrial biogenesis in adipose tissue is suppressed in db/db mice and mice fed with a HFD. The mitochondrial chaperones like Cpn60 were decreased in adipose tissue of ob/ob mice and rats under a high fat diet.<sup>103,104,94</sup> Furthermore, a positive association of circulating Hsp60 concentrations with BMI, leptin, HOMA-IR, and blood pressure has been shown.<sup>105</sup> It has been described that some proteins involved in the mtUPR are up-regulated under obese situations and chronic inflammation.<sup>86,116</sup> Our *in vitro* data revealed that Cpn60 is enhanced during the development of adipocytes. Due to these findings and the fact that Cpn60<sup>-/-</sup> mice are embryo lethal<sup>106</sup>, we evaluated the relevance of Cpn60<sup>+/-</sup> mice, to investigate the effect of Cpn60 in the development of obesity. Several animal and clinical studies have suggested that Cpn60 play a central role in various diseases and it was shown to be associated with type 2 diabetes mellitus.<sup>95</sup> Therefore, we fed Cpn60<sup>+/-</sup> mice and their wt littermates to a high fat diet or a control diet for 8 weeks.

In our experiment we could show that Cpn60<sup>+/-</sup> mice are more lightweight than the wt mice both under control and HFD. The lower body weight could be explained by the lower assimilation coefficient and higher oxygen consumption in the resting state, especially in the Cpn60<sup>+/-</sup>-HFD group. We assume that this effect would be significant if the feeding duration would be prolonged. In regard of the metabolic profile, we saw a difference in the plasma triglyceride level between the genotypes dependent of the diet. The Cpn60<sup>+/-</sup>-HFD group had significantly higher plasma triglycerides than the wt-HFD group. This could be the case if lipolysis was activated in the Cpn60<sup>+/-</sup>-HFD group. The process of adipose tissue lipolysis is a highly regulated pathway whereby the triglycerides stored in the adipocyte are hydrolyzed, and fatty acids delivered to the plasma.<sup>147</sup> In our mouse model, liver triglyceride levels of Cpn60<sup>+/-</sup>-HFD mice were comparable with that from the Cpn60<sup>+/-</sup>-Ctrl group. These findings also give a hint that the adipose tissue lipolysis was activated in Cpn60<sup>+/-</sup>-HFD mice. This could be an explanation for the difference in the plasma triglyceride level. This effect might be enhanced by prolonged exposure to the HFD. Furthermore, we looked in the morphology of WAT. Here we could show that Cpn60<sup>+/-</sup>-Ctrl mice exhibited significantly smaller adipocytes compared to the wt-Ctrl group. This effect completely disappeared under HFD. In the *in vitro* experiments and in C57BL/6N mice we could show that the mitochondrial chaperone Cpn60 increased during the development of adipocytes. The partial lack of Cpn60 might be the reason for smaller adipocytes in the Cpn60<sup>+/-</sup>-Ctrl mice. As hypertrophy appears to be also a risk factor for metabolic diseases<sup>125</sup>, we suggest that in Cpn60<sup>+/-</sup> mice fed with control diet the process of hypertrophy disturbed, because of the partial lack of Cpn60. These results also indicate that fat cell size is a stimulus for stress at a cellular level.

Looking at the protein level of Cpn60 in liver and in adipose tissue we could confirm further findings that with HFD of wt mice, the expression of genes involved in several mitochondrial processes and especially mitochondrial heat-shock proteins were downregulated.<sup>103</sup> As expected the Cpn60 level was reduced (by 50%) in the liver and adipose tissue of Cpn60<sup>+/-</sup>-Ctrl mice, but regarding the liver we observed an inverted effect in the Cpn60<sup>+/-</sup>-HFD group. The Cpn60 level was similar to wt-HFD mice. These finding suggests a posttranscriptional regulation, activated by HFD-induced stress pathways. We could show the opposite situation in the adipose

tissue. Here the Cpn60 levels decreased in the Cpn60<sup>+/-</sup>-HFD group. Additionally, PKR levels decreased in adipose tissue of Cpn60<sup>+/-</sup> mice independent of the diet. We assume that mitochondrial biogenesis in response to the HFD seems to be highly compromised in liver and adipose tissue from Cpn60<sup>+/-</sup> mice models. Therefore, the mitochondrial DNA content as well as the expression of various markers like COX IV or cytochrome c should be tested. A mitochondrial staining could also give information about mitochondrial biogenesis.

Furthermore, the partial reduction of Cpn60 could explain the strong adjustment of the onset of obesity (weight, adipocyte size) between Cpn60<sup>+/-</sup> and wt mice under HFD. In the liver we could also observe a compensatory effect of Grp78 in the Cpn60<sup>+/-</sup>-HFD group. In adipose tissue we could not find this effect of compensation. Here also the duration of the feeding might be very important, as it was assumed by Stanton *et al.* that metabolic changes first occur in adipose tissue and then shift towards the liver.<sup>143</sup> This could be the reason why only a part of the results are in line with other studies.<sup>148,103</sup> VCP was significantly increased independent of the diet in the WAT of Cpn60<sup>+/-</sup> mice. We assume that the up-regulation of ERAD could improve ER homeostasis, attenuate inflammation<sup>102</sup> and thus compensate the partial lack of the mitochondrial chaperonin 60. A recent study suggested a similar process like the ERAD in the mitochondria.<sup>149</sup> In stressed mitochondria, a mitochondria-associated protein degradation (MTAD) pathway is activated and misfolded and unfolded components are removed. Thus, the cell could prevent mitochondria from stress-induced damage by recruiting components in the ERAD pathway to the stressed mitochondria.<sup>150</sup> To confirm the hypothesis, that ERAD and/or MTAD is activated in the WAT of Cpn60<sup>+/-</sup> mice ubiquitination assays as well as western blot of transporter proteins should be performed.

In Figure 27 and Figure 29 the results of UPR markers in liver and in WAT of Cpn60<sup>+/-</sup> is shown. In figure 29, three mice of the Cpn60<sup>+/-</sup>-Ctrl group showed a signal for Cpn60 whereas two mice did not. As discussed before, we have a high variation within the group of our mice as we combined male and female mice and maybe there are metabolic changes between the mice because of the adolescence. That the difference for Cpn60 expression comes from the gender could be excluded as one male and one female mouse showed no signal. Therefore, it might be that some of the Cpn60<sup>+/-</sup> mice have another protein profile for Cpn60 and the reaction to a



HFD might be different. In the densitometric measurement all five mice are included, meaning the low value of Cpn60 in the Cpn60<sup>+/-</sup>-Ctrl group comes from the two mice where no Cpn60 could be detected. But, as there are artifacts – a dark cloud in the background – on the western blot itself results have to be interpreted with caution.

We finally conclude that Cpn60<sup>+/-</sup> mice show a weak phenotype if they were fed with a control diet. The mice had lower body weight, higher oxygen consumption and presumably higher adipose tissue lipolysis. All these factors are beneficial in view of obesity but it seems that under HFD the stress condition cannot be compensated. We think that in further experiments the cellular effects of reduced levels of Cpn60 in the tissues in our mouse model could provide a better understanding of the mechanisms by which various mammalian cell types compensate for unbalanced and/or deficient mitochondrial protein quality control under normal and stress conditions. Future feeding experiments with the Cpn60<sup>+/-</sup> mice and with the tamoxifen inducible floxed Cpn60<sup>+/-</sup> mice will probably answer the question of whether Cpn60 is able to prevent HFD-induced obesity.



## List of Figures and Tables

### List of Figures

Fig. I 1: Basic structure of white adipose tissue. ....	13
Fig. I 2: Schematic course of adipogenic progression (modified from Cristancho, AG et al. <sup>34</sup> ) ..	15
Fig. I 3: Secretory pattern of WAT in obese subjects (modified from Hauner H. <sup>43</sup> ) .....	16
Fig. I 4: Schematic view of the endoplasmic reticulum unfolded protein response .....	19
Fig. I 5: Interaction of the ER and the mitochondria under harmful environmental stress .....	22
Fig. M 1: Electrophoresis of the genotyping. ....	34
Fig. M 2: Schema of the indirect calorimetry. ....	36
Fig. M 3: Intraperitoneal glucose injection. ....	37
Figure 1: Course of HKs in differentiated SGBS cells .....	46
Figure 2: Course of HKs in differentiated murine 3T3-L1 cells .....	47
Figure 3: Secretion of adipokines during differentiation in different preadipocyte models....	48
Figure 4: Markers of erUPR during the course of differentiation in primary isolated human preadipocytes (A) and SGBS cells (B) .....	50
Figure 5: Markers of mtURP during differentiation in primary isolated human preadipocytes (A) and SGBS cells (B).....	51
Figure 6: The ERAD marker VCP during the course of differentiation in human preadipocytes .....	52
Figure 7: The course of JNK-activation during adipogenic differentiation in different preadipocyte models.....	53
Figure 8: Secretion of adipokines during differentiation in murine 3T3-L1 cells.....	54
Figure 9: erUPR marker during the course of differentiation in 3T3-L1 cells.....	55
Figure 10: mtUPR marker during differentiation in 3T3-L1 cells .....	56
Figure 11: VCP levels during differentiation of murine 3T3-L1 cells.....	56
Figure 12: Course of JNK activation during adipogenesis of 3T3-L1 cells.....	57
Figure 13: UPR marker proteins in primary isolated fat cells of different sizes and in adipose tissue from needle biopsies.....	60
Figure 14: Distribution of adipocyte sizes in epididymal adipose tissue from C57BL/6N mice of different age and HE staining of epididymal adipose tissue from C57BL/6N wild type mice .....	61
Figure 15: UPR markers in epididymal adipose tissue of C57BL/6N mice of different age...	62

## List of Figures and Tables

Figure 16: Weight development after eight weeks feeding trial as well as lean-/ fat-mass development of Grp78 <sup>+/-</sup> mice fed with a control and a high fat diet .....	64
Figure 17: Assimilation coefficient of Grp78 <sup>+/-</sup> mice at different time points during the feeding trial .....	65
Figure 18: Glucose tolerance test, insulin levels, and HOMA-IR as well as plasma triglycerides of Grp78 <sup>+/-</sup> mice after 8 weeks fed a control and a high fat diet .....	67
Figure 19: Liver triglyceride level in Grp78 <sup>+/-</sup> mice after an 8 weeks feeding trial .....	68
Figure 20: UPR markers in liver of Grp78 <sup>+/-</sup> mice fed either a control or a high fat diet.....	70
Figure 21: Fat cell size and the distribution of fat cell size of Grp78 <sup>+/-</sup> mice after 8 weeks fed with high fat diet or control diet.....	72
Figure 22: UPR markers in WAT of Grp78 <sup>+/-</sup> mice fed a control and a high fat diet .....	73
Figure 23: Weight development, weight gain and the lean-/ fat-mass development of Cpn60 <sup>+/-</sup> mice fed a control and a high fat diet.....	75
Figure 24: Assimilation coefficient of Cpn60 <sup>+/-</sup> mice during the 4 <sup>th</sup> and the 8 <sup>th</sup> week of feeding .....	76
Figure 25: Glucose tolerance test, insulin levels, and HOMA-IR as well as plasma triglycerides of Cpn60 <sup>+/-</sup> mice fed a high fat diet or a control diet.....	78
Figure 26: Triglyceride levels in the liver of Cpn60 <sup>+/-</sup> mice and their wt littermates after 8 weeks feeding a high fat diet or a control diet.....	79
Figure 27: Protein levels of UPR markers in liver of Cpn60 <sup>+/-</sup> mice after a feeding trial of 8 weeks.....	80
Figure 28: Fat cell size and the distribution of fat cell size of Cpn60 <sup>+/-</sup> mice after an eight week feeding experiment .....	82
Figure 29: UPR markers in WAT of Cpn60 <sup>+/-</sup> mice fed a high fat diet for 8 weeks .....	83

## **List of Tables**

Table M 1: Standard-PCR-MasterMix (for the Phire HotStart DNA Polymerase) .....	32
Table M 2: Standard-PCR-MasterMix (for the Taq DNA polymerase).....	33
Table M 3: Composition of the different diets .....	35
Table M 4: HE staining protocol .....	38
Table 1: Characteristics of four individual tissue donors and their fractionated adipocytes .	58
Table 2: Characteristics of NGT and T2D subjects (N=25) .....	59
Table 3: Weight of several organs of the Grp78 <sup>+/-</sup> mice .....	67
Table 4: Organ weights of Cpn60 <sup>+/-</sup> mice .....	78

## **Abbreviations**

AMP	adenosinmonophosphate
ANOVA	analysis of variance
ASK	apoptosis signal-regulating kinase
AT	adipose tissue
ATF	activating transcription factor
ATP	adenosintriphosphate
AUC	area under the curve
BAT	brown adipose tissue
BCA	bicinchoninic acid
BIP	binding immunoglobulin protein
BMI	body mass index
BSA	bovine serum albumin
C/EBP	CCAAT/enhancer binding protein
CHOP	C/EBP homologous protein
ClpP	Clp protease (caseinolytic peptidase)
Cpn	chaperonin
CRE	cAMP response elements
CRP	C-reactive protein
Ctrl	control diet
CVD	cardiovascular disease
DAPI	4', 6-Diamindin-2-phenylindol
DIO	diet-induced obesity
DM	differentiation media
DNA	deoxyribonucleic acid
ECM	extracellular matrix
EGF	epidermal growth factor
eIF	eukaryotic translation initiation factor
ELISA	enzyme linked immunosorbent assay
EP	epididymal
ER/er	endoplasmic reticulum
ERAD	ER-associated degradation
ERSE	ER stress elements
FA	fatty acid

## Abbreviations

FBS/FCS	fetal bovine serum / fetal calf serum
FGF	fibroblast growth factor
FM	feeding media
GAPDH	glyceraldehyde 3-phosphate dehydrogenase
GPDH	glycerol-3-phosphate dehydrogenase
GRP	glucose-regulated protein
H3	histone 3
H&E	hematoxylin and eosin
HFD	high fat diet
HK	housekeeping protein
HOMA-IR	Homeostasis Model Assessment – insulin resistance
HPRT	hypoxanthine-guanine phosphoribosyltransferase
HRP	horseradish peroxidase
HSP	heat shock protein
IBMX	isobutyl-methylxanthine
IL	interleukin
IP-GTT	intraperitoneal glucose tolerance test
IRE	inositol requiring enzyme
JNK	cJun-N terminal kinase
KRP	Krebs-Ringer-Phosphate
MCP	monocyte chemotactic protein
MCS	mesenchymal stem cells
Mes	mesenterial
MetS	metabolic syndrome
MT/mt	mitochondrial
MTAD	mitochondrial associated degradation
NFκB	nuclear factor κB
NGT	normal glucose tolerant
NMR	nuclear magnetic resonance
O.C.T.	for Optimal Cutting Temperature
OTC	ornithine transcarbamylase
PAI	plasminogen activator inhibitor
PBS	phosphate buffered saline
PCR	polymerase chain reaction
pen-strep	penicillin and streptomycin
PERK	PKR-like ER kinase

PGC	peroxisome proliferator-activated receptor gamma coactivator
PKR	double-stranded RNA-activated protein kinase
PM	proliferation media
PMSF	phenylmethylsulfonylfluorid
PPAR	peroxisome proliferator activated receptor
PVDF	polyvinylidene fluoride
RMR	resting metabolic rate
RNA	ribonucleic acid
ROS	reactive oxygen species
RT	room temperature
SDS-PAGE	sodium dodecyl sulfate polyacrylamide gel electrophoresis
SVF	stromal vascular fraction
T3	triiodothyronine
T2D	type 2 diabetes
TIM	translocase of the inner mitochondrial membrane
TNF	tumor necrosis factor
TOM	translocase of the outer mitochondrial membrane
TRAF	TNFR-associated factor
U	unit
UPR	unfolded protein response
UPRE	UPR elements
VCP	valosin-containing protein
WAT	white adipose tissue
WB	western blot
WHO	world health organization
wt	wildtype
XBP	X-box binding protein





## References

- 1 van Gaal LF, Mertens IL, Block CE de. Mechanisms linking obesity with cardiovascular disease. *Nature* 2006; 444: 875–880; doi:10.1038/nature05487.
- 2 Hauner H. Insulin resistance and the metabolic syndrome—a challenge of the new millennium. *Eur J Clin Nutr* 2002; 56 Suppl 1: S25–9; doi:10.1038/sj.ejcn.1601350.
- 3 Loos RJF, Bouchard C. FTO: the first gene contributing to common forms of human obesity. *Obes Rev* 2008; 9: 246–250; doi:10.1111/j.1467-789X.2008.00481.x.
- 4 Poirier P, Giles TD, Bray GA, Hong Y, Stern JS, Pi-Sunyer FX *et al.* Obesity and cardiovascular disease: pathophysiology, evaluation, and effect of weight loss. *Arterioscler. Thromb. Vasc. Biol* 2006; 26: 968–976; doi:10.1161/01.ATV.0000216787.85457.f3.
- 5 Khosla T, Lowe CR. Indices of obesity derived from body weight and height. *Br J Prev Soc Med* 1967; 21: 122–128.
- 6 Stefan N, Kantartzis K, Machann J, Schick F, Thamer C, Rittig K *et al.* Identification and characterization of metabolically benign obesity in humans. *Arch. Intern. Med* 2008; 168: 1609–1616; doi:10.1001/archinte.168.15.1609.
- 7 Manolopoulos KN, Karpe F, Frayn KN. Gluteofemoral body fat as a determinant of metabolic health. *Int J Obes (Lond)* 2010; 34: 949–959; doi:10.1038/ijo.2009.286.
- 8 Bray GA. Medical consequences of obesity. *J. Clin. Endocrinol. Metab* 2004; 89: 2583–2589; doi:10.1210/jc.2004-0535.
- 9 Klein S, Wadden T, Sugerman HJ. AGA technical review on obesity. *Gastroenterology* 2002; 123: 882–932.

## References

- 10 Kopelman PG. Obesity as a medical problem. *Nature* 2000; 404: 635–643; doi:10.1038/35007508.
- 11 Reaven GM. Banting lecture 1988. Role of insulin resistance in human disease. *Diabetes* 1988; 37: 1595–1607.
- 12 Kumar V, Robbins SL, Cotran RS. Robbins and Cotran pathologic basis of disease. [expertconsult, searchable full text online], 8th edn. Philadelphia, Pa: Elsevier Saunders, 2010.
- 13 Panzram G. Mortality and survival in type 2 (non-insulin-dependent) diabetes mellitus. *Diabetologia* 1987; 30: 123–131.
- 14 Atkins RC, Briganti EM, Lewis JB, Hunsicker LG, Braden G, Champion Crespigny PJ de *et al.* Proteinuria reduction and progression to renal failure in patients with type 2 diabetes mellitus and overt nephropathy. *Am. J. Kidney Dis* 2005; 45: 281–287.
- 15 Trayhurn P, Wood IS. Signalling role of adipose tissue: adipokines and inflammation in obesity. *Biochem. Soc. Trans* 2005; 33: 1078–1081; doi:10.1042/BST20051078.
- 16 Dandona P, Aljada A, Bandyopadhyay A. Inflammation: the link between insulin resistance, obesity and diabetes. *Trends Immunol* 2004; 25: 4–7.
- 17 Xu H, Barnes GT, Yang Q, Tan G, Yang D, Chou CJ *et al.* Chronic inflammation in fat plays a crucial role in the development of obesity-related insulin resistance. *J. Clin. Invest* 2003; 112: 1821–1830; doi:10.1172/JCI19451.
- 18 Weisberg SP, McCann D, Desai M, Rosenbaum M, Leibel RL, Ferrante AW. Obesity is associated with macrophage accumulation in adipose tissue. *J. Clin. Invest* 2003; 112: 1796–1808; doi:10.1172/JCI19246.
- 19 Skurk T, Hauner H. Sekretorische Aktivität des Fettgewebes. Vom Energiespeicher zum endokrinen Organ. *MMW Fortschr Med* 2005; 147: 41–43.

- 20 Skurk T, Kolb H, Müller-Scholze S, Röhrig K, Hauner H, Herder C. The proatherogenic cytokine interleukin-18 is secreted by human adipocytes. *Eur. J. Endocrinol* 2005; 152: 863–868; doi:10.1530/eje.1.01897.
- 21 Skurk T, Mack I, Kempf K, Kolb H, Hauner H, Herder C. Expression and secretion of RANTES (CCL5) in human adipocytes in response to immunological stimuli and hypoxia. *Horm. Metab. Res* 2009; 41: 183–189; doi:10.1055/s-0028-1093345.
- 22 Kintscher U, Hartge M, Hess K, Foryst-Ludwig A, Clemenz M, Wabitsch M *et al.* T-lymphocyte infiltration in visceral adipose tissue: a primary event in adipose tissue inflammation and the development of obesity-mediated insulin resistance. *Arterioscler. Thromb. Vasc. Biol* 2008; 28: 1304–1310; doi:10.1161/ATVBAHA.108.165100.
- 23 Kang K, Reilly SM, Karabacak V, Gangl MR, Fitzgerald K, Hatano B *et al.* Adipocyte-derived Th2 cytokines and myeloid PPARdelta regulate macrophage polarization and insulin sensitivity. *Cell Metab* 2008; 7: 485–495; doi:10.1016/j.cmet.2008.04.002.
- 24 Wang P, Mariman E, Renes J, Keijer J. The secretory function of adipocytes in the physiology of white adipose tissue. *J. Cell. Physiol* 2008; 216: 3–13; doi:10.1002/jcp.21386.
- 25 Kershaw EE, Flier JS. Adipose tissue as an endocrine organ. *J. Clin. Endocrinol. Metab* 2004; 89: 2548–2556; doi:10.1210/jc.2004-0395.
- 26 Trayhurn P. Endocrine and signalling role of adipose tissue: new perspectives on fat. *Acta Physiol. Scand* 2005; 184: 285–293; doi:10.1111/j.1365-201X.2005.01468.x.
- 27 Trayhurn P, Wood IS. Adipokines: inflammation and the pleiotropic role of white adipose tissue. *Br. J. Nutr* 2004; 92: 347–355.
- 28 Cinti S. The adipose organ: morphological perspectives of adipose tissues. *Proc Nutr Soc* 2001; 60: 319–328.

## References

- 29 Klaus S. Adipose tissue. Georgetown, Tex, Austin, Tex: Landes Bioscience; Eureka.com, 2001.
- 30 Arner E, Westermark PO, Spalding KL, Britton T, Rydén M, Frisén J *et al.* Adipocyte turnover: relevance to human adipose tissue morphology. *Diabetes* 2010; 59: 105–109; doi:10.2337/db09-0942.
- 31 Pagano C, Calcagno A, Giacomelli L, Poletti A, Macchi V, Vettor R *et al.* Molecular and morphometric description of adipose tissue during weight changes: a quantitative tool for assessment of tissue texture. *Int. J. Mol. Med.* 2004; 14: 897–902.
- 32 Hirsch J, Han PW. Cellularity of rat adipose tissue: effects of growth, starvation, and obesity. *J. Lipid Res* 1969; 10: 77–82.
- 33 Spalding KL, Arner E, Westermark PO, Bernard S, Buchholz BA, Bergmann O *et al.* Dynamics of fat cell turnover in humans. *Nature* 2008; 453: 783–787; doi:10.1038/nature06902.
- 34 Cristancho AG, Lazar MA. Forming functional fat: a growing understanding of adipocyte differentiation. *Nat. Rev. Mol. Cell Biol* 2011; 12: 722–734; doi:10.1038/nrm3198.
- 35 Hauner H, Entenmann G, Wabitsch M, Gaillard D, Ailhaud G, Negrel R *et al.* Promoting effect of glucocorticoids on the differentiation of human adipocyte precursor cells cultured in a chemically defined medium. *J. Clin. Invest* 1989; 84: 1663–1670; doi:10.1172/JCI114345.
- 36 Skurk T, Alberti-Huber C, Herder C, Hauner H. Relationship between adipocyte size and adipokine expression and secretion. *J. Clin. Endocrinol. Metab* 2007; 92: 1023–1033; doi:10.1210/jc.2006-1055.
- 37 Skurk T, Alberti-Huber C, Hauner H. Effect of conditioned media from mature human adipocytes on insulin-stimulated Akt/PKB phosphorylation in human skeletal muscle cells: role of BMI and fat cell size. *Horm. Metab. Res.* 2009; 41: 190–196; doi:10.1055/s-0028-1093342.

- 38 Pradhan AD, Manson JE, Rifai N, Buring JE, Ridker PM. C-reactive protein, interleukin 6, and risk of developing type 2 diabetes mellitus. *JAMA* 2001; 286: 327–334.
- 39 Harman-Boehm I, Blüher M, Redel H, Sion-Vardy N, Ovadia S, Avinoach E *et al.* Macrophage infiltration into omental versus subcutaneous fat across different populations: effect of regional adiposity and the comorbidities of obesity. *J. Clin. Endocrinol. Metab.* 2007; 92: 2240–2247; doi:10.1210/jc.2006-1811.
- 40 Ohashi K, Parker JL, Ouchi N, Higuchi A, Vita JA, Gokce N *et al.* Adiponectin promotes macrophage polarization toward an anti-inflammatory phenotype. *J. Biol. Chem.* 2010; 285: 6153–6160; doi:10.1074/jbc.M109.088708.
- 41 Horibe T, Hoogenraad NJ. The chop gene contains an element for the positive regulation of the mitochondrial unfolded protein response. *PLoS ONE* 2007; 2: e835; doi:10.1371/journal.pone.0000835.
- 42 Fain JN. Release of inflammatory mediators by human adipose tissue is enhanced in obesity and primarily by the nonfat cells: a review. *Mediators Inflamm.* 2010; 2010: 513948; doi:10.1155/2010/513948.
- 43 Hauner H. The new concept of adipose tissue function. *Physiol. Behav.* 2004; 83: 653–658; doi:10.1016/j.physbeh.2004.09.016.
- 44 Hartl FU, Hayer-Hartl M. Molecular chaperones in the cytosol: from nascent chain to folded protein. *Science* 2002; 295: 1852–1858; doi:10.1126/science.1068408.
- 45 Cotto JJ, Morimoto RI. Stress-induced activation of the heat-shock response: cell and molecular biology of heat-shock factors. *Biochem. Soc. Symp* 1999; 64: 105–118.

## References

- 46 Ron D, Walter P. Signal integration in the endoplasmic reticulum unfolded protein response. *Nat. Rev. Mol. Cell Biol* 2007; 8: 519–529; doi:10.1038/nrm2199.
- 47 Zhao Q, Wang J, Levichkin IV, Stasinopoulos S, Ryan MT, Hoogenraad NJ. A mitochondrial specific stress response in mammalian cells. *EMBO J* 2002; 21: 4411–4419.
- 48 Hotamisligil GS. Endoplasmic reticulum stress and the inflammatory basis of metabolic disease. *Cell* 2010; 140: 900–917; doi:10.1016/j.cell.2010.02.034.
- 49 Hendershot LM. The ER function BiP is a master regulator of ER function. *Mt. Sinai J. Med.* 2004; 71: 289–297.
- 50 Ozcan U, Cao Q, Yilmaz E, Lee A, Iwakoshi NN, Ozdelen E *et al.* Endoplasmic reticulum stress links obesity, insulin action, and type 2 diabetes. *Science* 2004; 306: 457–461; doi:10.1126/science.1103160.
- 51 Schröder M, Kaufman RJ. The mammalian unfolded protein response. *Annu. Rev. Biochem.* 2005; 74: 739–789; doi:10.1146/annurev.biochem.73.011303.074134.
- 52 Chen X, Shen J, Prywes R. The luminal domain of ATF6 senses endoplasmic reticulum (ER) stress and causes translocation of ATF6 from the ER to the Golgi. *J. Biol. Chem* 2002; 277: 13045–13052; doi:10.1074/jbc.M110636200.
- 53 Alzayady KJ, Panning MM, Kelley GG, Wojcikiewicz RJH. Involvement of the p97-Ufd1-Npl4 complex in the regulated endoplasmic reticulum-associated degradation of inositol 1,4,5-trisphosphate receptors. *J. Biol. Chem.* 2005; 280: 34530–34537; doi:10.1074/jbc.M508890200.
- 54 Ye Y, Meyer HH, Rapoport TA. The AAA ATPase Cdc48/p97 and its partners transport proteins from the ER into the cytosol. *Nature* 2001; 414: 652–656; doi:10.1038/414652a.

- 55 Ballar P, Fang S. Regulation of ER-associated degradation via p97/VCP-interacting motif. *Biochem. Soc. Trans.* 2008; 36: 818–822; doi:10.1042/BST0360818.
- 56 Lee RJ, Liu C, Harty C, McCracken AA, Latterich M, Römisch K *et al.* Uncoupling retro-translocation and degradation in the ER-associated degradation of a soluble protein. *EMBO J.* 2004; 23: 2206–2215; doi:10.1038/sj.emboj.7600232.
- 57 Sidrauski C, Walter P. The transmembrane kinase Ire1p is a site-specific endonuclease that initiates mRNA splicing in the unfolded protein response. *Cell* 1997; 90: 1031–1039.
- 58 Lee A, Iwakoshi NN, Glimcher LH. XBP-1 regulates a subset of endoplasmic reticulum resident chaperone genes in the unfolded protein response. *Mol. Cell. Biol* 2003; 23: 7448–7459.
- 59 Urano F, Wang X, Bertolotti A, Zhang Y, Chung P, Harding HP *et al.* Coupling of stress in the ER to activation of JNK protein kinases by transmembrane protein kinase IRE1. *Science* 2000; 287: 664–666.
- 60 Hu P, Han Z, Couvillon AD, Kaufman RJ, Exton JH. Autocrine tumor necrosis factor alpha links endoplasmic reticulum stress to the membrane death receptor pathway through IRE1alpha-mediated NF-kappaB activation and down-regulation of TRAF2 expression. *Mol. Cell. Biol* 2006; 26: 3071–3084; doi:10.1128/MCB.26.8.3071-3084.2006.
- 61 Harding HP, Zhang Y, Ron D. Protein translation and folding are coupled by an endoplasmic-reticulum-resident kinase. *Nature* 1999; 397: 271–274; doi:10.1038/16729.
- 62 Harding HP, Novoa I, Zhang Y, Zeng H, Wek R, Schapira M *et al.* Regulated translation initiation controls stress-induced gene expression in mammalian cells. *Mol. Cell* 2000; 6: 1099–1108.

## References

- 63 Harding HP, Zhang Y, Bertolotti A, Zeng H, Ron D. Perk is essential for translational regulation and cell survival during the unfolded protein response. *Mol. Cell* 2000; 5: 897–904.
- 64 Ma Y, Brewer JW, Diehl JA, Hendershot LM. Two distinct stress signaling pathways converge upon the CHOP promoter during the mammalian unfolded protein response. *J. Mol. Biol* 2002; 318: 1351–1365.
- 65 Shen J, Chen X, Hendershot L, Prywes R. ER stress regulation of ATF6 localization by dissociation of BiP/GRP78 binding and unmasking of Golgi localization signals. *Dev. Cell* 2002; 3: 99–111.
- 66 Yamamoto K, Sato T, Matsui T, Sato M, Okada T, Yoshida H *et al.* Transcriptional induction of mammalian ER quality control proteins is mediated by single or combined action of ATF6alpha and XBP1. *Dev. Cell* 2007; 13: 365–376; doi:10.1016/j.devcel.2007.07.018.
- 67 Nakatani Y, Kaneto H, Kawamori D, Yoshiuchi K, Hatazaki M, Matsuoka T *et al.* Involvement of endoplasmic reticulum stress in insulin resistance and diabetes. *J. Biol. Chem* 2005; 280: 847–851; doi:10.1074/jbc.M411860200.
- 68 Gregor MF, Yang L, Fabbrini E, Mohammed BS, Eagon JC, Hotamisligil GS *et al.* Endoplasmic reticulum stress is reduced in tissues of obese subjects after weight loss. *Diabetes* 2009; 58: 693–700; doi:10.2337/db08-1220.
- 69 Boden G, Duan X, Homko C, Molina EJ, Song W, Perez O *et al.* Increase in endoplasmic reticulum stress-related proteins and genes in adipose tissue of obese, insulin-resistant individuals. *Diabetes* 2008; 57: 2438–2444; doi:10.2337/db08-0604.
- 70 Wellen KE, Hotamisligil GS. Inflammation, stress, and diabetes. *J. Clin. Invest.* 2005; 115: 1111–1119; doi:10.1172/JCI25102.



- 71 Hotamisligil GS. Inflammation and endoplasmic reticulum stress in obesity and diabetes. *Int J Obes (Lond)* 2008; 32 Suppl 7: S52-4; doi:10.1038/ijo.2008.238.
- 72 Furukawa S, Fujita T, Shimabukuro M, Iwaki M, Yamada Y, Nakajima Y *et al.* Increased oxidative stress in obesity and its impact on metabolic syndrome. *J. Clin. Invest.* 2004; 114: 1752–1761; doi:10.1172/JCI21625.
- 73 Gregor MF, Hotamisligil GS. Thematic review series: Adipocyte Biology. Adipocyte stress: the endoplasmic reticulum and metabolic disease. *J. Lipid Res.* 2007; 48: 1905–1914; doi:10.1194/jlr.R700007-JLR200.
- 74 Song B, Scheuner D, Ron D, Pennathur S, Kaufman RJ. Chop deletion reduces oxidative stress, improves beta cell function, and promotes cell survival in multiple mouse models of diabetes. *J. Clin. Invest* 2008; 118: 3378–3389; doi:10.1172/JCI34587.
- 75 Cinti S, Mitchell G, Barbatelli G, Murano I, Ceresi E, Faloia E *et al.* Adipocyte death defines macrophage localization and function in adipose tissue of obese mice and humans. *J. Lipid Res* 2005; 46: 2347–2355; doi:10.1194/jlr.M500294-JLR200.
- 76 Henze K, Martin W. Evolutionary biology: essence of mitochondria. *Nature* 2003; 426: 127–128; doi:10.1038/426127a.
- 77 Stowe DF, Camara AKS. Mitochondrial reactive oxygen species production in excitable cells: modulators of mitochondrial and cell function. *Antioxid. Redox Signal* 2009; 11: 1373–1414; doi:10.1089/ARS.2008.2331.
- 78 Murgia M, Giorgi C, Pinton P, Rizzuto R. Controlling metabolism and cell death: at the heart of mitochondrial calcium signalling. *J. Mol. Cell. Cardiol* 2009; 46: 781–788; doi:10.1016/j.yjmcc.2009.03.003.
- 79 Green DR, Kroemer G. The pathophysiology of mitochondrial cell death. *Science* 2004; 305: 626–629; doi:10.1126/science.1099320.

## References

- 80 Frey TG, Mannella CA. The internal structure of mitochondria. *Trends Biochem. Sci* 2000; 25: 319–324.
- 81 Hoogenraad NJ, Ward LA, Ryan MT. Import and assembly of proteins into mitochondria of mammalian cells. *Biochim. Biophys. Acta* 2002; 1592: 97–105.
- 82 Rehling P, Brandner K, Pfanner N. Mitochondrial import and the twin-pore translocase. *Nat. Rev. Mol. Cell Biol* 2004; 5: 519–530; doi:10.1038/nrm1426.
- 83 Ryan MT, Hoogenraad NJ. Mitochondrial-nuclear communications. *Annu. Rev. Biochem* 2007; 76: 701–722; doi:10.1146/annurev.biochem.76.052305.091720.
- 84 Voos W, Röttgers K. Molecular chaperones as essential mediators of mitochondrial biogenesis. *Biochim. Biophys. Acta* 2002; 1592: 51–62.
- 85 Haynes CM, Petrova K, Benedetti C, Yang Y, Ron D. ClpP mediates activation of a mitochondrial unfolded protein response in *C. elegans*. *Dev. Cell* 2007; 13: 467–480; doi:10.1016/j.devcel.2007.07.016.
- 86 Rath E, Berger E, Messlik A, Nunes T, Liu B, Kim SC *et al.* Induction of dsRNA-activated protein kinase links mitochondrial unfolded protein response to the pathogenesis of intestinal inflammation. *Gut* 2011; doi:10.1136/gutjnl-2011-300767.
- 87 Martinus RD, Garth GP, Webster TL, Cartwright P, Naylor DJ, Høj PB *et al.* Selective induction of mitochondrial chaperones in response to loss of the mitochondrial genome. *Eur. J. Biochem* 1996; 240: 98–103.
- 88 Aldridge JE, Horibe T, Hoogenraad NJ. Discovery of genes activated by the mitochondrial unfolded protein response (mtUPR) and cognate promoter elements. *PLoS ONE* 2007; 2: e874; doi:10.1371/journal.pone.0000874.

- 89 Rath E, Haller D. Inflammation and cellular stress: a mechanistic link between immune-mediated and metabolically driven pathologies. *Eur J Nutr* 2011; 50: 219–233; doi:10.1007/s00394-011-0197-0.
- 90 Koh EH, Park J, Park H, Jeon MJ, Ryu JW, Kim M *et al.* Essential role of mitochondrial function in adiponectin synthesis in adipocytes. *Diabetes* 2007; 56: 2973–2981; doi:10.2337/db07-0510.
- 91 Kozak LP, Koza RA, Anunciado-Koza R. Brown fat thermogenesis and body weight regulation in mice: relevance to humans. *Int J Obes (Lond)* 2010; 34 Suppl 1: S23-7; doi:10.1038/ijo.2010.179.
- 92 Enerbäck S. Brown adipose tissue in humans. *Int J Obes (Lond)* 2010; 34 Suppl 1: S43-6; doi:10.1038/ijo.2010.183.
- 93 Nedergaard J, Bengtsson T, Cannon B. Unexpected evidence for active brown adipose tissue in adult humans. *Am. J. Physiol. Endocrinol. Metab* 2007; 293: E444-52; doi:10.1152/ajpendo.00691.2006.
- 94 Sutherland LN, Bomhof MR, Capozzi LC, Basaraba SAU, Wright DC. Exercise and adrenaline increase PGC-1{alpha} mRNA expression in rat adipose tissue. *J. Physiol. (Lond.)* 2009; 587: 1607–1617; doi:10.1113/jphysiol.2008.165464.
- 95 Imatoh T, Sugie T, Miyazaki M, Tanihara S, Baba M, Momose Y *et al.* Is heat shock protein 60 associated with type 2 diabetes mellitus? *Diabetes Res. Clin. Pract* 2009; 85: 208–212; doi:10.1016/j.diabres.2009.06.004.
- 96 Beal MF. Mitochondria take center stage in aging and neurodegeneration. *Ann. Neurol* 2005; 58: 495–505; doi:10.1002/ana.20624.
- 97 Imai Y, Ahima RS. Rodents as genetic models of obesity. *Drug Discovery Today: Disease Models* 2005; 2: 165–175; doi:10.1016/j.ddmod.2005.08.005.

## References

- 98 Kanasaki K, Koya D. Biology of obesity: lessons from animal models of obesity. *J. Biomed. Biotechnol.* 2011; 2011: 197636; doi:10.1155/2011/197636.
- 99 Collins S, Martin TL, Surwit RS, Robidoux J. Genetic vulnerability to diet-induced obesity in the C57BL/6J mouse: physiological and molecular characteristics. *Physiol. Behav.* 2004; 81: 243–248; doi:10.1016/j.physbeh.2004.02.006.
- 100 LOCHAYA S, LEBOEUF N, MAYER J, LEBOEUF B. Adipose tissue metabolism of obese mice on standard and high-fat diets. *Am. J. Physiol.* 1961; 201: 23–26.
- 101 Luo S, Mao C, Lee B, Lee AS. GRP78/BiP is required for cell proliferation and protecting the inner cell mass from apoptosis during early mouse embryonic development. *Mol. Cell. Biol* 2006; 26: 5688–5697; doi:10.1128/MCB.00779-06.
- 102 Ye R, Jung DY, Jun JY, Li J, Luo S, Ko HJ *et al.* Grp78 heterozygosity promotes adaptive unfolded protein response and attenuates diet-induced obesity and insulin resistance. *Diabetes* 2010; 59: 6–16; doi:10.2337/db09-0755.
- 103 Rong JX, Qiu Y, Hansen MK, Zhu L, Zhang V, Xie M *et al.* Adipose mitochondrial biogenesis is suppressed in db/db and high-fat diet-fed mice and improved by rosiglitazone. *Diabetes* 2007; 56: 1751–1760; doi:10.2337/db06-1135.
- 104 Wilson-Fritch L, Nicoloso S, Chouinard M, Lazar MA, Chui PC, Leszyk J *et al.* Mitochondrial remodeling in adipose tissue associated with obesity and treatment with rosiglitazone. *J. Clin. Invest* 2004; 114: 1281–1289; doi:10.1172/JCI21752.
- 105 Marker T, Sell H, Zillessen P, Glode A, Kriebel J, Ouwens DM *et al.* Heat Shock Protein 60 as a Mediator of Adipose Tissue Inflammation and Insulin Resistance. *Diabetes* 2012; 61: 615–625; doi:10.2337/db10-1574.

- 106 Christensen JH, Nielsen MN, Hansen J, Füchtbauer A, Füchtbauer E, West M *et al.* Inactivation of the hereditary spastic paraplegia-associated Hspd1 gene encoding the Hsp60 chaperone results in early embryonic lethality in mice. *Cell Stress Chaperones* 2010; 15: 851–863; doi:10.1007/s12192-010-0194-x.
- 107 Green H, Meuth M. An established pre-adipose cell line and its differentiation in culture. *Cell* 1974; 3: 127–133.
- 108 Wabitsch M, Brenner RE, Melzner I, Braun M, Möller P, Heinze E *et al.* Characterization of a human preadipocyte cell strain with high capacity for adipose differentiation. *Int. J. Obes. Relat. Metab. Disord* 2001; 25: 8–15.
- 109 van Harmelen V, Skurk T, Röhrig K, Lee Y, Halbleib M, Aprath-Husmann I *et al.* Effect of BMI and age on adipose tissue cellularity and differentiation capacity in women. *Int. J. Obes. Relat. Metab. Disord* 2003; 27: 889–895; doi:10.1038/sj.ijo.0802314.
- 110 Skurk T, Ecklebe S, Hauner H. A novel technique to propagate primary human preadipocytes without loss of differentiation capacity. *Obesity (Silver Spring)* 2007; 15: 2925–2931; doi:10.1038/oby.2007.349.
- 111 Wickelgren I. Obesity: how big a problem? *Science* 1998; 280: 1364–1367.
- 112 LOWRY OH, ROSEBROUGH NJ, FARR AL, RANDALL RJ. Protein measurement with the Folin phenol reagent. *J. Biol. Chem* 1951; 193: 265–275.
- 113 Gorzelnia K, Janke J, Engeli S, Sharma AM. Validation of endogenous controls for gene expression studies in human adipocytes and preadipocytes. *Horm. Metab. Res* 2001; 33: 625–627; doi:10.1055/s-2001-17911.

## References

- 114 Matthae S, May S, Hubersberger M, Hauner H, Skurk T. Protein Normalization in Different Adipocyte Models and Dependence on Cell Size. *Horm Metab Res* 2013; doi:10.1055/s-0033-1341429.
- 115 Harding HP, Zeng H, Zhang Y, Jungries R, Chung P, Plesken H *et al.* Diabetes mellitus and exocrine pancreatic dysfunction in *perk*<sup>-/-</sup> mice reveals a role for translational control in secretory cell survival. *Mol. Cell* 2001; 7: 1153–1163.
- 116 Nakamura T, Furuhashi M, Li P, Cao H, Tuncman G, Sonenberg N *et al.* Double-stranded RNA-dependent protein kinase links pathogen sensing with stress and metabolic homeostasis. *Cell* 2010; 140: 338–348; doi:10.1016/j.cell.2010.01.001.
- 117 Lee E, Yoon C, Kim Y, Bae Y. The double-strand RNA-dependent protein kinase PKR plays a significant role in a sustained ER stress-induced apoptosis. *FEBS Lett* 2007; 581: 4325–4332; doi:10.1016/j.febslet.2007.08.001.
- 118 Zhang K, Kaufman RJ. From endoplasmic-reticulum stress to the inflammatory response. *Nature* 2008; 454: 455–462; doi:10.1038/nature07203.
- 119 Laumen H, Saningong AD, Heid IM, Hess J, Herder C, Claussnitzer M *et al.* Functional characterization of promoter variants of the adiponectin gene complemented by epidemiological data. *Diabetes* 2009; 58: 984–991; doi:10.2337/db07-1646.
- 120 Lara-Castro C, Fu Y, Chung BH, Garvey WT. Adiponectin and the metabolic syndrome: mechanisms mediating risk for metabolic and cardiovascular disease. *Current Opinion in Lipidology* 2007; 18: 263–270; doi:10.1097/MOL.0b013e32814a645f.

- 121 Christiaens V, Sujatha R, Hellemans KH, Pipeleers D, Lijnen HR. Functional interactions between pancreatic beta cells and (pre)adipocytes. *Endocrine* 2010; 38: 118–126; doi:10.1007/s12020-010-9364-y.
- 122 Calkhoven CF, Müller C, Leutz A. Translational control of gene expression and disease. *Trends Mol Med* 2002; 8: 577–583.
- 123 Dagon Y, Avraham Y, Berry EM. AMPK activation regulates apoptosis, adipogenesis, and lipolysis by eIF2alpha in adipocytes. *Biochem. Biophys. Res. Commun.* 2006; 340: 43–47; doi:10.1016/j.bbrc.2005.11.159.
- 124 Reaven GM, Brand RJ, Chen YD, Mathur AK, Goldfine I. Insulin resistance and insulin secretion are determinants of oral glucose tolerance in normal individuals. *Diabetes* 1993; 42: 1324–1332.
- 125 Weyer C, Foley JE, Bogardus C, Tataranni PA, Pratley RE. Enlarged subcutaneous abdominal adipocyte size, but not obesity itself, predicts type II diabetes independent of insulin resistance. *Diabetologia* 2000; 43: 1498–1506; doi:10.1007/s001250051560.
- 126 Lönn M, Mehlig K, Bengtsson C, Lissner L. Adipocyte size predicts incidence of type 2 diabetes in women. *FASEB J.* 2010; 24: 326–331; doi:10.1096/fj.09-133058.
- 127 Gülден E, Märker T, Kriebel J, Kolb-Bachofen V, Burkart V, Habich C. Heat shock protein 60: evidence for receptor-mediated induction of proinflammatory mediators during adipocyte differentiation. *FEBS Lett* 2009; 583: 2877–2881; doi:10.1016/j.febslet.2009.07.049.
- 128 Gülден E, Mollérus S, Brüggemann J, Burkart V, Habich C. Heat shock protein 60 induces inflammatory mediators in mouse adipocytes. *FEBS Lett* 2008; 582: 2731–2736; doi:10.1016/j.febslet.2008.07.002.

## References

- 129 Wang XZ, Lawson B, Brewer JW, Zinszner H, Sanjay A, Mi LJ *et al.* Signals from the stressed endoplasmic reticulum induce C/EBP-homologous protein (CHOP/GADD153). *Mol. Cell. Biol* 1996; 16: 4273–4280.
- 130 Oyadomari S, Koizumi A, Takeda K, Gotoh T, Akira S, Araki E *et al.* Targeted disruption of the Chop gene delays endoplasmic reticulum stress-mediated diabetes. *J. Clin. Invest* 2002; 109: 525–532; doi:10.1172/JCI14550.
- 131 Meusser B, Hirsch C, Jarosch E, Sommer T. ERAD: the long road to destruction. *Nat. Cell Biol.* 2005; 7: 766–772; doi:10.1038/ncb0805-766.
- 132 Gupta S, McGrath B, Cavener DR. PERK (EIF2AK3) Regulates Proinsulin Trafficking and Quality Control in the Secretory Pathway. *Diabetes* 2010; 59: 1937–1947; doi:10.2337/db09-1064.
- 133 Kaufman RJ. Orchestrating the unfolded protein response in health and disease. *J. Clin. Invest.* 2002; 110: 1389–1398; doi:10.1172/JCI16886.
- 134 Prada PO, Zecchin HG, Gasparetti AL, Torsoni MA, Ueno M, Hirata AE *et al.* Western diet modulates insulin signaling, c-Jun N-terminal kinase activity, and insulin receptor substrate-1ser307 phosphorylation in a tissue-specific fashion. *Endocrinology* 2005; 146: 1576–1587; doi:10.1210/en.2004-0767.
- 135 Hajj S de, Bakker AC, van der Geest RN, Haegeman G, Vanden Berghe W, Aarbiou J *et al.* NF-kappaB mediated IL-6 production by renal epithelial cells is regulated by c-jun NH2-terminal kinase. *J. Am. Soc. Nephrol.* 2005; 16: 1603–1611; doi:10.1681/ASN.2004090781.
- 136 Ropelle ER, Flores MB, Cintra DE, Rocha GZ, Pauli JR, Morari J *et al.* IL-6 and IL-10 anti-inflammatory activity links exercise to hypothalamic insulin and leptin sensitivity through IKKbeta and ER stress inhibition. *PLoS Biol.* 2010; 8; doi:10.1371/journal.pbio.1000465.



- 137 Kim T, Wayne Leitner J, Adochio R, Draznin B. Knockdown of JNK rescues 3T3-L1 adipocytes from insulin resistance induced by mitochondrial dysfunction. *Biochem. Biophys. Res. Commun.* 2009; 378: 772–776; doi:10.1016/j.bbrc.2008.11.121.
- 138 Leppä S, Saffrich R, Ansorge W, Bohmann D. Differential regulation of c-Jun by ERK and JNK during PC12 cell differentiation. *EMBO J.* 1998; 17: 4404–4413; doi:10.1093/emboj/17.15.4404.
- 139 Salans LB, Cushman SW, Weismann RE. Studies of human adipose tissue. Adipose cell size and number in nonobese and obese patients. *J. Clin. Invest* 1973; 52: 929–941; doi:10.1172/JCI107258.
- 140 Björntorp P. Effects of age, sex, and clinical conditions on adipose tissue cellularity in man. *Metab. Clin. Exp.* 1974; 23: 1091–1102.
- 141 Knittle JL, Timmers K, Ginsberg-Fellner F, Brown RE, Katz DP. The growth of adipose tissue in children and adolescents. Cross-sectional and longitudinal studies of adipose cell number and size. *J. Clin. Invest.* 1979; 63: 239–246; doi:10.1172/JCI109295.
- 142 Oller do Nascimento CM, Ribeiro EB, Oyama LM. Metabolism and secretory function of white adipose tissue: effect of dietary fat. *An. Acad. Bras. Cienc.* 2009; 81: 453–466.
- 143 Stanton MC, Chen S, Jackson JV, Rojas-Triana A, Kinsley D, Cui L *et al.* Inflammatory Signals shift from adipose to liver during high fat feeding and influence the development of steatohepatitis in mice. *J Inflamm (Lond)* 2011; 8: 8; doi:10.1186/1476-9255-8-8.
- 144 Li J, Ni M, Lee B, Barron E, Hinton DR, Lee AS. The unfolded protein response regulator GRP78/BiP is required for endoplasmic reticulum integrity and stress-induced autophagy in mammalian cells. *Cell Death Differ.* 2008; 15: 1460–1471; doi:10.1038/cdd.2008.81.

## References

- 145 Sutherland LN, Capozzi LC, Turchinsky NJ, Bell RC, Wright DC. Time course of high-fat diet-induced reductions in adipose tissue mitochondrial proteins: potential mechanisms and the relationship to glucose intolerance. *Am. J. Physiol. Endocrinol. Metab.* 2008; 295: E1076-83; doi:10.1152/ajpendo.90408.2008.
- 146 Valladolid-Acebes I, Fole A, Martín M, Morales L, Victoria Cano M, Ruiz-Gayo M *et al.* Spatial memory impairment and changes in hippocampal morphology are triggered by high-fat diets in adolescent mice. Is there a role of leptin? *Neurobiol Learn Mem* 2013; 106: 18–25; doi:10.1016/j.nlm.2013.06.012.
- 147 Langin D. Adipose tissue lipolysis as a metabolic pathway to define pharmacological strategies against obesity and the metabolic syndrome. *Pharmacol. Res.* 2006; 53: 482–491; doi:10.1016/j.phrs.2006.03.009.
- 148 Pauw A de, Tejerina S, Raes M, Keijer J, Arnould T. Mitochondrial (dys)function in adipocyte (de)differentiation and systemic metabolic alterations. *Am. J. Pathol.* 2009; 175: 927–939; doi:10.2353/ajpath.2009.081155.
- 149 Heo J, Livnat-Levanon N, Taylor EB, Jones KT, Dephoure N, Ring J *et al.* A stress-responsive system for mitochondrial protein degradation. *Mol. Cell* 2010; 40: 465–480; doi:10.1016/j.molcel.2010.10.021.
- 150 Chatenay-Lapointe M, Shadel GS. Stressed-out mitochondria get MAD. *Cell Metab.* 2010; 12: 559–560; doi:10.1016/j.cmet.2010.11.018.

## **Publications and Presentations**

### **Peer-reviewed original manuscripts and reviews**

Gruber L, Kisling S, Lichti P, Martin F-P, **May S**, Lichtenegger M; Rychlik M, Haller D  
High Fat Diet Accelerates Pathogenesis of Murine Crohn's Disease-Like Ileitis  
Independently of Obesity  
*(submitted)*

**May S**, Matthä S, Blüher M, Hauner H, Haller D, Skurk T  
Adipogenic differentiation is not necessarily a condition for elevated ER-stress  
*(in preparation)*

Matthä S<sup>§</sup>, **May S**<sup>§</sup>, Hubersberger M, Hauner H, Skurk T  
Protein normalization in adipocyte models and dependence on cell size  
*Horm Metab Res. 2013 Apr 2. [Epub ahead of print]*  
<sup>§</sup> these authors contributed equally to the manuscript

### **Oral presentations**

Gruber L, **May S**, *Fiamoncini J, Müller V, Daniel H, Clavel T*, Haller D  
High-fat diet aggravates Crohn's Disease-like ileitis independently of  
obesity via alterations of epithelial barrier homeostasis

50. Wissenschaftlicher Kongress der Deutschen Gesellschaft für Ernährung (German Nutrition Society), March 20-22, 2013, Bonn, Germany

Berger E, **May S**, Haller D

Characterization of a chaperonin 60 deficient mouse model for the analysis of  
mitochondrial stress in metabolic organs

49. Wissenschaftlicher Kongress der Deutschen Gesellschaft für Ernährung (German Nutrition Society), March 14-16, 2012, Freising, Germany

## Publications and Presentations

**Schmidt S**, Schmidt J, Blüher M, Hauner H, Haller D, Skurk T

Kompetenznetz Adipositas - Regulation von Zellstressmarkerproteinen während der adipogenen Differenzierung

27. Jahrestagung der Deutschen Adipositas-Gesellschaft (DAG), October 06-08, 2011, Bochum, Germany

**Schmidt S**, Hauner H, Haller D, Skurk T

ER stress response during adipogenesis in murine 3T3-L1 and human SGBS cells

47. Wissenschaftlicher Kongress der Deutschen Gesellschaft für Ernährung (German Nutrition Society), March 11-12, 2010, Jena, Germany

### **Poster presentations**

Gruber L, **May S**, Haller D

High-fat feeding affects barrier protein expression and enhances pathogenesis in a murine model of Crohn's disease like ileitis

49. Wissenschaftlicher Kongress der Deutschen Gesellschaft für Ernährung (German Nutrition Society), March 14-16, 2012, Freising, Germany

**Schmidt S**, Blüher M, Hauner H, Haller D, Skurk T

Regulation der Adipositas-assoziierten chronischen Inflammation im Fettgewebe

26. Jahrestagung der Deutschen Adipositas-Gesellschaft (DAG), November 04-06, 2010, Berlin, Germany

**Schmidt S**, Haller D, Hauner H, Skurk T

ER-Stressantworten während der adipogenen Differenzierung humaner SGBS Zellen

25. Jahrestagung der Deutschen Adipositas-Gesellschaft (DAG) & Herbsttagung der Deutschen Diabetes-Gesellschaft (DDG), November 05-07, 2009, Berlin, Germany

### **Awards**

Poster award

25. Jahrestagung der Deutschen Adipositas-Gesellschaft (DAG) & Herbsttagung der Deutschen Diabetes-Gesellschaft (DDG), November 05-07, 2009, Berlin, Germany

## **Acknowledgements**

Doing a PhD was a personal goal in my life, which was not only easy but sometimes really hard and frustrating. Therefore the encouragement of a lot of people was very important for me and the finalization of my PhD thesis.

First of all, special thanks go to Prof. Dirk Haller and Prof. Hans Hauner, who gave me the opportunity to doing my PhD in a constant supporting and motivating collaboration during the last three years. I really appreciate the excellent discussions.

It is an honor for me to thank my supervisor PD Thomas Skurk, who contributed to this work by ceaseless discussions and ideas. He has made available his support in a number of ways by never-ending motivation as well as constant support.

I would like to show my gratitude to all my colleagues for their scientific and for the mental support. We had a lot of fun together, which makes me happy and the work a bit easier. My thanks go to Simone Matthä and Manuela Hubersberger, who shared my personal ups and downs and always had some friendly words for me. My thanks also go to Julia Stoll, Kathrin Rauh, Susanne Krug, Kerstin Ehlers and Tina Brand for the nice talks in our office. For me it always was a kind alternation to the work in the lab. The periods of plenty of candy will be always in my mind. Special thanks go to Emanuel Berger and Lisa Gruber for the discussion and motivation. Because of you I always felt as a part of the "Haller's group".

Ich möchte allen meinem Freunden für ihre Unterstützung und für ihr Verständnis danken. Die zahlreichen Spieleabende, Feiern und Telefonate waren ein großer Ausgleich und haben mir immer wieder neue Kraft und Durchhaltevermögen gegeben.

Von Herzen danke ich meinem Mann Alexander, der mich immer wieder aufgebaut hat und mir Mut und Kraft zugesprochen hat, mein Ziel zu erreichen. Herzlicher Dank gilt auch meinen Eltern Heidi und Bernd, sowie meiner Schwester Katja und meinem Schwager Sören dafür, dass Sie immer für mich da sind.



# Curriculum Vitae

## Personal Data

**Name:** Stephanie May geb. Schmidt

**Date of birth:** 19.04.1985

**Place of birth:** Gera, Thuringia, Germany

**Nationality:** German

## Education and Qualification

since Apr. 2012

**Recruiter, Kelly Scientific Resources, Kelly Services GmbH**

Oct. 2008 to Feb. 2012

**PhD student, Lehrstuhl für Ernährungsmedizin & Biofunktionalität der Lebensmittel, TU München**

Thesis: "Influence of adipogenesis and high fat diet on the development of cell stress markers in adipose tissue"

Major tasks: Paper writing and publishing, writing of proposals, supervision of Bachelor students, lab tasks

Oct. 2006 to Sep. 2008

**Master of Science in Molecular Biotechnology, TU München**

Master's Thesis: „Investigation of the Tat-dependent export in lactobacilli (using the reporter protein GFP)“

Main emphases: Molecular Medicine, Food Biotechnology, International Management

Grade: 1,6 (B)

Oct. 2003 to Oct. 2006

**Bachelor of Science in Molecular Biotechnology, TU München**

Bachelor's Thesis: "Influence of the bovine embryo to the expression of selected components of the complement system in the endometrium during the pre-implantation phase"

Grade: 2,3 (C)

## Curriculum Vitae

---

**Jun. 2003**

**Abitur (final secondary – school examination),  
Osterlandgymnasium, Gera**

Grade: 1,9

### **International Experience**

**Jul. 2008 to Aug. 2008**

**DAAD Exchange, Ulan Bator, Mongolia**

- Lessons in English and molecular biotechnology at the University of Ulan Bator
- Building of network with national and international DAAD students

**Jul. 2006 to Oct. 2006**

**Research Internship, UADY, Mexiko**

- Project at the University in Merida
- Fermentation processes in fruit and waste
- Language school for Spanish